

## USE OF ILLINOIS BY-PRODUCT RESIDUES FOR PAVING MATERIALS

N. Ghafoori<sup>1</sup>, L. Wang<sup>2</sup>, S. Kassel<sup>3</sup>  
Department of Civil Engineering  
Southern Illinois University at Carbondale  
Carbondale, Illinois 62901

Keywords: coal, combustion residue, and roller compacted concrete

### ABSTRACT

Tests were conducted in a field demonstration project to determine if by-products of fluidized bed and pulverized coal combustions (FBC and PCC) can be used in production of surface wearing course pavements for secondary/county roads. Various proportions of pre-hydrated FBC spent bed, as a fine aggregate; PCC fly ash, as a primary cementitious binder, with or without low dosage of portland cement; and crushed limestone coarse aggregate were blended at their optimum moisture content to produce zero-slump concrete mixtures. Pavement slabs of 6 ft by 12 ft were constructed by compacting 10 in. loose fresh matrix into 8 in. final thickness, in two lifts, using a self-propelled steel vibratory roller. No other surface finish treatments were used.

Information gathered in this paper makes the user of roller compacted concrete (RCC) containing FBC/PCC by-product residues aware of the fact that excellent engineering characteristics can be attained even when little or no portland cement is used. After 18 months from the date of initial casting, the pavement sections are crack-free and remain in excellent surface condition.

### BACKGROUND

In the United States, nearly 80% of the coal produced is used for electric power generation and about 15% of this amount is recovered as coal combustion by-products<sup>1</sup>. Currently, 90 million short tons of ash is produced annually and the level of production is expected to reach 200 million short tons by the year 2000<sup>2,3,4</sup>. The high cost of waste disposal, scarcity of disposal sites, and serious environmental damages associated with the disposal of coal combustion residues have encouraged innovative utilization strategies. Undoubtedly, the construction industry, with its already depleted natural resources and ability to assimilate large volumes of materials, is in a unique position to provide safe and economical solutions of by-product utilization in a variety of construction-related applications.

While past laboratory investigation had provided valuable scientific data on the engineering properties of various FBC/PCC concrete mixtures and identified a number of potentially viable applications, field feasibility studies were needed to bring the laboratory investigation a step closer to reality<sup>5,6</sup>. The paper presented herein reports on a field demonstration project aimed at evaluating the constructability and engineering performance of the experimental slabs utilizing FBC spent bed and PCC fly ash. A nearly 300 ft road, comprising of 25 different slab sections, was constructed at a site located in Carterville, Illinois. Both conventional (vibratory) and roller compacted concrete placement techniques were utilized. Once the pavement sections were placed and finished, a coat of chemical sealant was spread on the slab surface to maintain sufficient moisture for the hydration of cementitious binders. The road was seal-cured for nearly two weeks before it was opened to traffic.

The findings of the surface course roller compacted slabs are presented and discussed in the paragraphs to follow.

### MATERIALS AND METHODS

The FBC spent bed was obtained from a coal-fired circulating fluidized bed combustor at a co-generation plant burning high-sulfur Illinois coal. Its physico-chemical properties are shown in Tables 1 and 2. In order to eliminate the excess heat of hydration and subsequent expansive phases, the FBC residues were pre-hydrated prior to blending with other concrete constituents<sup>7</sup>. The fly ash selected for the study, a by-product of pulverized coal combustion process, complied with the requirements of ASTM C 618<sup>8</sup>. The chemical and physical characteristics associated with this fly ash are documented in Tables 1 and 3, respectively. A low dosage of Type V portland cement (5% by mass of total dry solids), as a complimentary cementitious binder, was used in some slab sections. The crushed limestone coarse aggregate was obtained from a quarry in southern Illinois.

<sup>1</sup>Associate Professor, <sup>2</sup>Research Graduate Assistant, and <sup>3</sup>Research Undergraduate Assistant

The physical properties are shown in Table 4. The mixture designation, solid constituents and proportions, nominal moisture content, and air-dry density are listed in Table 5.

Cylindrical (4" x 8") and beam-shaped (4" x 4" x 14") specimens were cored at different ages. They were tested for strength (ASTM C 39, ASTM C 496, and ASTM C 78)<sup>9</sup>, elasticity (ASTM C 469)<sup>9</sup>, length change (ASTM C 157)<sup>9</sup>, resistance to wear (ASTM C 779, Procedure C)<sup>9</sup> and freezing and thawing (ASTM C 666, Procedure A)<sup>9</sup>.

#### DISCUSSION OF RESULTS

The influence of mixture proportion, curing age, and testing condition on compression behavior of roller compacted FBC/PCC surface course slabs were investigated; and the results are presented in Figures 1 and 2. Similar to conventional concrete, the FBC/PCC mixes continued to gain strength with age. An average increase of 23% and 35% in compressive strength was attained when concrete age was extended from 60 to 90 and from 90 to 180 days, respectively, under dry conditions. When tested under wet conditions, the improvement in strength was 36 and 49% for the aforementioned periods. The compression properties also improved as the FBC spent bed to PCC fly ash ratio decreased. The increase in strength was higher under wet conditions (an average of 33%) than that obtained under dry conditions (a mean value of 18%). However, the influence of moisture (wet or dry) on compressive strength reduced as concrete age increased. Slabs without portland cement displayed compressive strengths superior to those obtained for pavement sections containing cement (21% and 10% for dry and wet compressive strength, respectively).

Table 5 demonstrates the variation of splitting-tensile strength with respect to time for the FBC/PCC core specimens. Similar to the compressive strength, the splitting-tensile resistance is a function of mixture proportion and fly ash content of the matrix. Insofar as strength development is concerned, roughly 83% of 90-day strength was achieved after 60 days from the date of initial casting. An average increase in splitting tensile strength of 15% was observed as concrete age was extended from 90 to 180 days. While the addition of portland cement did not improve the compressive strength, it enhanced the tensile splitting of RCC slabs. The average ratios of splitting-tension to compression were typical of those expected for conventional concretes.

Young's modulus of elasticity for the RCC slabs was determined at various ages, and the results are shown in Table 6. Static modulus of elasticity varied from  $2.51 \times 10^6$  to  $4.17 \times 10^6$  psi. The FBC/PCC roller compacted concrete exhibited a lower elastic modulus than that of conventional concrete of the same strength level.

The progression of flexural strength with respect to cementitious content is illustrated in Table 7. Based on the results obtained, the flexural strength of all matrices displayed a similar trend to those of compressive and splitting-tensile strengths; the flexural capacity steadily improved as the fly ash content of the matrix increased. When a low dosage of portland cement was incorporated into FBC/PCC mixtures, a slight improvement in flexural strength was observed (an average value of 4.4%).

Figure 3 documents the linear expansion of the surface course FBC/PCC roller compacted concretes. The strain properties of the field slabs was stabilized after 2-4 weeks from the date of construction and, to date, remain insignificant. The addition of portland cement reduced, to some extent, the overall expansion strain of FBC/PCC slabs.

Figure 4 illustrates the abrasion resistance of roller compacted concrete mixes under wet surface conditions. In general, the depth of wear increased with abrasion time, and the rate of increase in expansion was fairly uniform as time of wear increased. A reduction in FBC spent bed to PCC fly ash ratio or addition of a low dosage portland cement enhanced abrasion resistance of RCC slabs (12.5% decrease in abrasion wear with addition of portland cement). This improvement is attributed to a stronger cementitious mortar of the concrete surface which displayed more resistance to wear.

Resistance to rapid freezing and thawing of the beam-shaped specimens cored from the non air-entrained experimental slabs is shown in Table 8. The addition of fly ash, and to a great extent portland cement, increased the resistance to freezing and thawing. After a year of exposure to the freezing and thawing cycles of the winter climate, no deterioration or surface scaling has been experienced by any of the FBC/PCC roller compacted concrete slabs.

#### CONCLUDING REMARKS

In general, test results for FBC/PCC roller compacted concrete slabs were extremely encouraging. Strength and elastic modulus followed the well-known patterns of conventional concrete, and

improved as cementitious content of the matrix increased. Expansion strains, based on internal sulfate attack, were minimal and virtually nonexistent. The slabs containing a low dosage of portland cement exhibited an improved tensile strength, linear expansion, abrasion wear, and freezing and thawing properties. Bi-weekly inspections of the paved surfaces indicated that, after 18 months from the date of initial casting, the sections are crack-free and remain in excellent surface condition.

#### ACKNOWLEDGEMENTS

This research was funded, in part, by grants made possible by the Illinois department of Energy and Natural Resources through its Coal Development Board and Illinois Clean Coal Institute, and by the U. S. Department of Energy (Grant number DE-FC22-92PC92521). However, any opinions, findings, conclusions, or recommendations expressed herein are those of the authors and do not necessarily reflect the views of IDENR, ICCI and the DOE.

Thanks are extended to a number of manufacturers who contributed materials used in this field project.

#### REFERENCES

1. Energy Information Administration "Cost and Quality of Fuels for Electric Utility Plants 1991", Office of Coal, Nuclear, Electric and Alternate Fuels, U.S. Department of Energy, Washington, DC 20585, August, 1992, 58 pp.
2. EPA report to Congress, "Wastes from the Combustion of Coal by Electric Utility Power Plants", United States Environmental Protection Agency, February, 1988, 45 pp.
3. Tyson, S.S., "Guidance for Coal Ash Use: Codes and Standard Activities for High-Volume Applications", Proceedings of 9th Annual International Pittsburgh Coal Conference, Pittsburgh, PA, 1992, pp. 815-817.
4. Coal Combustion Byproduct (CCB), "Production and Use: 1966-1993", Report for Coal Burning Utilities in the United States, American Coal Ash Association, Alexandria, VA 1995, 68 pp.
5. Ghafoori, N., "Engineering Characteristics and Durability of Roller Compacted Non-Cement FBC Mixes for Secondary Roads", Annual Report, Illinois Clean Coal Institute and Illinois Department of Natural Resources, September, 1994, 31 pp.
6. Ghafoori, N., "A Field Demonstration Project Utilizing FBC/PCC Residues for Paving Materials", Annual Report, Illinois Clean Coal Institute, September, 1995, 22 pp.
7. Ghafoori, N., and Sami, S., "A Simplified and Practical Approach for Effective Prehydration of Fluidized Bed Combustion Residues", Proceedings of the Coal, Energy and Environmental Conference, October 12-16, 1992, Ostrava, Czechoslovakia, Section IV, pp. 1-9.
8. Standard Specification for Fly Ash and Raw or Calcined Natural Pozzolan for Use as a Mineral Admixture in Portland Cement Concrete, ASTM C 618, American Society for Testing and Materials, Philadelphia, PA, 1987, 3 pp.
9. American Society for Testing and Materials, Annual Book of ASTM Standard, Part 14 and 19, Philadelphia, PA, 1989.
10. American Concrete Institute (ACI) Committee 226, "Fly Ash in Concrete", ACI Materials Journal, 1987, pp. 381-410.
11. Ghafoori, N., and Chang, W.F., "Roller Compacted Concrete Utilizing Dihydrate Phosphogypsum, Journal of Transportation Research Record, September, 1990, Vol. 1, No. 1301, pp. 139-148.
12. Helmuth, R., "Fly Ash in Cement and Concrete", Portland Cement Association, SP040-OIT, 1987, 203 pp.
13. Mindess, S., and Young, Y.F., "Concrete", Prentice-Hall Inc., Englewood Cliffs, NJ, 1981, 671 pp.
14. Neville, A.M., "Properties of Concrete", John Wiley and sons, New York, NY, 1981, 779 pp.
15. Sukandar, B.M., "Abrasion of Concrete Block Pavers", Master Thesis, Department of Civil Engineering and Mechanics, Southern Illinois University, Carbondale, IL, January, 1993, 165 pp.
16. Yoder, E.J., and Witzcak, A., "Principles of Pavement Design, 2nd Edition, John Wiley and Sons, 1975, 711 pp.

**Table 1: Chemical Test Data of FBC Spent Bed and PCC Fly Ash**

Chemical Composition	"FBC" Spent Bed	"PCC" Fly Ash	Fly Ash Specifications (ASTM C 618)
Silicon Oxide ( $SiO_2$ )	9.70	49.10	----
Aluminum Oxide ( $Al_2O_3$ )	3.69	25.50	----
Iron Oxide ( $Fe_2O_3$ )	2.16	16.60	----
Total ( $SiO_2+Al_2O_3+Fe_2O_3$ )	15.55	91.20	50.0 Minimum, Class C 70.0 Minimum, Class F
Sulfur Trioxide ( $SO_3$ )	24.42	0.50	50.0 Maximum
Calcium Oxide ( $CaO$ )	53.10	1.56	Less than 10%, Class F More than 10%, Class C
Magnesium Oxide ( $MgO$ )	0.88	0.89	----
Loss on Ignition	0.80	0.38	6.0 Maximum
Free Moisture	0.0	0.16	3.0 Maximum
Water of Hydration	2.65	0.0	----
Total $Na_2O$	0.16	0.37	----
Available Alkalies as $Na_2O$	N/A	0.08	1.5 Maximum
Total $K_2O$	0.39	2.26	----
Others ( $TiO_2+P_2O_5+BaO$ )	2.04	2.60	----

**Table 2: Physical Properties of FBC Spent Bed**

Fineness Modulus	Specific Gravity (OD)	Specific Gravity (SSD)	Absorption (%)	Organic Impurities
1.80	1.92	2.19	14.60	None

**Table 3: Physical Properties of PCC Fly Ash**

#325 Sieve Fineness		Specific Gravity	Autoclaved Expansion		Water Requirement		7-Day Compressive Strength		
Actual	Limit		Actual	Limit			Actual	ASTM	AASHTO
22.60	Max. 34%	2.39	0.03	0.80%	93.30	Max. 105	85.40	Min. 75%	Min. 60%

**Table 4: Physical Properties of Crushed Limestone Coarse Aggregate**

Maximum Size (Max. Normal Size)	Specific Gravity (OD)	Specific Gravity (SSD)	Absorption (%)	Rodded Unit Weight (OD) (lb/ft <sup>3</sup> )	Rodded Unit Weight (SSD) (lb/ft <sup>3</sup> )	Void Ratio
1 (3/4)	2.64	2.67	0.75	93.50	94.20	43.75

**Table 5: Mixture Proportion Details for FBC/PCC Roller Compacted Concrete Mixtures**

Mix No.	FBC Spent Bed (%) *	Silicious Fine Aggregate (%)	PCC Fly Ash (%)	Portland Cement (%)	Limestone Coarse Aggregate (%)	Nominal Moisture Content (%)	Air-Dry Density (lb/ft <sup>3</sup> )
C3	26.67	---	13.33	---	60.0	7.67	144.47
C5	20.0	---	20.0	---	60.0	7.74	145.12
C1P	29.5	---	5.5	5.0	60.0	8.27	140.66
C3P	24.17	---	10.83	5.0	60.0	7.95	144.43
C5P	17.5	---	17.5	5.0	60.0	7.62	142.43

\* Note: All percentages are by mass of total dry solids

**Table 6: Splitting-Tensile Strength and Static Modulus of Elasticity of FBC/PCC Roller Compacted Concrete Mixtures**

Mix No.	Splitting-Tensile Strength (psi)			Splitting-Tension to Compression Ratio			Modulus of Elasticity (10 <sup>6</sup> psi)		
	Curing Age (Days)			Curing Age (Days)			Curing Age (Days)		
	60	90	180	60	90	180	60	90	180
C3	323	406	476	0.078	0.098	0.087	3.54	3.80	4.06
C5	442	500	549	0.103	0.092	0.096	3.70	3.94	4.17
C1P	236	300	362	0.111	0.110	0.108	2.51	2.78	3.09
C3P	352	438	530	0.106	0.109	0.120	3.30	3.48	3.66
C5P	467	536	571	0.120	0.119	0.121	3.41	3.60	3.79

**Table 7: 90-Day Flexural Strength of FBC/PCC Roller Compacted Concrete Mixtures**

Mix. No.	Flexural Strength (psi)	Strength Ratio	
		Flex./Comp.	Flex./Split
C3	646.88	0.127	1.60
C5	701.25	0.128	1.40
C1P	486.3	0.189	1.62
C3P	665.35	0.165	1.52
C5P	743	0.165	1.39

**Table 8: Freezing and Thawing of FBC/PCC Roller Compacted Concrete Mixtures (Mass Loss %)**

Mix No.	Number of Freezing and Thawing Cycles									
	5	10	15	20	25	30	35	40	45	
C3	0.43+	7.42#	17.1#	30.5#						
C5	0	0.41+	0.41+	1.03*	3.08#	44.8#				
C1P	0.44-	2.44+	22.6#	41.2#						
C3P	0.21-	0.42-	5*	15.2#	55.7#					
C5P	0	0	0.22-	0.43-	1.3+	4.11+	10.6#	29.2#		

- slight flaking; + slight chipping; \* noticeable cracking in specimen; # severe flaking and chipping

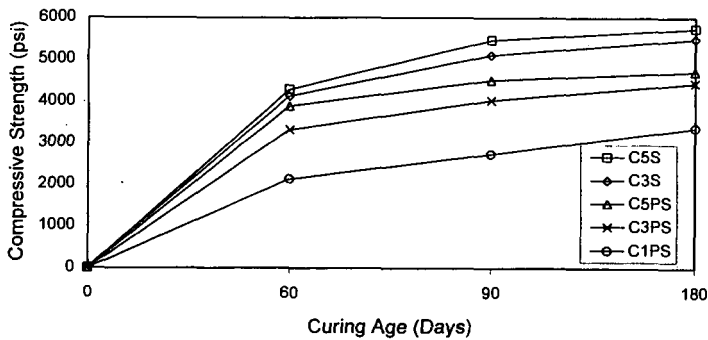


**Figure 1: Field Air-Dry Compressive Strength of Surface Course FBC/PCC Roller Compacted Concrete Mixtures**

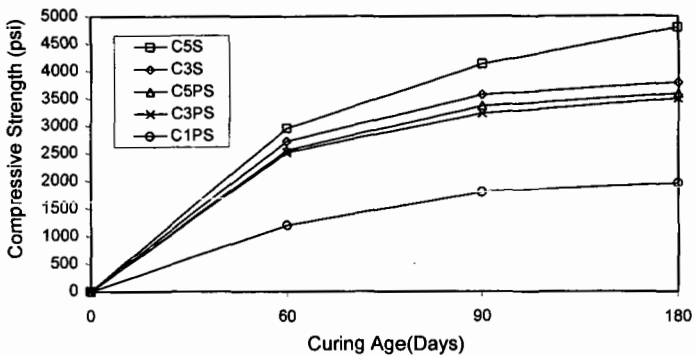


Figure 2: Field Soaked Compressive Strength of Surface Course FBC/PCC Roller Compacted Concrete Mixtures

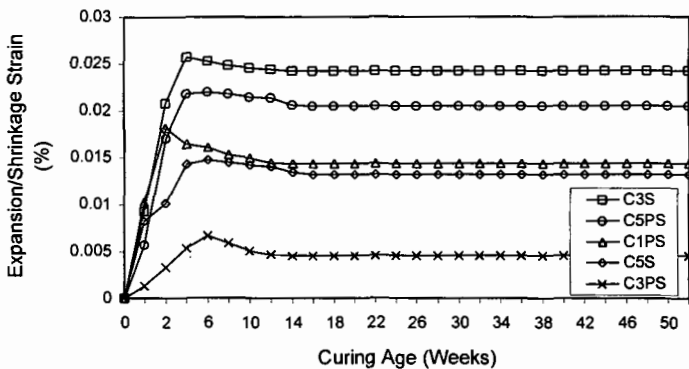


Figure 3: Field Expansion/Shrinkage of Surface Course FBC/PCC Roller Compacted Concrete Mixtures

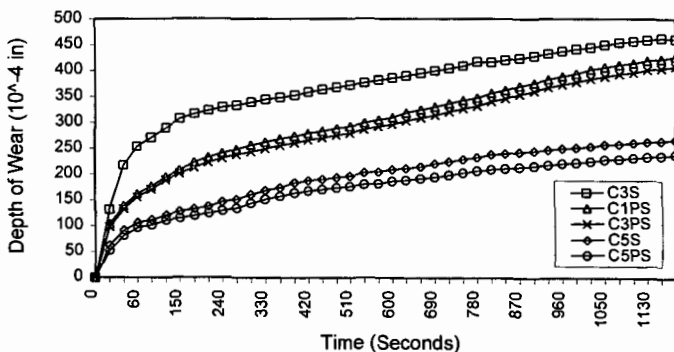


Figure 4: Field Abrasion Resistance of Surface Course FBC/PCC Roller Compacted Concrete Mixtures (Wet at Testing)

## Roller Compacted Base Course Construction Using Lime Stabilized Fly Ash and Flue Gas Desulfurization Sludge By-Product

Joel H. Beeghly, Project Manager  
Dravo Lime Company Research Center  
3600 Neville Road  
Pittsburgh, Pennsylvania 15225

Keywords: lime, stabilization, flue gas desulfurization

### ABSTRACT

Dewatered calcium sulfite and calcium sulfate sludges from unoxidized flue gas desulfurization (FGD) processes at coal fired power plants can be mixed with coal fly ash and lime to cause a cementitious chemical reaction used to construct a roller compacted base course (RCFGD) or an impermeable pond liner. The chemical reaction is described as lime reacting with alumina from the fly ash which in turn reacts with the calcium sulfite and sulfate FGD waste to form calcium sulfo-aluminate compounds. Leachate data is similar to primary drinking water quality standards. Two field demonstrations of RCFGD and a proposed mix design procedure are described. Factors that affect strength gain and freeze-thaw durability such as optimum moisture content, fly ash to FGD ratio, and age of FGD are discussed. Better understanding is needed on how to predict long term strength performance and expansive potential given the nature of long term hydration forming ettringite compounds and the vulnerability to destructive freeze-thaw cycles.

### INTRODUCTION

Lime is commonly used as a reagent to remove  $SO_2$  from power plant emission burning medium and high sulfur bituminous coal. A leading supplier of lime products for flue gas treatment applications, the Dravo Lime Company is also extensively involved in the development of lime-based environmental technologies, including ways to better manage the large volume of waste product resulting from these efforts to clean the stack gases from large coal-fired publicly owned utilities. In the United States alone, over 68 million tons of coal ash materials and 20 million tons of flue gas desulfurization (FGD) materials must be handled. Most of the ash and nearly all of the FGD by-products must be disposed in landfills.<sup>1</sup> This huge volume of waste material disposal applies to unoxidized FGD systems that use either lime or limestone as the alkaline sorbent.

A common practice for landfill disposal with twenty years experience is a sludge fixation process whereby the FGD sludge is dewatered by vacuum filtration or centrifuges, and the cake solids are mixed with the plant's fly ash that was collected separately and some pulverized quicklime. This mixture is referred to as fixated scrubber sludge solids (FSSS). As it is being placed and compacted in a landfill disposal cell, chemical reactions begin causing the material to harden.

The Dravo Lime Company (DLC) serves 14 power stations in the Ohio River Valley generating about 13,500 MW of power. Twelve of these stations practice the above lime-fly ash stabilization process, often called by the original process tradename, POZ-O-TEC. The strength of FSSS for landfill disposal is not high enough at 200 psi @ 28 days curing or durable enough for heavy traffic and freeze-thaw conditions. However, when compared to natural soils, fixated FGD scrubber sludge solids have been shown to have high natural strength and low permeability.<sup>2</sup> Although important, permeability testing and results will not be covered in this paper.

This paper will discuss the progress of on-going research at Dravo Lime Company on how this fixated scrubber sludge solids (FSSS) mixture can be upgraded in terms of strength gain and durability and be used as a roadbase pavement or structural fill material that would be applied by placing it using construction techniques similar to those for roller compacted concrete (RCC).

### ROLLER COMPACTED CONCRETE OR STABILIZED BASE COURSE

Conventional RCC is a dry and stable mix of aggregate, portland cement or lime, and water. It is also similar to lime stabilization of soil or aggregate base course which is widely used to improve the strength and durability of soils by ion exchange and cementitious reactions, enabling their use as engineering materials in the construction of pavements and structural fills. RCC is typically laid by modified asphalt pavers or a road grader and compacted by rollers that follow close behind. The material should show tremendous stability in the fresh state. As the FGD-fly ash-lime mixture hydrates, the material acquires strength but not likely as much strength as

conventional portland cement concrete. Adequate strength for stabilized base course is about 400 psi in 28 days curing for most applications. It is believed the FSSS mixture using additional lime and coal ash material can be designed to attain 400 psi. It will be called roller compacted FGD stabilized base material (RCFGD).

However, the RCC made from FSSS is not suited to perform as a highway wearing course pavement because of low abrasion resistance. Some experience suggests it can exhibit suitable durability in terms of freeze-thaw resistance but more proof is needed to define the durability limitations which is discussed further.

#### **CHARACTERIZATION OF FSSS COMPONENTS**

Fixed scrubber sludge solids (FSSS) is the term to apply to the mixture of sludge cake, fly ash, and lime to allow stabilization of the sludge cake for landfill disposal. The term for upgraded FSSS for use as roller compacted base course will be labeled roller compacted FGD (RCFGD). The FGD scrubber solids mineralogical composition from a lime scrubber, most of which are based on the Dravo Lime magnesium enhanced lime Thiosorbic process and some inhibited oxidation limestone scrubbers, is mostly calcium sulfite hemi-hydrate ( $\text{CaSO}_3 \cdot \frac{1}{2}\text{H}_2\text{O}$ ) ranging 75-85% and some calcium sulfate dihydrate ( $\text{CaSO}_4 \cdot 2\text{H}_2\text{O}$ ) ranging 10-20% with minor amount of calcium carbonate ( $\text{CaCO}_3$ ) ranging 5-15% and minor amounts fly ash minerals. Coal fly ash is mostly clay like minerals composed of alumina, silica, and iron oxide. A geochemical oxide or elemental form analysis is listed in Table 1. Also listed in the composition of the quicklime component which is closer to a unhydrated calcitic quicklime than a dolomitic lime.

One method to evaluate pavement performance is the unconfined compression test (ASTM D2166). In this procedure strengths of specimens compacted to a known density and water content according to ASTM D698 (Standard Proctor Test) are evaluated after different curing periods and conditions.<sup>3</sup>

#### **MIX PROPORTION FOR LANDFILL DISPOSAL**

The proportion of the components as they are mixed to stabilize the FGD sludge for landfill disposal varies somewhat from plant to plant and from day to day depending on the percent solids of the dewatered sludge cake and the availability of the fly ash. The objective is to make a mixture that can be compacted to a density required by the solid waste regulatory authority. Generally, the ratio of fly ash to scrubber solids is 0.75 or less for every 1.0 on a dry weight basis. The predominately calcium sulfite sludge comes from large diameter thickeners and then is dewatered by drum vacuum filters or centrifuges to about 40% solids based on the total wet weight. The cake is mixed with the fly ash and 2-3% pulverized quicklime (CaO) in a pug mill. Only enough lime is added to cause enough hardening to stabilize the sludge and prevent leachate by adequate strength development and resultant clay-like impermeability. The approximately 35-42% FGD sludge solids is increased to about 60-65% solids in the FSSS. Smith presents a good description of the FSSS process.<sup>4</sup> The mixture is conveyed to a stockpile area to cure for a few days and stiffen to facilitate placement and compaction in the landfill. The state EPA regulatory operating permit will specify for landfill disposal the density and permeability of the compacted solids, thereby governing the amount of compaction effort.

#### **ENVIRONMENTAL WATER QUALITY IMPACT**

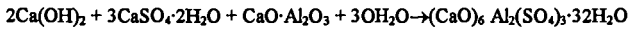
From combustion of bituminous coal, the FGD solids and fly ash are classified by the USEPA as non-hazardous. Presented in August, 1993, their final regulatory decision on wet FGD emission control waste stated that these materials are not regulated as hazardous wastes under CERCLA Subtitle C and officially placed them under Subtitle D as solid wastes under the jurisdiction of individual states. Classified as a residual solid waste, the State of Ohio EPA program encourages beneficial reuse of FSSS as long as water quality of the surrounding area is not affected. They require each specific project submit a proposal and description for beneficial use status. However, the process of mixing a FSSS with additional fly ash and lime makes the roller compacted mix a product and thus exempt from requiring Ohio EPA approval. However, correspondence with local and state regulatory officials is prudent to foster understanding of the technology and minimal environmental impact of beneficial uses of RCFGD.

The Ohio EPA judges from leachate water quality testing any potential risk. As shown in Table 2 the leachate from one FSSS and fly ash source being utilized are one example showing concentrations of heavy metal elements very much below concentrations considered hazardous (RCRA limits) and actually similar to primary drinking water standards. As permitted by Ohio EPA, the ASTM leachate procedure 3987-85 using distilled water was used instead of the TCLP method that uses acid. The levels are well below Ohio EPA residual waste Class III limits. Leachate concentration for elements other than the TCLP metals are shown.

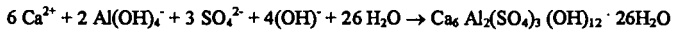
## CEMENTITIOUS POZZOLANIC AND SULFO-POZZOLANIC REACTIONS

There are two basic but related types of chemical reactions that are responsible for the hardening process. Both are a type of pozzolanic reactivity commonly used in stabilization and solidification of waste materials. The first hardening reaction is the more understood pozzolanic reaction where the high pH lime (CaO) solubilizes the silica (SiO<sub>2</sub>), glassy amorphous alumina (Al<sub>2</sub>O<sub>3</sub>), and aluminosiliceous glass from the fly ash component in the presence of high pH and water. These reactions are similar to the hydration of portland cement. This relatively slow reaction solidification is noticeable in about four hours by the stiffening to a mortar or stiff paste like consistency. If compacted, this consumption of free moisture in the FSSS cake material will cause the sludge cake to harden and gain bearing strength. Calcium silicate hydrates (xCaO - ySiO<sub>2</sub> - zH<sub>2</sub>O), calcium aluminate hydrates (xCaO - yAl<sub>2</sub>O<sub>3</sub> - zH<sub>2</sub>O), calcium silica-alumina hydrates (wCaO - xAl<sub>2</sub>O<sub>3</sub> - ySiO<sub>2</sub> - zH<sub>2</sub>O) and calcium alumina-ferro hydrates (wCaO - xAl<sub>2</sub>O<sub>3</sub> - yFe<sub>2</sub>O<sub>3</sub> - zH<sub>2</sub>O) are the reaction products.

A secondary reaction begins once the calcium aluminate hydrates are formed. Often called sulfo-pozzolanic, calcium aluminate at high pH reacts with calcium sulfite and calcium sulfate react to form a class of compounds called calcium sulfo-aluminate or calcium aluminosulfate minerals. This type of chemical compound, called ettringite, is represented by the following reaction.



Another molecular formula for ettringite is written as 3CaO·Al<sub>2</sub>O<sub>3</sub> - CaSO<sub>4</sub>·32H<sub>2</sub>O. This reaction continues to occur for more than one year. It utilizes 32 moles of water for every 3 moles of available CaO and 3 moles of CaSO<sub>4</sub> consumed, and thus ettringite is a big contributor to long term development of compressive strength. However, as noted later, its long term stability is questioned. McCarthy and Tishmack express the reaction differently as follows:



They state the actual phase is more complex, with some carbonate substitution for sulfate and variable H<sub>2</sub>O content. Also, Si can substitute for Al, forming solid solutions with thaumasite, Ca<sub>6</sub> Si<sub>2</sub> (SO<sub>4</sub>)<sub>2</sub> (CO<sub>3</sub>)<sub>2</sub> (OH)<sub>12</sub> · 24H<sub>2</sub>O.<sup>5</sup>

## PRODUCTION OF RCFGD: TWO CASE HISTORIES

FSSS that is produced for landfill disposal on any given day may not be suitable for beneficial uses such as structural fill, road base, or pond liner. A more controlled and batch type mixing process is preferable where quality and productivity are more assured. A quality control / quality assurance program can be more effective if there is a smaller or secondary pug mill to mix the FSSS containing extra fly ash with additional lime or lime related materials, i.e., lime kiln dust, and additional ash by-products i.e. bottom ash. The addition of both can offer a good means to help the FSSS achieve both more pozzolanic reactivity and a higher percent solids and therefore be closer to its optimum dry density necessary for facilitate the compaction effort. Otherwise, excessive levels of moisture or variations in the amount of fly ash in the FSSS component would prevent a uniform mix and hinder product quality control.

A process for developing RC base course mixes that will satisfy mix design criteria, i.e. 400 psi at 28 days, is being researched by DLC in cooperation with other organizations namely American Electric Power Service Corporation (AEP), VFL Technology Corporation (VFL), and The Ohio State University (OSU).

1993 OSU Cattle Feedlot Pavement: In 1993 DLC and OSU, Department of Civil Engineering performed laboratory studies that showed adequate RCFGD strengths could be made for a base course pavement at a cattle feedlot. In cooperation with the American Electric Power Service Corporation, FSSS from their Conesville plant was converted into RCFGD for a pavement to keep cattle out of the mud during the winter at the feedlot and a storage area for large round hay bales. As shown in Table 3, the ratio of fly ash to FGD was doubled from 0.8:1.0 for the FSSS control (landfill product) to 1.6:1.0 for the RCFGD product. Also, the lime content was increased from 2.0% in the FSSS to 6.5% for two test sections and 11.5% in a third section. Samples of each material were taken to lab and allowed to cure. The 28 day strength increased from 45 psi for the FSSS mix to 190-260 psi for the RCFGD mixes at 6.5% CaO. The 90 day strengths increased likewise from 100 psi to 480-580 psi. A third test at 11.5% lime did not increase strengths at the higher amount. A block of pavement was cut out and removed after

the first winter at 9 months age. A strength of 400 psi was found. More detail on this first RCFGD project has been previously reported.<sup>2</sup>

**1995 Bob Evans Farm Cattle Feedlot Pavement:** In the summer of 1995, an opportunity arose to use a portable pug mill to make lime activated RCFGD, operated by VFL Technology and in cooperation with American Electric Power Gavin Plant personnel. This means of secondary mixing provides a way to add extra ash, i.e., bottom ash or boiler slag, and extra lime bearing material into the FSSS in order to maintain better quality of the RCFGD mix by controlling the percent solids and cementitious reagent. The FSSS was specified to have minimum 1:1 FA to FGD. The pug mill has two variable speed feed hoppers. One is for the FSSS and one for additional bottom ash. A silo will store and feed the cementitious reagent. It produces continuous quantities upon demand much like an asphalt hot mix or ready mix concrete plant at a rate of about 120-150 tons per hour.

One of project objectives was to compare the extra lime fines to the use of lime kiln dust, which is generally 20% ± 5% quicklime and 75% pulverized limestone. Therefore, more is required. The dosages compared in the plant mixes described in Table 4 are 8% lime fines and 20% lime kiln dust (LKD). More research will determine the optimum dosage of each. Table 4 also shows a lab mix of 8% LKD. Unconfined compressive strengths with 8 and 20% LKD tests surpassed the 400 psi at 28 days age criteria. These strength and densities agreed closely with similar lab mixes performed earlier by American Electric Power's Civil Engineering Laboratory.<sup>6</sup> Details of results including costs and durability tests i.e. freeze-thaw resistance, will be the subject of a future report.

#### MIX DESIGN PROCEDURE TO MAKE RCFGD FROM FSSS

A proposed procedure is outlined for designing and confirming a mix design to meet the design strength for RCFGD and can be summarized in four steps:

**Step 1 - Specification for FSSS:** The first stage is to develop a specification or criteria for the fixated scrubber sludge solids (FSSS) that is to be the main component in the RCFGD mix. When placing an order for RCFGD, a separate stockpile of "high grade" FSSS can be segregated on the concrete storage pad. To start with, the filter cake solids should be maximized or have a minimum of 40% solids (wet weight basis). The amount of fly ash and lime added to make FSSS should be mixed to increase the percent solids to about 66% or more (a 66% solids wet weight basis equals to 51.5% on a dry weight basis). The ratio of fly ash to filter cake solids on a dry weight basis should approximate 1:1. More fly ash if available up to 1.6:1.0 may be better for more moisture control. At least 2-3% pulverized quicklime should be added to initiate the chemical reaction. Experience has shown the FSSS should cure at least one day in a stockpile before using it to make RCFGD but not more than 3 days. Over four days, the strength gain in the FSSS mix alone would be destroyed when re-mixing for RCFGD.

**Step 2 - Develop procedure to design RCFGD:** The second stage is to determine the optimum moisture content (OMC) so as to determine the amount of additional extra dry pozzolanic and cementitious material to increase the strength of RCFGD. Excessive water contents would prevent optimum compaction or maximum dry density. However, 2-5% of extra moisture is desirable to hydrate the extra lime required (~5% CaO as free, available and pulverized quicklime or equivalent).

- a) The amount of free moisture that achieves a compacted base course of maximum dry density is determined by constructing / generating a OMC curve according to ASTM D-698<sup>3</sup>. It is reported on a dry weight basis i.e. weight of moisture divided by the weight of dry solids. An example is shown in Table 5.
- b) The optimum moisture content is apt to be much lower than the moisture content of the FSSS. Additional ash and/or lime based cementitious fines, i.e. pulverize quicklime or lime kiln dust, needs to be added in a second mixing operation like that described at the VFL pugmill to closely approach the OMC. The amount of additional ash material needed can be represented by the following formula:

$$OMC = \frac{\text{water content present in FSSS}}{\text{solids in FSSS} + \text{additional solids needed}} \times 100$$

Example: Assume an OMC is found to be about 35% on a dry weight basis. Assume the FSSS is 66% solids on the wet basis. It contains 34% water. The amount of additional

ash required calculates to 0.31 lb for every 1.0 lb of FSSS. The added ash is assumed here to be dry. Variable speed settings of each hopper feeder can be set accordingly.

$$35\% \text{ OMC} = \frac{0.34 \text{ water}}{0.66 \text{ FSSS} + 0.31 \text{ added ash}} \times 100$$

- c) Strength gain should be confirmed. In this phase of Step 2, one is to mold specimens to determine unconfined compression strength (UCS) of the OMC mix. This should be done in conjunction with checking levels of extra cementitious reagent in order to confirm strength gain from at least 7 to 28 days but as early as 4 days curing. UCS should be determined according to ASTM D-2166-85. Dry and wet density would be calculated. The water content of the broken procter cylinders for strength should be determined and recorded.

Step 3 - Field Demonstration Mix and Conformation, Field Sampling for UCS, Water Content, and Density: Once placed and compacted in the field in place densities and water content should be determined and compared to that designed. Molded samples for UCS should be made to cure and break for strength gain confirmation.

### **FIELD SAMPLING FOR UNCONFINED COMPRESSIVE STRENGTH, MOISTURE, AND DENSITY**

The specimens would be extruded on site, kept moist, and transported safely to a laboratory curing chamber. Unconfined compressive strength is determined at 7, 14, 28, and 60 days. Two specimens are broken on at least two of the days to check for repetition/consistency. Each molded sample should be weighed and checked for wet density. After compaction and extrusion of the specimen, only a small amount of water should be observed on the base of the mold. Surfaces of the specimens should appear damp. The dry density can be determined after determining the free moisture of the uncompacted material assuming very little if any water was compacted out of the specimen during the molding process. Extra specimens for durability testing such as wet-dry or freeze-thaw resistance would also have to be made.

In place density measurements using the sand cone volumetric displacement procedure (ASTM D4914) or a Troxler nuclear densiometer should be taken for comparison to the procter mold densities. The free moisture should be a few percentage points in excess of the OMC content to account for quicklime hydration.

### **RCFGD BENEFICIAL USE - NEED FOR CAUTION, PROOF OF DURABILITY**

Road base construction using RCFGD in the thousands of tons have been applied in Florida and Texas.<sup>7,8,9</sup> Both lime and portland cement has been used as the stabilizing agent, and other sources than coal FGD wet sludge have been used. In the Ohio River Valley, power plants that scrub are more interested in learning how to design and construct beneficial use applications such as roller compacted pavement or structural fill. One of the major concerns for successful long term applications of this cementitious reaction in the more northern climate is the long term durability, most specifically resistance to degradation from freeze-thaw cycles.

The first record of attempting FSSS for roadbase construction in the Ohio Valley region was near Pittsburgh, PA, in 1977.<sup>10</sup> Cores of the road base were taken after 3 and 7 years for freeze-thaw testing by the vacuum saturation method as stipulated in ASTM C-593.<sup>11</sup> Strengths were not decreased as one might expect by this severe test.

The only recent work has been reported by researchers at OSU, AEP and VFL. They all used ASTM D 560 method titled "Freezing and Thawing Compacted Soil-Cement Mixtures."<sup>3</sup> However, Wolfe, Chen, and Hargroves at OSU<sup>12,13</sup> modified the procedure to gauge results by testing UCS rather than measuring weight loss after each freeze-thaw cycle. VFL and AEP are researching a pass-fail criteria based on volume change and strength as opposed to the conventional practice of measuring weight loss per ASTM D560.<sup>9</sup> More research needs to confirm if this criteria can be met for RCFGD using extra lime and fly ash at the respective OMC.

Chen and Wolfe of OSU found good strengths under freeze-thaw conditions provided 5% extra lime was added to the FSSS before compaction and the time from compaction to first freeze was at least 60 days. Also, they showed that water contents above 40% (dry weight) exhibited low strength after 12 cycles of freeze-thaw.<sup>12</sup> Hargroves of OSU showed that after 60 days curing the 12 cycles of freeze-thaw lowered compressive strengths from about 600 psi to 300-

500 psi.<sup>13</sup> More research must confirm if this loss in strength is acceptable. In general, more experience by various researchers is needed before a consensus can be found on how to perform freeze-thaw testing and what criteria and parameters to judge user acceptance.

Another major need for answers to questions from highway construction design engineers is the potential for swelling reactions like those reportedly caused by other types of compacted FGD by-product materials. Specifically, dry FGD by-products from fluid bed combustion and duct injection systems have similar chemical and mineralogical composition and cementitious strength gaining reactions when conditioned with water and then compacted. Studies have reported dry FGD by-products have swelling characteristics due to the slow hydration and formation of ettringite.<sup>14</sup> Swelling has been known to occur after clay soils high in sulfate content were stabilized with lime in order to construct a road.<sup>15</sup> Graham et.al. reported that under a confining pressure, ettringite formed preferentially inside available pore space, indicating that the formation mechanism may be regulated by a surcharge.<sup>16</sup> Others fear the subsequent formation of thaumosite ( $\text{Ca}_6\text{Si}_2(\text{CO}_3)_2(\text{SO}_4)_2(\text{OH})_{12}\cdot 24\text{H}_2\text{O}$ ) may further degrade performance.<sup>17</sup> Still others have reported studies where the addition of extra pulverized fly ash improved durability of the dry FGD mixtures for structural fill or pelletized for use as construction aggregates.<sup>18</sup> Papers on FSSS by the noted author Charles Smith of Conversion Systems, Inc. have never mentioned potential swelling or descriptive tests to predict same.<sup>4,5,8</sup> Saylak et.al. states ettringite is stable if there is ample supply of sulfate available.<sup>6</sup> They recommend using low alumina content portland cement as the cementitious stabilizing agent. Long term swelling tests need to be conducted using ASTM method D4546.<sup>2</sup>

#### ASTM SUB-COMMITTEE 50.03

The ASTM E50.03 coal ash task group recently published a standard ASTM P5 23-95 "Guide for the Use of Coal Combustion Fly Ash Structural Fills".<sup>19</sup> This provisional guide covers the design and construction procedures for consideration of engineering, economics, and environmental factors in the development of fly ash structural fills. Committee E-50 covers environmental risk assessment. The sub-committee E50.03 is responsible for pollution prevention, reuse, recycling, and environmental efficiency. Utilization of coal combustion fly ash conserves land, natural resources, and energy. A similar effort in creating guidelines should be considered for RCFGD for use as a stabilized base and structural fill.

#### SUMMARY AND CONCLUSIONS

Roller compacted stabilized base course for construction projects required to withstand heavy weight traffic is a potential high volume beneficial use for fixated FGD scrubber sludge solids (FSSS) that are enhanced by the addition of extra fly ash/bottom ash and quicklime in order to efficiently compact to maximum density and thereby attain higher compressive strength and long-term durability.

The chemical composition of the mix components and cementitious chemical reactions that cause increases in bearing strength are discussed. The common practice of producing FSSS for landfill disposal is compared to the advanced mixing process to obtain higher strengths for beneficial use applications in land construction. Leachate water quality of FSSS is non-toxic and similar to primary drinking water standards. State of Ohio regulatory policy encourages large scale demonstrations of beneficial use. Processing to enhance the FGD by-products for beneficial use eliminates the requirement for regulatory approval, but the EPA authorities still need information for better understanding and public support.

Two case histories and a procedure for designing a mix to have optimum moisture content (OMC) were discussed. One recent case used a portable pug mill to obtain OMC and increased strength by addition of extra coal ash and lime. Twenty percent lime kiln dust was successfully used as a substitute for 8% pulverized quicklime. Adequate strength of 400 psi can be achieved.

Concerns about long term durability are discussed. There is not enough field demonstration evidence that satisfactory long term durability can be attained under freeze-thaw conditions. Better consensus is needed on how to test for durability. The risk of potential swelling from expansive long term hydration reactions of ettringite formation must be clarified. ASTM E-50 committee on environmental risk assessment using recycled products offers a means to write a specification for designing roller compacted base course using FGD and coal ash by-products. Efforts to develop beneficial uses of these materials should be enhanced by the growing public interest in concepts and the example of environmental sustainability.

#### REFERENCES

1. American Coal Ash Association, 1995, "1993 Coal Combustion By-Product Production and Use," Alexandria, VA.
2. Wolfe, W.E. and Cline, J.H., 1995, "A Field Demonstration of the Use of Wet and Dry Scrubber Sludges in Engineered Structures," Proceedings: Eleventh International Symposium on Use and Management of Coal Combustion By-Products, American Coal Ash Association, Alexandria, VA, Paper No. 7.
3. American Society Testing & Materials, 1989, Annual Book of ASTM Standards, Vol. 4.08, Philadelphia, PA.
4. Smith, C.L., 1985, "Lime-Based Fixation of Flue Gas Desulfurization Wastes," ASTM Symposium STP 931. Lime for Environmental Uses, Philadelphia, PA, June, pp 52-68.
5. McCarthy, G.J. and Solem-Tishmack, J.K., 1994, "Hydration Mineralogy of Cementitious Coal Combustion By-Products," Advances in Cement and Concrete Materials Engrg. Div/ASCE, NY, NY, Proceedings: 87th Annual Meeting Air & Waste Management Association, Cincinnati, Ohio, June 19-24, 1994.
6. Personal Communications with R.J. Collins of VFL Technology and P. Amany and E. Booth of American Electric Power, November 15, 1995.
7. Smith, C.L., 1993, "15 Million Tons of Fly Ash Yearly in FGD Sludge Fixation," Proceedings: Tenth International Symposium on Coal Ash Utilization, American Coal Ash Association, Alexandria, VA, Paper No. 2.
8. Saylak, D., Sorensen, G., and Golden, D.M., 1994, "Construction Applications for FGD By-Products," Proceedings: 87th Annual Meeting Air & Waste Management Association, Cincinnati, Ohio, June 19-24, 1994.
9. Prusinski, J.R., et al., 1995, "Development and Construction of Road Bases from Flue Gas Desulfurization Material Blends," Proceedings: Eleventh International Symposium on Use and Management of Coal Combustion By-Products, American Coal Ash Association, Alexandria, VA, Paper No. 22.
10. Smith, C.L., 1989, "Fixated FGD Scrubber Solids," Proceedings: Power-Gen, 1989, New Orleans, LA, December, 1989, pp 312-325.
11. American Society for Testing & Materials, 1993, Annual Book of ASTM Standards, Vol. 4.01, Philadelphia, PA.
12. Chen, X. and Wolfe, W.E., 1995, "The Durability of Stabilized Flue Gas Desulfurization Sludge," Proceedings: University of Kentucky Ash Utilization Conference, Lexington, KY, October 23-25, 1995.
13. Hargroves, M.D., 1994, "The effect of Freeze-Thaw Cycles on the Strength of Flue Gas Desulfurization Sludge," Master Thesis, The Ohio State University, Department of Civil Engineering.
14. Adams, D.A. and Wolfe, W.E., 1993, "The Potential for Swelling in Samples of Compacted Flue Gas Desulfurized By-Product," Proceedings: Tenth Ash Use Symposium, American Coal Ash Association, Alexandria, VA, Vol. 2, Paper No. 61.
15. Mitchell, J.K. and Dermatas, D., 1992, "Clay Soil Heave Caused by Lime-Sulfate Reactions," Innovations and Uses for Lime, ASTM STP 1135, American Society for Testing and Materials, Philadelphia, PA, pp 41-64.
16. Graham, V.M., et al., 1993, "Mineralogical Transformations of Ettringite in Concrete Derived from Dry FGD By-Products," Proceedings: Pittsburgh Coal Conference, University of Pittsburgh, School of Engineering, Pittsburgh, PA, pp 864-868.
17. Weinberg, A. and Hemmings, R.T., 1995, "Results from Continued Monitoring of Advanced Coal Combustion By-Products: The Effects of Mineral Transformations on Material Properties," Proceedings: University of Kentucky Ash Utilization Conference, Lexington, KY, October 23-25, 1995.
18. Wu, M.M., et al., 1995, "Composition Effects on Durability of Aggregates made from Coal Combustion By-Products," Proceedings: University of Kentucky Ash Utilization Conference, Lexington, KY, October 23-25, 1995.
19. American Society Testing Materials, 1995, "Provisional Standard Guide for Use of Coal Combustion Fly Ash in Structural Fills," designation PS 23-95, Philadelphia, PA

**Table 1**  
**Chemical Composition of RCFGD Components**

	<u>Range, % by weight</u>		
	<u>Conesville FGD Solids</u>	<u>Fly Ash</u>	<u>Quick Lime</u>
CaO	29 - 35	1 - 3	87 - 95
MgO	1.3 - 1.5	0.5 - 1.0	3 - 6
SiO <sub>2</sub>	10 - 17	33 - 45	1.8 - 2.9
Al <sub>2</sub> O <sub>3</sub>	5 - 10	17 - 22	0.5 - 0.7
Fe <sub>2</sub> O <sub>3</sub>	5 - 10	20 - 34	0.2 - 0.3
Na <sub>2</sub> O	<0.2	0.2 - 0.6	trace
K <sub>2</sub> O	0.2 - 0.8	1.3 - 2.2	trace
SO <sub>3</sub>	26 - 33	1.0 - 2.4	<0.20
LOI	10 - 13	1 - 6	0.4 - 1.5

**Table 2**  
**Leachate Tests of Conesville FSSS and Fly Ash**  
**ASTM Distilled Water Extraction (18 hr., 20:1 water : solid)**

units: mg/l	FSSS Conesville	Fly Ash Conesville	Class III Residual Waste	RCRA Limits	Primary Drinking Water Standards
<b>Parameters - toxic metals:</b>					
As	0.008	0.15	1	5	0.05
Ba	0.22	0.13	30	100	1
Cd	<0.005	0.01	0.2	1	0.01
Cr	<0.002	0.02	1	5	0.05
Pb	<0.002	<0.002	1	5	0.05
Hg	<0.0002	<0.0002	0.04	0.2	0.002
Se	0.007	<0.005	0.2	1	0.01
Ag	<0.005	<0.003	1	5	0.05
<b>Other Trace Elements :</b>					
B	0.36	--	--		
Cu	0.001	0.27	--		
Cl	61	2	7,500		
F	0.8	0	120		
Fe	<0.01	5	9		
Mn	<0.01	0	9		
SO <sub>4</sub>	36	650	7,500		
Na	7.4	10.5	7,500		
TDS	560	940	10,000		
pH	10.5	4.1			
alkalinity	260	<1			
acidity	<1	202			

**Table 3**  
**RCFGD at OSU Feedlot made from Conesville Plant FGD Solids (FSSS)**  
**plus extra Fly Ash and Lime, September, 1993**

	<u>Control Mix (FSSS)</u>	<u>Extra Lime Added at OSU Feedlot</u>	<u>Extra Lime Added at Conesville</u>	<u>Extra Lime, Conesville and OSU</u>
FA:FGD (dry)	1.0 : 1.0	1.6 : 1.0	1.6 : 1.0	1.6 : 1.0
Total Lime Added, %	2	6.5	6.5	11.5
Per Cent Solids	52.6	61.7	63.1	62.8
Wet Density, lbs./cu.ft.	101.5	97.2	99.8	99.1
Dry Density, lbs./cu.ft.	68.8	70.3	72.9	72.2
<b>Unconfined Compressive Strength, psi :</b>				
28 day	45	190	260	220
90 day	100	580	480	310

**Table 4**  
**Roller Compacted FGD Base Course made at Bob Evans Feedlot**  
**and mixed at Gavin AEP - VFL Pug Mill, August, 1995**

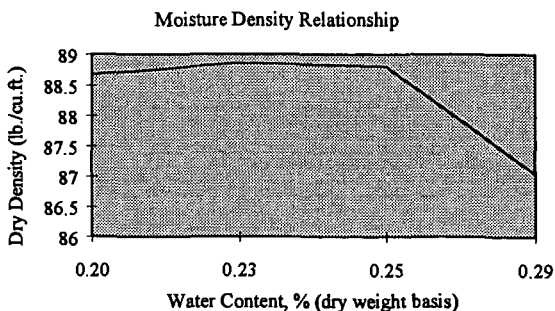
Extra Lime:	Plant Mix	Plant Mix	Lab Mix
	8% Lime Fines	20% Lime Kiln Dust	8% Lime Kiln Dust
<b>Mix Design:</b>			
FA:FGD (1)	1.0:1.0	1.0:1.0	
FSSS (2)	80%	80%	100%
BA (3)	20%	20%	0%
<b>Results:</b>			
Moisture	29%	32%	34%
Wet Density: lbs./cu.ft.	107.2	110.1	103.8
Dry Density: lbs./cu.ft.	83.2	83.6	85.0
<b>Unconfined Compressive Strength: psi</b>			
7 day	90	100	114
14 day	190	220	270
28 day	350	470	400
60 day	520	790	510 (87 day)

Notes: 1) FA = Gavin flyash; FA:FGD ratio is on dry weight basis to make FSSS.  
 2) FSSS is the FA:FGD mixture plus 2% quicklime mixed at Gavin pugmill.  
 3) BA is the bottom ash mixed along with extra lime at VFL pug mill.

**Table 5**  
**Moisture-Density Relationship for Gavin FSSS + 20% Lime Kiln Dust**  
*Proportions adjusted to meet the criteria for the 4 different WC ratios.*

SAMPLE	WC2	WC3	WC4	WC5
WT MOLD + WS (lb.)	13.96	14.06	14.12	14.16
WT MOLD (lb.)	10.42	10.42	10.42	10.42
VOL MOLD (cu. ft.)	0.0333	0.0333	0.0333	0.0333
WET DENSITY (lb./cu.ft.)	106.3	109.3	111	112.3
WT TARE + WS (g)	232.9	234.7	242.2	224.3
WT TARE + DS (g)	197.9	194.8	198.2	178.6
WT TARE (g)	21.9	21.9	21.9	21.9
WT DS (g)	176	172.9	176.3	156.7
WT WATER (g)	35	39.9	44	45.7
WATER CONTENT %	0.20	0.23	0.25	0.29
DRY DENSITY (lb./cu.ft.)	88.67	88.86	88.8	87.05

*(legend: WT = weight, WS = wet solids, DS = dry solids)*



**ACKNOWLEDGMENTS**

The author wishes to thank Professor Wm. Wolfe of The Ohio State University, Department of Civil Engineering, and Mr. Pedro Amanya and Mr. Greg Keenan of the American Electric Power Service Corporation for their advice and information in preparing this paper.

## THE EFFECT OF CARBONATION REACTIONS ON THE LONG TERM STABILITY OF PRODUCTS MADE FROM DRY FGD MATERIALS.

T.L. Robl<sup>1</sup>; U.M. Graham<sup>1</sup>; D.N. Taulbee<sup>1</sup> and W. Giles<sup>2</sup>, 1. University of Kentucky, Center for Applied Energy Research, 3572 Iron Works Pike, Lexington, KY 40511, 2. Freeman United Coal Mining Co., Crown Complex, P.O. Box 259 Farmersville, IL 62533

Keywords: Ettringite, Carbonation, FGD-Material Stability

### ABSTRACT

Flue gas desulfurization (FGD) technologies such as spray dryers and fluidized bed combustors produce a dry by-product which often has substantial quantities of unreacted lime or hydrated lime. The reactivity of the lime with the other constituents upon hydration, imparts a cementitious property. The major early hydration reactions include: the hydration of calcium sulfate to gypsum, the formation of the cementitious mineral ettringite, a calcium sulfo-aluminate-hydrate and the formation of CAS gels. Weathering is found to decrease the strength and integrity of these materials. Field studies, based on soil gas analysis, indicate that these materials rapidly absorb CO<sub>2</sub>. Studies of the mineralogic transformation which take place upon hydration and subsequent weathering indicate that carbonation reactions result in extensive calcium carbonate formation over time. However, carbonate formation takes place at the expense of gypsum, not ettringite as suggested by laboratory studies. Based on field evidence and X-ray data, ettringite appears to be relatively stable.

### INTRODUCTION

Dry lime and limestone based flue gas desulfurization methods, such as fluidized bed combustion and spray dryer technologies, produce a dry product which typically contains free lime in a hydrated or unhydrated form. Free lime along with water, the products of sulfation, typically anhydrite CaSO<sub>4</sub>, or hemi-hydrate (CASO<sub>4</sub>.1/2H<sub>2</sub>O), and the decrystallized aluminosilicate mineral matter from the coal readily react to form a hardened mass. Because of this cementitious characterization many uses for these materials have been proposed such as structural fill in mines, road base stabilization, grouts and, in a pelletized form, artificial aggregates for concrete and asphalt application. The use of this material is dependent in most cases on the material's strength, durability and long term stability.

However, the principal cementitious mineral, ettringite, has long been known to be susceptible to attack and degradation from carbonation. Laboratory experiments have determined that ettringite can be readily broken down with high concentrations of CO<sub>2</sub> under hydrous conditions to more fundamental compounds.<sup>1,2</sup> This results in a loss of strength and material integrity.

### STUDY OBJECTIVES, METHODS AND MATERIALS

The objective of this work is to determine how important carbonation reactions are and their effect on the nature of the materials. Studies are being conducted of CO<sub>2</sub> uptake in field lysimeters filled with materials from the U.S. Department of Energy and U.S. the Environmental Protection Agency sponsored demonstration of the Coolside technology at Ohio Edison's Edgewater Power Plant (Coolside #2).<sup>3</sup> The Coolside demonstration material was placed in three large (3x3x3.5 m deep) field lysimeter cells. These lysimeters were packed at densities within 5% of 1,100 Kg/m<sup>3</sup> (cell L3), 1,040 Kg/m<sup>3</sup>(L2), and 720 Kg/m<sup>3</sup>(L1). The cells were monitored for their mineralogical changes after having been exposed for three seasonal cycles. Drill cores were prepared from the upper 0.5 meters of the three lysimeters and the cored material was analyzed for ettringite formation using X-ray diffraction and scanning electron microscopic analyses. Ettringite was observed to have formed in all lysimeters upon reaction of the FGD waste material with the downward penetrating rain water. In April of 1994 the lysimeters were equipped with gas monitoring wells at 20, 40 and 76 cm of depth (Table I). The wells consist of glass tubes, which are open at one end to a given depth and capped with a septum to allow gas to be withdrawn for analysis. In April of 1995, wells at 107 cm of depth were added.

The impact of weathering on the mineralogy of the materials was conducted on samples collected at the Freeman United Coal Company's Crown III Mine, located in central Illinois. The company has pioneered fluidized bed combustion backhaul and disposal methods at this site which was open in 1991. Circulating fluidized bed combustion (CFBC) fly ash is hauled in semi-trailer dump trucks to the mine. The ash is dumped into a hopper and metered out with screw feeders and mixed with water before being pumped to the disposal site. The solids are settled from the slurry and the water returned to the mixer. The solids settle into a mud-like paste that typically hardens within days. In addition to the fly ash materials, coarser bottom ash representing about 20% of the total material received is also handled at the mine. It is disposed of dry in the landfill area and

then wetted.

#### EARLY HYDRATION AND CEMENTITIOUS REACTIONS

The comparison of the dry fluidized bed combustion materials varies but generally the materials consist of anhydrite ( $\text{CaSO}_4$ ), lime ( $\text{CaO}$ ), quartz ( $\text{SiO}_2$ ), minor calcite ( $\text{CaCO}_3$ ) and glassy silicious ash particles. In spray dryer and duct injection materials the lime and anhydrite may be partially or fully hydrated. The important early hydration reactions consist of the hydration of the lime to portlandite  $\text{Ca}(\text{OH})_2$ , and its partial dissolution to form a highly alkaline solution, or

$$(1) \text{CaO} + \text{H}_2\text{O} \rightarrow \text{Ca}(\text{OH})_2 = \text{Ca}^{2+} + 2\text{OH}^-$$

and the hydration of anhydrite to gypsum ( $\text{CaSO}_4 \cdot 2\text{H}_2\text{O}$ ), or

$$(2) \text{CaSO}_4 \rightarrow \text{Ca}^{2+} + \text{SO}_4^{2-} + 2\text{H}_2\text{O} = \text{CaSO}_4 \cdot 2\text{H}_2\text{O}$$

Anhydrite is an orthorhombic mineral and is much denser ( $2.98 \text{ g/cm}^3$ ) and more soluble ( $K_s = 4.2 \times 10^{-5}$ ) than monoclinic gypsum ( $2.32 \text{ g/cm}^3$  and  $K_s = 2.4 \times 10^{-5}$ ). The anhydrite-gypsum transition probably does not occur in the solid state, but rather through a dissolution-precipitation mechanism. Another very important reaction which takes place rapidly upon hydration is the formation of ettringite ( $\text{Ca}_6\text{Al}_2(\text{SO}_4)_3(\text{OH})_{12} \cdot 26\text{H}_2\text{O}$ ),

$$(3) 6 \text{Ca}^{2+} + 2 \text{Al}(\text{OH})_3 + 3 \text{SO}_4^{2-} + 4 \text{OH}^- + 26 \text{H}_2\text{O} \rightarrow \text{Ca}_6\text{Al}_2(\text{SO}_4)_3(\text{OH})_{12} \cdot 26\text{H}_2\text{O}$$

The formation of ettringite is a competing reaction to that of gypsum. However, it also requires alumina and hydroxide ions and is typically found on, or near, coal ash particles, its source of alumina.

The ideal form of ettringite is  $\text{Ca}_6\text{Al}_2(\text{SO}_4)_3(\text{OH})_{12} \cdot 26\text{H}_2\text{O}$ . Stoichiometric ettringite, however, is an artifact of the laboratory, and in nature it is variable in composition. Another important member of the ettringite family is thaumasite,  $\text{Ca}_3\text{Si}_2(\text{SO}_4)_3(\text{CO}_3)_2(\text{OH})_{12} \cdot 24\text{H}_2\text{O}$  which contains silica in substitution for some of the alumina and carbonate for some of the sulfate. It is now believed by some that thaumasite and ettringite form a solid solution series.<sup>4</sup>

The structure of ettringite is complex. Work by Moore and Taylor determined that ettringite had a trigonal hexagonal unit cell which consists of columns which have the composition  $(\text{Ca}_6[\text{Al}(\text{OH})_6]_2 \cdot 24\text{H}_2\text{O})^{6+}$  which are aligned along the crystallographic c-axis ( $\text{Al}^{3+}$  ions are octahedral coordinated by  $(\text{OH})^-$ ) and are accompanied by channels of the composition  $(\text{SO}_4)_3 \cdot \text{H}_2\text{O})^{6-}$ .<sup>5</sup>

#### CARBONATION REACTIONS

The rapid reaction of carbon dioxide with fresh CFBC material, where ettringite had not yet formed, was measured in our own laboratory experiments and presented previously. We found that the rate of uptake and quantity of gas absorbed was highly dependent upon the degree of hydration.<sup>6</sup> Dry samples of ettringite also do not react significantly with  $\text{CO}_2$ . Hydrated samples of ettringite rapidly reacted with  $\text{CO}_2$  and decomposed to form gypsum, aluminum hydroxide and calcite.

The reactivity of  $\text{CO}_2$  with synthetic ettringite in the laboratory is not directly relatable to complex mineral assemblages under field conditions. As part of our field study of the leaching potential of the materials generated by the Coolside process, we measured the concentration of  $\text{CO}_2$  in both the soil gas and the gas in the Coolside FGD materials. Concentrations of  $\text{CO}_2$ , as high as 3% were measured in the soil gases overlying the Coolside materials but were either near the limits of detection or unmeasurable in the gases within the materials themselves or near the soil-FGD material boundary (Table I). Thus, field observations confirmed the absorption of  $\text{CO}_2$  by the FGD materials found in the laboratory experiments.

#### MINERALOGIC TRANSFORMATIONS

The mineralogic transformations which take place during weathering was studied in samples collected from the Freeman United FDG disposal area. A suite of 19 samples were collected, ranging in age from fresh unhydrated materials to severely weathered samples which were approximately 3 years old.

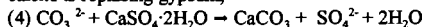
The fresh unhydrated samples were composed of anhydrite, lime and glassy silicious material derived from the coal. Ettringite was found to form rapidly, as it is an important mineral in the 1 day and 1 month old samples and was the dominant mineral phase present in some of the more aluminum rich samples (Figure 1). The total amount of ettringite formed correlated strongly with the amount of alumina in the samples, suggesting that its formation was limited by the availability of this component.

The older samples collected strongly showed the effects of carbonation. They were in general weak and friable compared to the freshly hydrated samples. The amount of calcite present in the older samples was found to be much higher. The hydrated fly ash samples had an average of 6.7% CO<sub>2</sub> versus 16.7% in the fly ash samples older than one year. Thus atmospheric CO<sub>2</sub> is a major reactant in the system.

At very high pHs, i.e. ~12, such as developed by a solution saturated with Ca(OH)<sub>2</sub>, CO<sub>2</sub> is readily absorbed, reacts directly with the hydroxide and disassociates to the carbonate ion, (3) CO<sub>2</sub> + OH<sup>-</sup> = HCO<sub>3</sub><sup>-</sup> = H<sup>+</sup> + CO<sub>3</sub><sup>2-</sup>

The carbonate and calcium ions form calcium carbonate, which is highly insoluble at an elevated pH.

The concentration of sulfate in the samples was found to decrease in older samples by about 25%. This was concomitant with the increase in carbonate, which suggests that, in the longer term, calcite is replacing gypsum,



Gypsum all but disappeared in the older samples. This is not unexpected, as calcite has a lower solubility product than gypsum (pK<sub>s</sub>~ 8.4 for calcite vs pK<sub>s</sub>~4.6 for gypsum at 25 °C), and is much less soluble under alkaline conditions.

In general the field study indicated that ettringite is highly stable in the weathering environment, as the X-ray diffraction results indicated its presence in abundance in all of the older samples (Figure 1). The most severely weathered sample contained no gypsum and did show some attenuation of the ettringite peaks relative to the other samples, and the ettringite in this sample may have undergone some weathering induced decay. However, in general the ettringite in the samples was found to be highly stable relative to other neoformed hydrous minerals such as gypsum and portlandite.

#### SUMMARY

The field studies fully confirmed the laboratory measurements indicating the highly reactive nature of the dry FGD materials with respect to CO<sub>2</sub>. However, direct carbonation of ettringite was not found. The primary carbonation reaction is the replacement of gypsum by calcite and the presumable loss of sulfate from the system. Only when the gypsum was exhausted was evidence found for the carbonation of ettringite. McCarthy et al. found thaumasite forming in weathered AFBC and LIMBs materials which they studied and noted that the samples lost strength when thaumasite appeared.<sup>7</sup> No Thaumasite was detected in any of the weathering products for these materials. The loss of competency and strength in these samples appeared to be a function of the breakdown of matrix minerals other than ettringite, such as gypsum and calcite.

#### ACKNOWLEDGEMENTS

This work was supported in part with funds provided by the United States Department of Energy Through Cooperative Agreement No.DE-FC21-93MC30251.

#### REFERENCES

1. Grounds, T. H.G. Midgley and D.V. Nowell, 1988, Carbonation of Ettringite by Atmospheric Carbon Dioxide. *Thermochimica Acta*, V 135, p. 347-352.
2. Ghorab, H.Y., D. Heinz, U. Ludwig, T. Meskendahl and A. Wolter, 1980, On the Stability of Calcium Aluminate Sulfate Hydrates in Pure Systems and in Cements. *7th International Congress on the Chemistry of Cement*, V IV, Paris, France, p. 497-502.
3. Kanary, D.A., R.M. Statnick, H.Yoon, D.C McCoy, J.A. Withum and G.A. Kudlac, 1990, Coalside Process Demonstration at the Ohio Edison Company Edgewater Plant Unit 4 - Boiler 13. *Proceedings, 1990 SO<sub>2</sub> Control Symposium*, EPRI and U.S. EPA, Ses.7A, V 3, 19p.
4. McCarthy, G.J. and J.K. Solem-Tishmack, 1994, Hydration Mineralogy of Cements Coal Combustion By-Products, Proceedings of an Engineering Foundation Conference, *Advances in Cement and Concrete*, p. 103-121.
5. Moore, A.E. and Taylor, 1968, *Nature*, V 268, p.1085.
6. Taulbee, D., U.M. Graham, R.F. Rathbone and T.L. Robl, 1995, Investigation of the CO<sub>2</sub> Absorption Capacity of Dry FGD Wastes. *Preprints, Division of Fuel Chemistry, ACS*, V 40, p.858-862.
7. McCarthy, G.J. D.G. Grier, J.A. Parks, S.D. Adamek, 1995, Long Term Stability of Disposed Cementitious Coal Combustion By-Products. *Proceedings, 1995 International Ash Utilization Symposium*, University of Kentucky, CAER, Lexington, KY, 6p.

Lysimeter	Material	Depth	N	Avg %CO <sub>2</sub>	Std Dev	Max	Min
L1-Coolside	Soil	20	39	0.531	0.392	1.9	0.05
	Soil	48	38	0.152	0.100	0.4	dl
	Soil/FGD	76	38	0.008	0.033	0.2	dl
	FGD	107	14	0.002	0.005	0.015	dl
L2-Coolside	Soil	20	39	0.486	0.314	1.4	0.05
	Soil	48	39	0.115	0.114	0.83	dl
	Soil/FGD	76	39	0.013	0.031	0.15	dl
L3-Coolside	FGD	107	14	0.001	0.003	0.01	dl
	Soil	20	30	0.693	0.620	2.8	dl
	Soil	48	29	0.992	0.892	3.2	0.02
L4-PCC FA	Soil/FGD	76	31	0.098	0.351	2	dl
	FGD	107	10	0.007	0.007	0.015	dl
	Soil	20	39	0.218	0.221	0.8	dl
	Soil	46	38	0.084	0.068	0.3	dl
L4-PCC FA	Soil/FA	76	39	0.223	0.214	0.84	dl
	Fly Ash	107	14	0.313	0.280	1	0.04

Table I. CO<sub>2</sub> Concentration Measured in Gas Wells Located Above and in Lysimeter Field Cells Filled with Coolside FGD Materials. Control Cell L4 is Filled with Conventional Fly Ash. CO<sub>2</sub> is in Percent Volume. Atmospheric CO<sub>2</sub> Concentration is Approximately 0.036% (360 ppm) at This Site, Detection Limit (dl) is ~0.0150% (150 ppm).

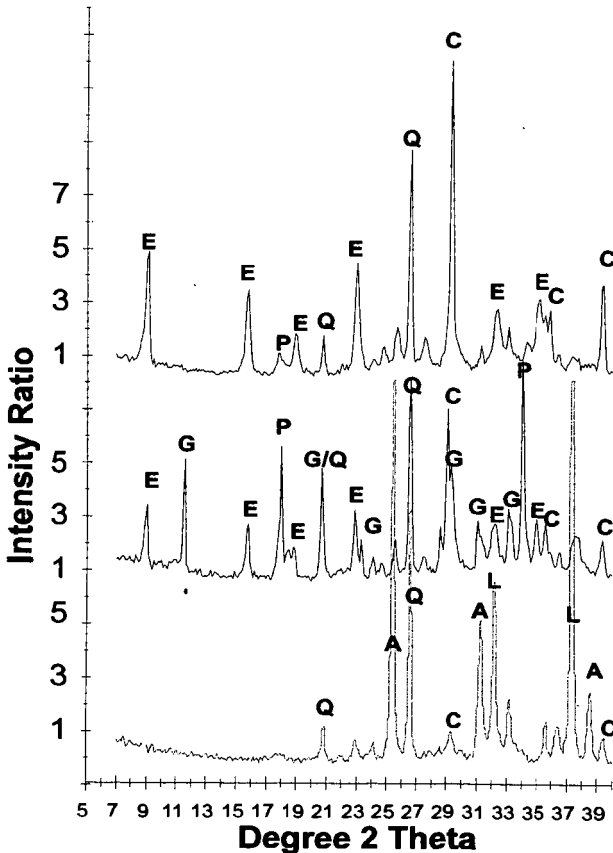


Figure 1. X-ray Diffraction Spectra for As-Received dry FGD Material (Lower, Dotted Trace), Recently Hydrated Material (1 Week Old) and Highly Weathered Material (Upper, Approximately 2.2 years Old). Peaks for Calcite (C), Gypsum (G) Anhydrite (A) Ettringite (E), Portlandite (P), Quartz (Q), Lime (L) are Indicated.

# CHARACTERISTICS OF PNEUMATICALLY-EMPLACED DRY FLUE GAS DESULFURIZATION MATERIALS

S.D. Carter, R.F. Rathbone, U.M. Graham, and T.L. Robl  
Center for Applied Energy Research  
University of Kentucky  
3572 Iron Works Pike, Lexington, KY 40511

K.G. Sutterer  
Department of Civil Engineering  
University of Kentucky  
Lexington, KY 40506

**Keywords:** Dry flue gas desulfurization material, pneumatic emplacement, mineralogy

## ABSTRACT

The University of Kentucky in collaboration with the Department of Energy, Addington, Inc. and Costain Coal is currently developing a commercial concept for the haul back of dry flue gas desulfurization materials (FGDM) into highwall mine adits. The University's Center for Applied Energy Research (CAER) is investigating emplacement systems for a mine demonstration which is planned for the third quarter of 1996. A laboratory-scale transport system has been built at the CAER to evaluate the potential of pneumatic transport for FGDM emplacement. The system is modeled after shotcreting systems in which water is mixed with cement (FGDM) in a nozzle at the end of the pneumatic pipe. Solids travel approximately 70 ft in the lab-scale system at a rate of up to 6 lb FGDM/minute prior to impingement onto a sample collector. Prehydrated FGDM from a circulating fluidized bed combustor has been successfully emplaced onto vertically positioned sample surfaces without excessive dust liberation. The test program is focussed on determining the pneumatic conditions necessary to maximize the strength of the emplaced FGDM under anticipated mine curing conditions while minimizing dust formation. The mineralogy and strength of a pneumatically created sample are described following curing for 60 days.

## INTRODUCTION

An important potential advantage of the FGDM haul-back concept for a highwall mining company is that 100% coal recovery is possible. Current highwall techniques must leave behind a structural web of coal, recovering approximately 65 to 75% of the resource. By leaving coal webs equivalent to the width of the mining head, it is possible with the haul-back scheme to fill the empty adits with FGDM and then mine the remaining coal web by using the hardened FGDM for structural support. This concept requires that the emplaced FGDM be sufficiently strong to provide support during the second phase of coal mining. The overall strength of the emplaced FGDM depends not only on its physical properties but also on the efficiency of emplacement. A relatively strong material is useless in this application if only, say, 75% of the adit is filled. Therefore, an essential characteristic of the emplacement technology for this haul-back concept is high fill efficiency. Another essential feature is that the material must be emplaced remotely because no worker should ever be required to enter a highwall mine with an unbolted roof. It is almost certain that roof bolting, accompanied by some amount of manual emplacement, would not be economically feasible.

A pneumatically-based system was chosen for initial consideration in this project because of the potential of shotcrete technology to completely fill the mine adit without forms. Hydraulic backfill of highwall adits is difficult because the adits are normally horizontal and slump prevents fill to the ceiling. With pneumatically-based (shotcrete) technology, however, concrete can be applied to vertical and even overhead surfaces, making it ideal for underground tunnel support. A prime example is its use in portions of the Metro subway system in Washington, D.C. For underground mining environments, Krantz found that shotcreting was successful in sealing, preventing spalling, and providing roof stability.<sup>1</sup> The ability to remotely line tunnels and shafts using shotcrete technology has also been demonstrated.<sup>2,3</sup> A disadvantage of shotcrete technology is that its production rates are relatively low compared to hydraulic concrete emplacement methods. Shotcreting has been primarily used for lining applications and not for bulk filling. However, it has been reported that a hybrid shotcreting system, the "Blastmixer," is capable of placing 50 tons of concrete per hour using large volumes of low-pressure air.<sup>4</sup>

## EXPERIMENTAL

**System Description.** The source of pneumatic air for the emplacement test unit (ETU), Figure 1, is a vortex blower with a capacity of 220 ft<sup>3</sup>/min @ 0 psig and 50 ft<sup>3</sup>/min @ 7.9 psig. Therefore, the system is limited to low pressure operation. A pitot tube is used to measure the air flowrate at the inlet of the blower. A metered stream of water can be added at the

inlet of the blower to create a mist of water, if desired. The air flowrate is controlled by a gate valve downstream of the blower. The tstream of the blower. The temperature and pressure are measured at the outlet of the blower to provide a secondary measure of the air flowrate from performance curves provided by the blower manufacturer. Pressure is measured just downstream of the controlling gate valve to monitor the system for blockages.

Solids are injected into the two-inch schedule-40 steel pipe by a rotary valve. The valve can deliver FGDM at a rate of up to 6 lb/minute. A sealable hopper with a volume of 0.86 ft<sup>3</sup> supplies solids to the valve. Purge air is injected into the bin at three points to fluidize the solids and facilitate the feeding of the solids through the valve. An electric vibrator is mounted on the bin to alleviate problems with solids flow in the hopper. Addition of solids to the hopper during operation is not possible with the system in this configuration.

Solids are pneumatically transferred over a distance of 70 ft within 2-inch schedule-40 steel pipe which is covered by 0.5 inches of foam insulation. The pipe is insulated so that the extent of hydration reactions involving free lime (CaO) may be estimated when water is present during pneumatic conveyance. Thermocouples are located at 20-ft intervals to monitor any increase in temperature caused by hydration reactions. The pressure drop across the straight run of pipe is measured to monitor the air and solid flowrates.

The flexible metal hose connecting the last pipe section to the main run of pipe serves to permit the manual positioning of the nozzle. The nozzle must be maneuvered so that the FGDM shotcrete is evenly distributed over the sample panel. A thermocouple is placed through the bottom of the sample panel at its mid point so that it minimally intrudes in the path of the shotcrete jet. The nozzle is constructed of 1.5-inch schedule-40 PVC pipe and fittings (1.61-inch inside diameter). Water is injected radially inward through a ring of 24 holes (each 0.0145 inches in diameter) in the pipe.

**Testing Objectives.** The basic goal of the experimental plan is to evaluate the performance of FGDM as a function of shotcreting parameters so that the requirements for the mine demonstration technology can be specified. Once the important shotcreting parameters are determined for the FGDM, a robotic vehicle based on state-of-the-art mining technology can be fitted with a shotcrete nozzle for remote emplacement. While any new material to be considered for shotcrete emplacement must be experimentally evaluated, the high free lime (CaO) content of many types of FGDM makes testing doubly important. Substantial amounts of heat are generated during the hydration of CaO to form Ca(OH)<sub>2</sub>, promoting concerns about ignition of the coal seam and about possible steam explosions during emplacement. In addition, hydration of FGDM containing free lime in excess water has been shown to decrease the strength of sample pellets.<sup>5</sup> By prehydrating the FGD material with only enough water to hydrate the CaO, the strength of sample pellets following subsequent hydration was increased. The experimental plan addresses several scenarios regarding CaO hydration sequences, including the addition of water mist to the pneumatic transport pipe. The potential advantages of pre-wetting the FGDM during pneumatic transport are that the solids can be cooled by external heat exchange prior to emplacement and that the nozzle performance will be improved (i.e. less dust liberation). For this paper, the FGDM was prehydrated prior to pneumatic transport. While a fundamental goal of this effort is to optimize the workability of the material during emplacement, another important objective is to characterize the establishment of strength as a function of time. This paper examines the chemical and physical characteristics of a shotcrete sample produced from prehydrated FGDM after curing for 60 days.

**X-Ray Diffraction Analyses.** X-ray diffraction (XRD) analyses were performed on the prehydrated feedstock and on three samples of the cured FGDM slab 60 days after emplacement. Cu K $\alpha$  radiation from 7° to 40° (63° for the feedstock) 2 $\theta$  at 0.1° increments was utilized. Crystalline phases were identified using the JCPDS file on CD-rom. Samples were ground with a mortar and pestle prior to analysis.

**Material Studied.** Fly ash from the Archer Daniel Midland (ADM) co-generation plant in Decatur, IL was used in this study. The plant utilizes circulating fluidized bed combustion (CFBC). Freeman United Mining Co. disposes of the FGDM at its Crown III facility in Farmersville, IL. The sample was collected in air-tight plastic drums upon arrival at the Freeman United facility. The FGDM was prehydrated at a weight ratio of 1 part water to 10 parts FGDM. This ratio was determined from previous work to slake the free lime without initiating cementitious reactions. The following minerals comprised the majority of the crystalline phases of the prehydrated FGDM as determined by XRD: anhydrite (CaSO<sub>4</sub>), portlandite (Ca(OH)<sub>2</sub>), quartz (SiO<sub>2</sub>), hematite (Fe<sub>2</sub>O<sub>3</sub>), magnetite (Fe<sub>3</sub>O<sub>4</sub>), calcite (CaCO<sub>3</sub>), periclase (MgO), and lime. In addition to these major minerals, ettringite (Ca<sub>6</sub>Al<sub>2</sub>(SO<sub>4</sub>)<sub>3</sub>(OH)<sub>12</sub>·26H<sub>2</sub>O) and gypsum (CaSO<sub>4</sub>·2H<sub>2</sub>O) were identified in minor amounts.

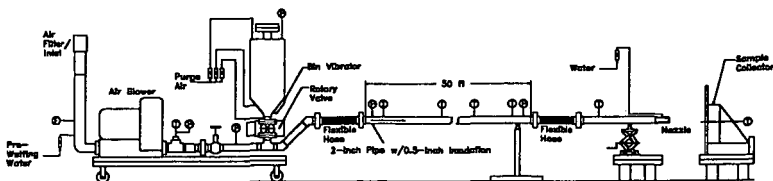


Figure 1. Schematic diagram of the pneumatic laboratory-scale emplacement test unit (ETU).

From this analysis it was determined that the free lime was almost completely converted and that cementitious reactions had not occurred to a significant degree. Therefore, it was confirmed that an optimal quantity of prehydrating water had been utilized.

## RESULTS AND DISCUSSION

**Nozzle Optimization.** Shotcreting involves the creation of a turbulent jet of air that contains a mixture of solids and water mist. Ideally, the jet impinges on a surface, and particle-free air exits parallel to the surface, leaving the water and solids behind. In reality, however, a significant amount of water and solid particles remain airborne. A study was performed to determine the amount of mist loss as a function of air velocity and distance of the nozzle to the collection surface. While these water-only experiments may not be truly representative of the solid-water mix that remains airborne, it should at least indicate the trends that can be expected for these parameters. During these experiments, water at a rate of 15 gal/hr was injected into the nozzle. The air/water jet then impinged onto a flat plywood surface mounted vertically so that all the water that adhered to the surface would drain into a container and could be measured. The best results, approximately 80% retention efficiency, were obtained for the higher air velocity runs (362 ft/sec) at a distance of 4 ft between the collector and the nozzle. These conditions were used for the production of the shotcrete sample studied in this paper.

**Production of FGDM Shotcrete Samples.** For each test, a full hopper (0.86 ft<sup>3</sup>) of dry FGDM is used. Complete mass balances are impossible to achieve because the system is not closed, permitting the escape of dust and mist. However, as discussed previously, it is estimated that 80% of the particles and droplets in the air jet are retained on the sample collector under the conditions of this study. Several slabs of FGDM shotcrete, approximately 3 inches in thickness and 1 foot in diameter, have been successfully prepared to-date. The pneumatically emplaced FGDM adhered to the vertically positioned plywood without slumping. The FGDM/water mixture exhibited stiffness immediately upon deposition suggesting a consistency that, in larger volumes, would be advantageous for bulk fill applications without the need for forms. For the FGDM shotcrete sample that is the focus of this paper, a water/FGDM ratio of 0.45 was utilized. This ratio was chosen because it was shown during previous tests to provide the best emplacement results. A relatively high water addition rate is beneficial because it reduces dust formation and it gives the material good workability for even deposition. Excessive water is squeezed out of the sample because of the force of the impingement. Therefore, the moisture content of the sample immediately after emplacement was likely lower than the 0.45 water/FGDM ratio that was produced in the nozzle. Moreover, the water content of freshly deposited shotcrete is not a highly variable parameter because the water content tends to be self regulating for the range of water addition rates that produce good shotcrete consistency.

Immediately after formation, the sample slab was covered with damp cloth and then with plastic to prevent moisture evaporation without providing excessive water. For strength tests, 2-inch-long 1.4-inch-diameter cores were produced using a carbide-steel-tipped hole saw. The cores were then kept moist prior to testing.

**Strength Development During Curing.** Unconfined compression tests were performed on core samples at 20 and 50 days following emplacement. The 20 day strength was 200 psi, and the

apparent density of the core sample was determined to be 1.47 g/cm<sup>3</sup>. The strength at 50 days was determined to be greater than 650 psi. A more precise measure of the compressive strength at 50 days was not obtained because the testing apparatus was not set up for stresses greater than 1000 lb to be placed on the sample. An uncompressive strength of at least 500 psi will be necessary for the emplaced FGDM to prevent subsidence when the structural web of coal is removed during the second phase of mining. Previous work has shown that compressive strengths greater than 1000 psi are possible with these materials when the samples are formed and cured within a rigid container.<sup>3</sup> The present study has now confirmed that pneumatically emplaced FGDM will be able to develop sufficient strength for this backhaul concept.

**Mineralogy of Cured FGD Shotcrete.** A highwall coal mine adit can contain essentially no water, or it can be completely filled with water. Therefore, the amount of excess water that is available to the emplaced FGDM during curing can be quite variable. Curing of the slab of shotcrete was performed under conditions most closely related to a dry mine environment. This sample will be subsequently referred to as 'dry-cured' for simplicity, even though it was stored with some moisture present. A subsample of the main slab was removed after 7 days and completely immersed in water to simulate a water-saturated mine. Samples of the dry-cured and the water-immersed shotcrete were analyzed by XRD 60 days after pneumatic emplacement. To observe the change in mineral forms as a result of the hydration of the feedstock and the different curing environments, selected mineral peaks were standardized to the quartz {101} peak (Figure 2). By doing so, it is assumed that quartz remained unaffected by the curing condition and that quartz was not selectively eliminated or concentrated in the shotcrete during emplacement.

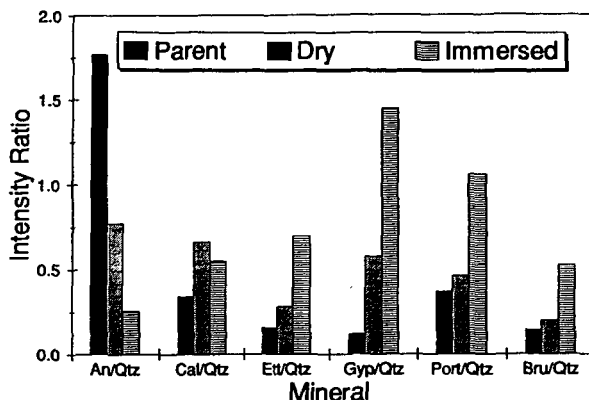


Figure 2. Comparison of major XRD peak intensities, normalized by quartz {101}, for the feedstock, dry-cured shotcrete, and water-immersed shotcrete samples.

The decreased abundance of anhydrite and corresponding increase in gypsum for the dry-cured sample compared to the feedstock (Figure 2) illustrates a major hydration reaction for this material. Other hydration reactions include the additional formation of ettringite, portlandite, and brucite (Mg(OH)<sub>2</sub>). The formation of ettringite and gypsum are responsible for the strength that was shown to develop for the dry-cured slab. The amount of calcite was highest for the dry-cured sample because of contact with atmospheric CO<sub>2</sub>. Continued hydration reactions were observed for immersed sample as illustrated by increased quantities of ettringite, gypsum, portlandite, and brucite. While the formation of additional ettringite can promote extra strength, the continued formation of gypsum from anhydrite by reaction with water that is diffusing back into the solid can reduce strength. Ettringite needles tend to fill pores which increase the density and strength of the FGDM cement. Gypsum also fills pores, but it can swell sufficiently to create cracks and decrease the strength of the solid. While no strength tests were performed for the immersed sample, it was obvious during sample preparation for XRD that the strength of the sample was diminished compared to the dry-cured sample. The formation of additional gypsum in the immersed sample may have been responsible for its reduced strength.

#### SUMMARY

Prehydrated FGDM from a CFBC was successfully emplaced onto a vertical surface by shotcrete technology. The strength developed by the dry-cured sample after 50 days was determined to be greater than 650 psi which is sufficient to support the mine roof during

mining of the structural web of coal. The levels of ettringite and gypsum in the dry-cured sample were consistent with the strength which had developed. It appears that some decrease in strength can be expected for these materials if subjected to excess water during curing in an unconfined environment.

#### ACKNOWLEDGMENTS

This work was supported by the U.S. Department of Energy under Cooperative Agreement No.: DE-FC21-93MC30251 (such support does not constitute an endorsement by the USDOE of the views expressed in this article). The authors would like to thank E. Coffey, M. Yewell and D. Taulbee of the CAER for assistance with this work. Also, W. Giles of Freeman United is acknowledged for providing FGDM to the project.

#### REFERENCES

1. Krantz, Gary W., *Information Circular 8994*, 1984, US Bureau of Mines.
2. Goff, James S., *Use of Shotcrete for Underground Structural Support*, Engineering Foundation Conference, 1974, ACI Pub. SP-45, pp. 405-417.
3. Monaghan, David A., Hoadley, David J. and Anderson, Grant L., *Shotcrete for Ground Support*, Engineering Foundation Conference, 1977, ACI Pub. SP-54, pp. 225-240
4. Ryan, T.F., *Gunite: A Handbook for Engineers*, 1973, Cement and Concrete Association, London, p. 26
5. Graham, U.M., Rathbone, R.F., Sutterer, K.G., and Robl, T.L., *1995 International Ash Utilization Symposium*, University of Kentucky, Center for Applied Energy Research, Oct. 23-25, Lexington.

## STABILIZATION OF METAL-LADEN HAZARDOUS WASTES USING LIME-CONTAINING ASH FROM TWO FBC's AND A SPRAY-DRIER

J. Cobb, R. D. Neufeld, J. Pritts and V. Clifford  
School of Engineering, University of Pittsburgh, Pittsburgh, PA 15261  
C. Bender, Mill Service Co.; J. Beeghly, Dravo Lime Company., Pittsburgh, PA

**Keywords:** clean coal technology by-product reclamation, hazardous waste management, chemical stabilization

### ABSTRACT

Clean coal technology by-products, collected from commercial operations under steady state conditions, are reacted at bench-scale with metal-laden hazardous wastes. Reaction conditions involve mixing calibrated weight ratios of by-product to hazardous waste with attention to minimizing added moisture. Of the 15 heavy metals monitored, lead appeared to be the element of greatest concern both from a leaching and a regulatory point of view. While leaching information is focused on lead stabilization, similar information exists for other metals as well. Stabilized solid products of reactions are sampled for TCLP evaluations. For samples showing evidence of metal stabilization, further experimentation was conducted evaluating optimum moisture content and development of physical strength (measured as compressive strength) over time of curing. Results show that certain hazardous wastes are highly amenable to chemical stabilization, while others are not; certain by-products provided superior stabilization, but did not allow for strength generation over time.

### INTRODUCTION

The general objective this two-year project (*which has just completed the first year*) is to provide useful information and data on the ability of new and emerging sources of chemical treatment substances, in this case by-products from advanced clean coal technologies, to be used by the hazardous waste management community. These studies fall into two categories: (i) characterization of selected critical properties of by-products and (ii) observation of their ability to stabilize and solidify characteristic metal-laden solid hazardous wastes. A more commercial objective of the project is to link the producers of by-product with operators of hazardous waste treatment facilities in a mutually profitable manner. From the treatment facility operators' point of view, new sources of treatment material with abilities to stabilize and solidify their feed wastes can be added to their material source list. From the producers' point of view, new uses for by-products of their advanced coal combustors and desulfurizers will be developed and demonstrated. These producers have implemented various emission control technologies at coal-fired (and coal waste fired) electric power plants and are studying a number of others. The technologies currently in use generate significant amounts of by-products with limited commercial value. Consequently, much of the by-products are disposed as solid wastes. In particular, companies employing wet scrubber technologies for the desulfurization of flue gases have found few alternatives to disposal for the sludges generated in the processes due to the excess moisture present in the by-product. On the other hand, the contemporary development of dry desulfurization technologies offers great promise that these process by-products may have beneficial commercial application, such as those studied as part of this project.

**Background:** The project focuses on characteristic metal-laden hazardous waste. Federal regulations and many state regulations require generators of solid wastes to determine if the wastes they produce are hazardous. The determination process requires the generators to analyze leachates produced when the wastes are mixed with an extraction fluid and compare the results of that analysis to a published list that defines which parameters are of concern and the extract concentrations at which a waste containing those parameters is considered hazardous. Wastes that contain extract constituents on the list at concentrations that equal or exceed the published concentrations are considered to be characteristically hazardous (unless they are specifically excluded) and said to exhibit the "toxicity characteristic". Among the parameters included on the toxicity characteristic list published in the Federal regulations<sup>1</sup> are eight metals; the

<sup>1</sup> See 40 CFR 261.24.

concentrations at which a waste extract containing them is considered hazardous, are:

<u>Metal Parameter</u>	<u>Hazardous Concentration in Leachate (mg/l)</u>
Arsenic (As)	5.0
Barium (Ba)	100.0
Cadmium (Cd)	1.0
Chromium (Cr)	5.0
Lead (Pb)	5.0
Mercury (Hg)	0.2
Selenium (Se)	1.0
Silver (Ag)	5.0

Once a waste is determined to be hazardous, generators are restricted from directly disposing that waste anywhere in the United States. Prior to disposal, the waste must be treated to an extent that renders the resulting waste non-hazardous. The purpose of the treatment prior to disposal is to reduce the likelihood of migration of hazardous waste constituents from the waste. Wastes that are treated to meet the established standards can be disposed.

For purposes of this first-year research, toxic metal-laden wastes were treated at bench-scale by stabilization and solidification methods. Stabilization/solidification is a treatment technology used to reduce the hazard potential of a waste by converting the contaminants into their least soluble, mobile, or toxic form. Solidification refers to techniques that encapsulate the waste in a monolithic solid of high structural integrity. Solidification does not necessarily involve a chemical interaction between the wastes and the solidifying reagents but may mechanically bind the waste into the monolith. Similarly, stabilization does not necessarily involve solidification, since precipitation and complexation are also mechanisms of stabilization.

#### BY-PRODUCTS

The Clean Coal Technology (CCT) Program is a cooperative effort to demonstrate a new generation of innovative coal processes, which are environmentally cleaner and more efficient than conventional coal-burning processes [US DOE, 1991]. In dry CCT systems, a calcium-based sorbent (usually slaked lime, limestone, or dolomite) is injected directly into a furnace, ductwork, precipitator, or scrubber vessel that produces powdered or granular by-products, as opposed to the slurries associated with traditional wet scrubber systems. All these processes produce a by-product which is removed in the particulate control equipment. Dry by-products from lime or limestone injected into the furnace, such as in FBC systems, have neutralizing, sorptive, and cementitious properties that make them interesting as potential reagents for hazardous waste stabilization because of their high free quicklime (CaO) and anhydrous calcium sulfate (CaSO<sub>4</sub>) contents. The specific composition of a particular type of by-product may vary widely depending upon the CCT process employed, the coal and sorbent composition, and the plant operating conditions. Since the chemical, physical, and engineering properties of dry CCT by-products are directly related to their history of use within the system and specific mineralogy, it is essential to accurately determine the mineralogical composition of these wastes and process configurations if safe and economical uses are to be defined.

Four clean-coal technology by-products were originally identified, but only the first three were used in this research.

1- Dry Scrubber Residue, supplied by CONSOL Inc. This material is from a spray drier at the outlet of a pulverized coal boiler burning high-sulfur eastern coal. Within the process, ash laden flue gas enters the bottom of the spray drier and all of the sulfur-capture residue rises through the upper port with the fly ash. The residue contains 45% fly ash, 36% CaSO<sub>4</sub>/CaSO<sub>4</sub>, 10% Ca(OH)<sub>2</sub>, 2% CaCO<sub>3</sub>, and 7% other inert material with moisture content of 2% or less.

2- Residue from a Coal-Fired Pressurized Fluid Bed Combustor (PFBC) at the Tidd Station of Ohio Power Company. This demonstration facility was constructed and is operated in cooperation with the U.S. Department of Energy in Round I of the Clean Coal Technology Program. The sorbent fed to the plant, rather than lime or limestone, is dolomite. Dolomite is used at the Tidd Station because it is both more porous (and thus more reactive) and easier to handle without bridging in the piping system. By operating

at high pressure, little of the dolomite in the residue is in the oxide form - most is present as carbonate. The dolomitic character of the sorbent yields a residue that is lower in pH than that produced from lime-based sorbents. This characteristic is particularly advantageous in stabilizing arsenic-laden waste solids. As this by-product contains magnesium, it will buffer the stronger lime alkalinity. The chemical composition of the residue is 50-60% equivalent  $\text{CaCO}_3$  and 1-2% available (free or uncombined)  $\text{CaO}$ .

3- Residue from a Coal-Waste-Fired CFBC operated by the Ebensburg Power Company. Approximately 200,000 tons/year of this material is trucked back to the mines from which the coal wastes are derived. Some or all of this by-product could be diverted to nearby sites for beneficial use if they could be identified. The coal waste fed to the boiler has a sulfur content between 1.4 and 2.0 percent. The limestone is 83%  $\text{CaCO}_3$ . It is sized at 12 mesh x 0 and contains between 5 and 10 percent through 140 mesh. The fly ash is removed in a ten-segment baghouse and conveyed to a silo. Approximately 70% of the by-product in the silo is baghouse ash; 30% is bottom ash. Thus, the by-product is a relatively coarse material containing 82% ash, 12.5% limestone equivalent and 5.5%  $\text{CaSO}_3/\text{CaSO}_4$ .

4- Residue from a Coal-Fired Circulating Fluid Bed Combustor (CFBC), supplied by Anker Energy Corporation. This material is produced by the cogeneration project of Applied Energy Service at its Thames River Plant near Uncasville, Connecticut. Anker Energy Corporation supplies the coal used in the plant and through early 1995 had to backhaul the residue to its mines in West Virginia. It was anticipated that some or all of the approximately 100,000 tons/year of this by-product could be easily diverted to hazardous waste treatment plants along the general rail route from Connecticut to West Virginia. The AES Thames River Plant is base-loaded, operating at 95-96 percent of capacity constantly, thus the ash from it is very uniform. The residue is a relatively coarse material, as it contains both bottom and fly ash from the boiler, and contains 45% limestone equivalent, 28% ash and 27%  $\text{CaSO}_3/\text{CaSO}_4$ . Dravo Lime Company provided assistance in obtaining and transporting multiple representative samples from each clean coal technology site in accordance with ASTM-C-311. Samples were split for analysis and use at the University of Pittsburgh and the Dravo Lime Company.

#### HAZARDOUS WASTES

Six different hazardous wastes have been selected for examination by Mill Service, Inc., a regional centralized hazardous waste treater, from among the materials processed commercially at their facility. The table below outlines significant properties of each hazardous waste: note that lead is the contaminant of primary concern since it is the TCLP lead levels that exceed appropriate limits.

HAZARDOUS WASTES STABILIZED

Hazardous Waste Source	Hazardous Constituents of Concern	Total Concentration (mg/kg solids)	TCLP Concentration (mg/l)	TCLP Regulatory Limit (mg/l)
Sludge from Lead-Acid Storage Battery Production	Lead	3,000	20	5.0
	Cadmium	3	0.19	1.0
	Chromium	12	—	5.0
Contaminated Soil from a Munitions Depot	Lead	1,200	26	5.0
	Cadmium	4.8	—	1.0
	Chromium	59	—	5.0
	Copper	210	1.8	—
	Zinc	580	8.2	—
Contaminated Soil from a Multi-Use Industrial Site	Lead	5,000	80	5.0
	Cadmium	5.4	—	1.0
	Chromium	22	—	5.0
	Copper	260	—	—
	Zinc	660	17	—

Baghouse Dust from Basic Oxygen Furnace (BOF) Steelmaking	Lead	1,400	14	5.0
	Cadmium	55	—	1.0
	Chromium	260	—	5.0
	Copper	57	—	—
	Nickel	130	—	—
	Vanadium	76	—	—
Ash from a Municipal Solid Waste Incinerator	Zinc	41,000	4.4	—
	Lead	5,700	20	5.0
	Barium	550	—	100
	Cadmium	630	—	1.0
	Chromium	130	—	5.0
	Copper	1,300	—	—
Contaminated Soil from a Former Waste Water Treatment Plant	Zinc	23,000	2.1	—
	Lead	750	7.8	5.0

## RESULTS & CONCLUSIONS

Bench-scale stabilization experiments consisted of mixing by-products with hazardous wastes at weight ratios ranging from 0 to 1:2 with minimal moisture addition. Sampling of the stabilized mass was done immediately after treatment for evaluation of TCLP leachate compositions. As may be expected, some combinations of by-product/wastes exhibited stabilization more consistently than others. Figures 1 and 2 provide contrasting resultant information for two representative sets of stabilization experiments: figure 1 shows information illustrating lead stabilization while figure 2 shows failure to stabilize lead.

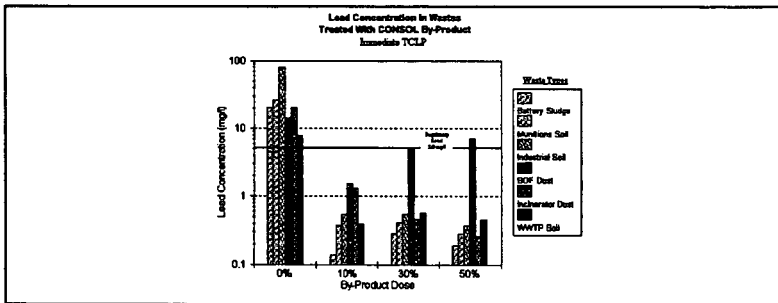


Figure 1  
Successful Lead Stabilization

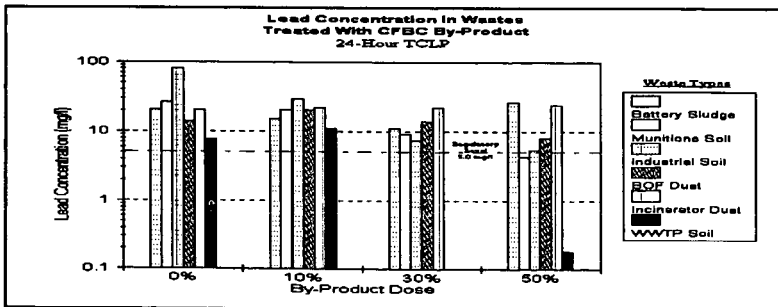


Figure 2  
Unsuccessful Lead Stabilization

**Solidification/Strength Development:** In addition to chemical stabilization, aliquots of hazardous waste and by-products were evaluated for development of strength over time when prepared at optimal moisture contents. Optimal moisture values were determined to be that at which the "stiffened" mass would produce a "slump" in the neighborhood of 1 inch to 2 inches when tested in accordance with standard concrete testing procedures. Figure 3, a representative plot of compressive strength development over time, indicates that for some samples, strength development is considerable while little strength development is achieved for others.

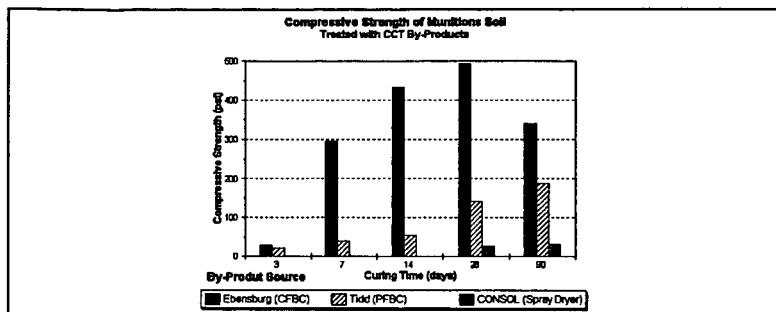


Figure 3  
Strength Development over Time

#### SUMMARY

- Clean Coal Technology by-products may be used for heavy metal stabilization of a number of hazardous waste sources, however laboratory evaluations must be conducted to assure final product quality.
- Pozzolanic properties of clean coal technology by-products are useful in making a hardened product for reuse or disposal.
- By-products producing a highly stabilized materials do not often produce the strongest product. Thus, evaluation of final product use and/or disposal options must be made on a case-by-case basis.
- Commercial-scale stabilization testing will be undertaken during the second year of this project in conjunction with developing an understanding of underlying principles governing the behavior of these new treatment chemicals.

#### REFERENCES:

"Clean Coal Technology - The New Coal Era", Washington, DC: U.S. Department of Energy, Assistant Secretary for Fossil Energy, January, 1991.

#### ACKNOWLEDGMENT:

*This paper was prepared with the support of the U.S. Department of Energy, under Cooperative Agreement No. DE-FC21-94MC3117. However, any opinions, finding, conclusions, or recommendations expressed herein are those of the authors and do not necessarily reflect the views of the DOE.*

## THE USE OF FLUIDIZED BED COMBUSTER ASH IN THE SOLIDIFICATION OF HIGH OIL AND GREASE SEDIMENTS

R. Gregory Bennett and Ernest F. Stine Jr., Ph.D  
IT Corporation, 312 Directors Drive, Knoxville, TN 37923

Keywords: Fluidized bed combustor ash; High oil and grease sediment; Treatability study

### INTRODUCTION and BACKGROUND

It has been common practice at petroleum refineries to dispose of oil sludges (containing oil, grease solids and water) in onsite pits. Remediation of these pits has typically involved in-situ solidification of the sludges using mixtures of Portland cement and fly ash. While this leaves the oily material in place, the resulting form is less permeable than the resulting sludge and has significant strength to support a cap. The supported cap reduces the infiltration rate of water to contact the solidified sludges. Due to the cumulative impact of the solidification and capping process the mobility of these materials is therefore reduced.

Since 1991 an oil refinery has been investigating the closure of several large storm water impoundment ponds. These ponds contain sediments that are high in oil and grease and mostly low in solids. Oil and grease content ranges from 1.5 to 20% by EPA Method 9071<sup>1</sup>. Consistencies and liquid content of the sediments vary from a very wet free flowing emulsion to a congealed sludge with about 70% solids. The primary concern of closure was to solidify the residues while still maintaining the low leachability and mobility of both metals and volatile organic hydrocarbons (VOCs).

During the project evaluation phase, a consulting engineering firm conducted a treatability study that evaluated Portland cement, cement kiln dust, Class C fly ash and pulverized quicklime for solidification of various pond sediment samples. The goal of this study was to develop formulations that would reduce the leachability of metals and VOCs below regulatory limits and obtain unconfined compressive strengths greater than 0.98 kilograms/sq.cm (Kg/sq.cm). The study's recommendations ranged from formulations with 20% Portland cement and 10% fly ash blend to formulations using 30 to 35% Portland cement. At these recommended cement loadings, the cost of the remediation was unacceptably very high. IT-Davy, a joint venture between IT Corporation and Davy Environmental, was hired to provide final engineering design and investigate lower cost solidification formulations. IT-Davy successfully demonstrated the use of by-product blends through field studies, a laboratory bench-scale confirmation study and a full-scale pilot demonstration.

#### Preliminary Field Screening Studies

Two stages of testing were performed in the field as a screening of reagents for later laboratory work. The first stage consisted of testing single reagents and blended reagents for strength development, rate of hardening, heat generation, and water absorption after hydration. Experiments consisted of testing 12 single reagents and 30 blends of these reagents. Reagents included four Class C fly ashes, five fluidized bed combustor ashes, two cement kiln dusts and Type I Portland cement.

The second screening stage consisted of mixing different single reagents and reagent blends that harden on hydration with a sediment sample (composited from several lagoons on the site) to achieve the highest strength. Seven of the more promising single reagents from the first stage that had good water adsorption, possible strength formation and low heats of reaction were mixed with a composite sediment sample in various dosages and measured for strength using development. Strength was measured by penetration resistance using a pocket penetrometer at seven days of cure. Various blended combinations of these reagents were then compared for strength using penetration resistance as measured by pocket penetrometer at seven days. These blends included cement/fly ash, cement kiln dust/fly ash, cement/fluidized bed combustor ash and mixtures of other by-products. Ratios of blend components were changed in increments of 20% to find the optimum mixture of reagents for the blend. The dosage of reagent blends was compared for formulations that met  $> 1.0$  Kg/sq.cm penetration resistance. Additional field screening was performed to optimize the reagent dosages of cement only and fly ash/fluidized bed combustor ash (FA/FBCA) blends.

Results showed that strengths could be achieved using cement or blends of fly ash and fluidized bed combustor ash at high dosages. Further testing was done on individual samples from each of the six lagoons on site (A, B, C, D, E, F). The percent solids and oil and grease content of these lagoons are found in Table 1. To increase the strength and lower the dosages, an absorptive soil was added to formulations with cement and FA/FBCA blend. The soil absorbed free water and thickened low solid sediments. With the addition of the soil, the strength criterion was increased to  $> 3.0$  Kg/sq. cm at seven days of cure increasing the oil retention of the formulations.

#### Bench-Scale Confirmation Testing

Four of the six lagoons were sampled and sediments were sent to IT's Environmental Technology Development Center in Oak Ridge, Tennessee for bench-scale testing. Sediment samples were designated A, B, C, D to identify the lagoon that they were taken. Using the results from the field screening, the

potential formulations shown in Table 2 were chosen for a bench-scale verification test. Two or three formulations were selected for each of four lagoon sample locations, labeled A, B, C, and D. Each location had varying amounts of solids, moisture, and oil and grease content. Percent solids and oil and grease are shown for all six lagoons in Table 1. In most of the mixes, adsorptive soil was added to increase the solids content of the sediments. At all of the sample locations, formulations were tested using cement (as a control reagent for comparison) and the FA/FBCA blend. For samples A and B the formulations from the previous treatability study that used cement only or cement/fly ash blend without soil were made for comparison. Formulations were tested for the following:

- Unconfined compressive strength (UCS) at 3, 7, 28, 90 days measured by ASTM D2166-91<sup>2</sup>
- Permeability at seven days measured by ASTM D5084<sup>3</sup>
- Oil retention at seven days measured by liquid loss at 42 psi of compression for five minutes
- Sample cohesiveness in water after 14 days
- Volume increases
- Compliance with Toxicity Characteristic (TC) regulatory limits by analyzing the material using the Toxicity Characteristic Leachate Procedure (TCLP)<sup>4</sup>

#### Full-scale Demonstration

Successful FA/FBCA blend mix formulations were used in a full-scale in-situ pilot demonstration. A large area of a sediment pond was diked for this demonstration. Free standing water and oil were removed before the addition of fill soil and reagent. Various mixing and reagent addition techniques were explored. The optimized laboratory formulations were tested against various reduced reagent formulations to confirm dosage rates. Samples were taken to measure the success of the remediation. The goal was to confirm the strength of 1.4 Kg/sq.cm and permeability less than  $1 \times 10^{-5}$  cm/sec achieved during laboratory investigations. Test samples were made in 7.6 x 15.2 cm cylinders during daily production. Each was tested for UCS at 3, 7, and 28 days of cure. Permeability was tested at seven days.

## **RESULTS and DISCUSSION**

### Preliminary Field Screening Studies

The first stage of field reagent screening began by testing various possible cement substitutes for cement like properties of hardening, heat evolution, and water absorption. Water was added to various Class C fly ashes, fluidized bed combustor ashes and cement kiln dust. Portland cement was hydrated for comparison. Test results identified potential reagents from each group, but showed that the Class C ashes as a group performed most like cement.

Sediment formulations were then prepared using reagent dosages of 40 to 60 g per 100 g of sediment. Strength development was tested at seven days by penetration resistance. Of the 11 reagents, only one Class C fly ash and two FBCAs showed strengths over 1 Kg/sq.cm at seven days. However, at 40 to 60% loadings these could not compare favorably to cement loadings of 20%.

Cement and Class C fly ash blends from the earlier study were reevaluated. Ratios of cement to fly ash were varied in 20% increments. In all cases 7-day strength decreased as cement was replaced with fly ash. This test was repeated using FA/FBCA blends and gave similar results. In an attempt to eliminate the need for cement, cement kiln dust were blended with various Class C fly ash mixes using loadings up to 45%. None met the desired strength after seven days. The by-product blends were then evaluated using various fluidized bed combustor ashes with Class C fly ash. At specific ratios, these blends exhibited strengths almost equal to cement mixtures. The mix ratios of reagents were unique for each specific combination of by-products (ashes). Since the cost of the coal burner by-products was very low compared to cement, higher ratios of reagents could be used at a significant cost savings.

Similar formulations were made using fill soil as an absorbent and to increase the solids content of the mixture. Results revealed that reductions could be made in the loading of both single and blended reagents. The addition of soil allowed some previously unsuccessful blend combinations to show strengths above 3 Kg/sq.cm with greater oil retention. Even with the soil addition the use of cement kiln dust was not effective.

The reagents with the most potential were then tested at different soil to sediment and reagent loadings. Results are in Table 3.

These results confirmed that the addition of soil to absorb the excess oil and water and increase the solid content of the sediment would reduce the dosage rate for cement. Results also showed that when using an optimum soil to sediment ratio of 1 to 0.75 that the FA/FBCA performed as well as cement alone. Not only was the performance equal, but the reagent cost was reduced by 40% when using the FA/FBCA blend even at slightly higher dosages.

Final field treatability testing was performed using sediment samples from all six lagoons, bracketing the range of conditions on the site. Final mixes were made using two ratios of FA/FBCA in the dry blend that was mixed with the sediment.

The final field tests confirmed the previous test results. As a general trend using the reagent FA/FBCA blend at a high mix ratio, significant strength formed at lower dosages a lower blend ratio. Soil to sediment comparisons showed that the ratio of soil to sediment to get an acceptable compressive strength are dependent on the sample location. Since a lower ratio would reduce the bulking factor, the lowest ratio of soil to sediment was preferred. At the optimum soil ratio of 1:0.75 and at a high blend mix ratio a reagent dosage of 25% met strengths of  $> 3 \text{ Kg/sq.cm}$  for all sediment locations. These mix formulations were selected for the next phase, a controlled bench-scale verification study. These formulations are the subject of a patent application.

#### Bench-scale Verification Study

Sample formulations were made in two to three kilogram batches. Mixes were made using a Hobart mixer, with a spade shaped blade. The mix was placed into 5.1 x 10.2 cm cylindrical molds. Molds were allowed to cure in sealed containers at room temperature on the bench top. Bulk density was determined on the uncured mix by weighing the filled molds. No significant changes in volume of the mix occurred as the samples cured. Raw sample bulk densities varied from  $1.07 \text{ g/cm}^3$  for the four sample locations. Grout mix densities for these sample varied from 1.2 to  $1.6 \text{ g/cm}^3$ .

Unconfined compressive strengths were tested by ASTM Method D2166 at 3, 7, 28, and 90 days. The passing criterion was  $> 1.4 \text{ Kg/sq.cm}$  at seven days of cure, which is based on developing enough strength to support construction equipment during the remediation phase of the project. No other specific criteria were established, but the total strength at 28 days of each sample were compared. See Table 4 for the UCS data. All the formulations using the FA/FBCA blend met the desired strengths. The cement formulations using soil were lower than the desired strength and the cement only formulations were much lower than the desired strength.

Sample molds were tested for permeability at seven days of cure by ASTM method D5084. Passing criteria was to have lower permeability than the permeability of the surrounding basin. The closure plan established  $1 \times 10^{-5} \text{ cm/sec}$  as the passing goal. All of the tested formulations met this requirement.

Liquid retention capacity was tested at seven days of cure. Samples used to measure unconfined compressive strength were crushed and reworked by hand. This material was placed into a 3.6 cm diameter stainless steel Carver mold. The mold was configured with a porous bottom plate that was covered with a filter paper to separate the sample from the plate. The mold was filled with sample, manually compacted and a  $3.0 \text{ Kg/sq.cm}$  load was applied for 5 min. Liquid retention was measured as a percentage of the weight retained. All of the samples retained between 89 and 96.6 % of their total liquid content. The FA/FBCA blend formulations all retained over 95% of their weights. Values for the cement mixes were generally 5% lower. When the percent liquid retention was graphed against the unconfined compressive strength, the graph showed that retention values improve with increasing strength up to  $1.8 \text{ Kg/sq.cm}$ .

The durability of 14 day cure samples was tested by submerging them in water. Blocks of solidified samples were immersed in beakers of water. Covers were placed on top to prevent evaporation. Results were recorded as visual observations. Cohesiveness, precipitation and oil sheen were noted. Observations were recorded over 90 days. These results show that slight oil sheens are present on all sample surfaces. In all cases the cement formulations exhibited more sheen than the FA/FBCA blend mixes. After two days the sheen was reduced in all beakers. White precipitate formed in cement mixes at two hours. At later time a smaller quantity of similar precipitate also formed in the by-product blend mixes. This precipitate is thought to be calcium hydroxide or calcium sulfate, by-products of cement hydration. No evidence of physical deterioration was seen in any of the samples. No changes occurred between nine and ninety days.

Samples were extracted at seven days using the TCLP method. The extracts were analyzed for semi-volatiles, volatiles and metals. No concentrations were expected above regulatory requirements because the original materials were within passing criteria. The leachability of the treated materials were all less than or equal to the leachabilities of the untreated sediments, and therefore below the TC regulatory criteria for these compounds.

The following recommendations were made from the bench-scale verification results:

- The FA/FBCA blend is an effective and economical replacement for cement in the stabilization of oily sediment.
- Absorbent fill soil is suitable for reducing reagent loading, while maintaining high strength, durability and low permeability.
- Controlling solids content is critical to effective solidification.
- Oil and grease in concentrations  $< 20\%$  has little effect on the reagent dosages in the proposed mix designs.

The recommend mix designs are: 1) Removal of free water before solidification; 2) Use absorbent fill soil to obtain 55 to 60% solids content; and 3) Add 25 to 30% FA/FBCA blend.

Recommendations from bench-scale verification were used to design a full-scale in-situ pilot demonstration.

#### Full-scale In-situ Demonstration

The purpose of the pilot demonstration was to test the ability to use the laboratory designs in the field. Many operational performance goals were addressed in this study that are beyond the scope of this paper. The technical goals of strength, mixing and permeability will be addressed.

Before stabilization a large sediment basin was divided using several dikes. The demonstration area was then dewatered by pumping free liquid from above the sediment. Solids content was increased to between 55 and 60% using fill soil. A long-stick trackhoe was used to mix soil into the sediment. Blending took place over several days so that the moisture could be absorbed by the soil. Additional soil was added as determined by field moisture determinations. Reagents were added to the mixture by delivery using a pneumatic tanker. Mixing was by three different techniques: 1) Long-stick trackhoe blending; 2) In-situ rotary mixer blending; and 3) Bulldozer blending.

The first two methods were done in-situ while the bulldozer blending was done on a pad. Both the bulldozer and the trackhoe mix were of a satisfactory consistency. Rotary mixer blending was unsatisfactory due to entanglements of debris with the mixer and the consistency of the mixes.

Variations in mix formulations were made to test the criticality of percent solids and reagent dosages. Samples were taken during mixing to be tested for compressive strength and permeability. Samples were aged in sealed containers on laboratory bench top separate from the remediation areas. Table 5 contains soil sediment ratios, percent reagents, final percent solids, compressive strengths, and permeabilities. Mixes with above 55% solids before adding the by-product blend gave acceptable strengths above 1.4 Kg/sq.cm at seven days. Permeabilities for all mixes were below  $1 \times 10^{-5}$  cm/sec which is ten times greater than the permeability of the surrounding soil. These data show that field results are consistent with earlier field screening and bench scale verification data.

#### CONCLUSIONS

IT-Davy demonstrated that an alternative solidification reagent is available to stabilize sediment with oil and grease contents below 20%. When used at the proper solids content a FA/FBCA blend gave equal or better strength and permeability compared to Portland cement. Because the cost of these combined reagents is lower than cement, larger dosages can be used at a lower cost. The practicality of these reagents has been demonstrated by field screening, bench-scale verification and a full-scale in-situ demonstration.

#### REFERENCES

- 1 EPA Method 9071, "Oil and Grease Extraction Method for Sludge and Sediment Samples", Test Methods for Evaluating Solid Waste Physical/Chemical Methods SW 846, 3rd Ed. Vol 1C
- 2 ASTM D2166, "Test Method for Unconfined Compressive Strength of Cohesive Soils", American Society of Testing and Materials, 1991. Vol. 04.08
- 3 ASTM D5084, "Test Method for Measurement of Hydraulic Conductivity of Saturated Porous Materials Using a Flexible Wall Permeameter", American Society of Testing and Materials, 1991. Vol. 04.08
- 4 EPA Method 1311, "Toxicity Characterization Leaching Procedure", Test Methods for Evaluating Solid Waste Physical/Chemical Methods SW 846, 3rd Ed. Vol 1C

**TABLE 1. PERCENT SOLIDS AND OIL AND GREASE FOR ALL SIX LAGOON SITES**

SAMPLE LOCATION	% SOLIDS	% OIL and GREASE
A	20	6
B	35	12
C	29	11
D	20	11
E	46	11
F	67	20

**TABLE 2. BENCH-SCALE VERIFICATION TEST FORMULATIONS**

SAMPLE LOCATIO N	REAGENT	DOSAGE PER 100 g OF SEDIMENT	ABSORPTIVE SOIL PER 100 g OF SEDIMENT
A	PORTLAND CEMENT	17	125
	FA/FBCA BLEND	30	125
	PORTLAND CEMENT	25	0
B	PORTLAND CEMENT	17	75
	FA/FBCA BLEND	20	75
	CEMENT/FLY ASH BLEND	25	0
C	PORTLAND CEMENT	22	75
	FA/FBCA BLEND	30	75
D	PORTLAND CEMENT	17	75
	FA/FBCA BLEND	20	75

**TABLE 3. PENETRATION RESISTANCE AT 7 DAYS (Kg/sq.cm)**

SOIL/SEDIMENT (w/w)	DOSAGE PER 100 g OF SEDIMENT	PENETRATION RESISTANCE USING EACH REAGENT		
		TYPE I PORTLAND CEMENT	CLASS C FLY ASH	FA/FBCA BLEND (MID-LEVEL RATIO)*
1/1	10	1.6	-	0.4
1/1	15	4.0	0.1	1.5
1/1	20	-	0.2	2.5
1/0.75	15	3.0	-	3.1
1/0.75	20	3.5	-	4.2
1/0.75	25	-	0.5	>4.5
1/0.5	15	1.2	-	-
1/0.5	20	3.0	-	2.6
1/0.5	25	>4.5	0.3	3.4
1/0.5	30	-	1.3	>4.5

\* Multiple ratios of FA/FBCA were investigated. These results are for the mid-level ratio blend of FA/FBCA.

**TABLE 4. UNCONFINED COMPRESSIVE STRENGTH**

SEDIMENT SAMPLE	MIX FORMULATION	UCS (kg/sq.cm)			
		3 DAYS	7 DAYS	28 DAYS	90 DAYS
<b>A</b>	Sed:Soil:Cement (100g:125g:17g)	0.35	0.42	0.84	0.98
	Sed:Soil:FA/FBCA Blend (100g:125g:30g)	1.62	3.52	4.29	4.71
	Sed:Cement (100g:25g)	ND	1.12	2.04	ND
<b>B</b>	Sed:Soil:Cement (100g:75g:17g)	0.84	1.34	1.90	2.81
	Sed:Soil:FA/FBCA Blend (100g:75g:20g)	0.56	1.62	1.97	2.53
	Sed:Cement/Fly ash (100g:25g)	ND	0.63	1.20	ND
<b>C</b>	Sed:Soil:Cement (100g:75g:22g)	0.14	0.14	0.21	0.28
	Sed:Soil:FA/FBCA Blend (100g:75g:30g)	0.77	2.95	4.22	4.71
<b>D</b>	Sed:Soil:Cement (100g:75g:17g)	1.12	1.62	2.39	2.95
	Sed:Soil:FA/FBCA Blend (100g:75g:20g)	0.63	1.76	2.25	2.53

**TABLE 5. FULL-SCALE IN-SITU DEMONSTRATION DATA**

	ISOLATION DIKE AREA		SOUTH DEMONSTRATION AREA				DOZER MIX AREA
	Cell No. 1	Cell No. 2	Cell No. 1	Cell No. 2	Cell No. 3	Cell No. 4	
Sediment to Soil Ratio	1:2.8	1:2.1	1:2.5	1:1.4	1:0.9	1:0.7	1:0.75
Percent Solids, Sediment and Soil	68%	65%	54%	53%	48%	45%	54%
Percent FA/FBCA Blend, by Wet Weight							
- Of Sediment	55%	42%	39%	29%	17%	14%	25%
- Of Sediment/Soil	14%	14%	16%	12%	9%	8%	17%
Final Mix, Percent Solids	72%	69%	60%	58%	52%	49%	60%
-Density, Kg/sq.cm	7.45	7.38	6.61	6.19	--	--	6.75
Compressive Strength, Kg/sq.cm							
- 3 days	0.70	0.70	0.42	0.28	Soft	Soft	Soft
- 7 days (ave. of 2)	1.69	2.04	1.27	0.28	Soft	Soft	--
- 28 days	4.50	3.30	2.18	1.41	Soft	Soft	--
Permeability, cm/sec x 10 <sup>7</sup>							
- 7 days	--	1.6	1.7	1.6	--	--	5.7

## CHARACTERIZING SYNTHETIC GYPSUM FOR WALLBOARD MANUFACTURE

P. J. Henkels  
USG Corporation Research Center  
700 N. Highway 45  
Libertyville, IL 60048

J.C. Gaynor  
United States Gypsum Company  
125 S. Franklin  
Chicago, IL 60606

**Keywords:** FGD Synthetic Gypsum, Gypsum Wallboard, Test Methods

### INTRODUCTION

United States Gypsum Company (USGC) has developed specifications and guidelines covering the chemical and physical aspects of synthetic gypsum to help predict end use acceptability in wallboard manufacture. These guidelines are based in part on past experiences with natural and synthetic gypsum. Similarly, most wallboard manufacturers in North America have developed their own guidelines based in part on its unique history and particular experiences with synthetic gypsum. While there are similarities between manufacturers' guidelines, differences do exist.

This paper discusses the importance of selected parameters contained in the FGD gypsum guidelines. In most cases, the parameters are equally relevant to other synthetic gypsums and the naturally occurring gypsum mineral as well.

USGC's general guidelines of FGD gypsum along with guidelines from the German Gypsum Association are listed in Table One. The guidelines are not an all inclusive list of every gypsum property important to the wallboard manufacturer. The guidelines serve as a starting point in negotiating sales agreements between the wallboard manufacturer and synthetic gypsum supplier. The product specification agreement at USGC is tailored to each individual source depending in large part to the percent usage at the wallboard facility, type of synthetic gypsum and capabilities of the supplier.

### GYPSUM CHARACTERIZATION

**Gypsum Purity.** Obviously, gypsum ( $\text{CaSO}_4 \cdot 2\text{H}_2\text{O}$ ) purity is an important attribute. Purity is key in manufacturing wallboard. Purity of mined natural rock varies widely usually from 80 - 96%. High purity is desired because lower weight gypsum board may be produced. Generally, a higher purity is desired for synthetic gypsum compared to natural rock in wallboard manufacture. Usually, high purity synthetic gypsum can be reasonably obtained by the supplier. Therefore, a higher purity synthetic gypsum will have increased value.

Impurities found in synthetic as well as natural gypsum can be quite detrimental to the wallboard produced. The higher purity reduces the chance of deleterious effects from these impurities.

Purity can be determined by several test methods including Differential Scanning Calorimetry/Thermal Gravimetry (DSC/TGA), X-Ray Fluorescence Spectroscopy (XRF) and  $\text{SO}_3$  analysis.

**Free Moisture.** Many synthetic gypsums discharged from by-product manufacturers are in the form of a wet cake. The free or surface moisture of the cake is usually in the range of 6 - 25%. Natural mined rock will vary from 0 - 3% moisture. Often, the amount of synthetic gypsum that a wallboard plant can blend in with the natural rock will be dictated by the thermal capacity of the rock drying system. High moisture reduces the amount of synthetic gypsum that can be blended. This reduces its value.

Often a wallboard manufacturer will enter a sales agreement with a supplier prior to the availability of the synthetic gypsum. When the actual free moisture is significantly greater than contracted, processing capacity problems will arise. This could be due to both thermal drying limits and because of the more challenging handling characteristics of high moisture gypsum. High moisture gypsum has a greater tendency to stick and build up on conveying equipment.

Free moisture of natural and synthetic gypsum materials are determined using a simple oven weight loss method per ASTM C471. In addition, heat and moisture determining balances are used.

**Impurities.** The type and quantity of impurities have the greatest impact on qualifying the use of a synthetic and natural gypsum. The guidelines list the predominant impurities found in FGD gypsum. Discussion of selected impurities follow.

**Residual Carbonates.** Unreacted limestone ( $\text{Ca/MgCO}_3$ ) is the predominant impurity found in many synthetic gypsum sources. Limestone is a common impurity in natural gypsum as well. Fortunately, limestone remains chemically inert through the board conversion process. However, increased wear on processing equipment results when encountering high amounts of limestone (Mohs value 3 - 4) since it is a harder substance than gypsum (Mohs value 1.6 - 2).

Limestone quantity can be determined through XRF oxide analysis of calcium and magnesium in conjunction with carbon dioxide ( $\text{CO}_2$ ) analysis by coulometric titrimetry. Alternatively,  $\text{CO}_2$  can be quantified through DSC scans.

**Flyash.** One concern with flyash in FGD gypsum is the chemical variability associated with burning different fuel sources (e.g. various coals and Orimulsion™). Flyash can affect paper to core bond during wallboard manufacture. The variability can cause intolerable problems in wallboard conversion. Also, flyash laden with silica and iron causes increased wear on process equipment.

An important concern with flyash is the amount of trace elements that may accompany it. This can raise serious industrial hygiene issues. Trace elements and the analysis will be discussed in a later section.

Flyash is easily detected using a scanning electron microscope (SEM). By using image analysis, an estimate of the amount of flyash present can be established. Fly ash can also be calculated by determining the mass balance around the scrubber and dust collection system. Figure One is an SEM photo of flyash impurity in a FGD gypsum sample.

**Silica ( $\text{SiO}_2$ ).** Silicon dioxide is an important impurity from an industrial hygiene perspective and a process issue for all mineral industries. Silica is common in both natural and synthetic gypsums. It can be part of a clay, flyash or quartz impurity.

High quantities of respirable (0 - 4 microns) silica could present an industrial hygiene issue.

Crystalline silica or quartz is a very hard substance (Mohs value 7). Even low amounts (1-2%) can cause dramatic accelerated wear on gypsum processing equipment.

Amorphous silica is also contained in a variety of clays. Clays negatively impact the amount of water required to form a fluid slurry and thus, create a higher thermal demand to drive off the excess water in the board conversion process.

Silica can be quantified using XRF. X-Ray diffraction (XRD) is used to identify whether the  $\text{SiO}_2$  present is amorphous or crystalline in nature. In addition, ASTM C-471 describes a wet chemistry method to determine  $\text{SiO}_2$  and insoluble matter.

**Calcium Sulfite ( $\text{CaSO}_3 \cdot 1/2\text{H}_2\text{O}$ ).** FGD systems may be designed to produce unoxidized gypsum or calcium sulfite instead of calcium sulfate dihydrate. This material is always landfilled. Sulfite impurities are a much greater concern at the gypsum producing FGD systems because they lead to scaling and other processing problems. The fine particle size of sulfite will cause cake washing and dewatering problems. Calcium sulfite is an unwanted impurity in any gypsum.

Thermal analysis and XRF will detect sulfite above 0.1%. Titration procedures are considered a better method to determine sulfite. A titration procedure is listed in EPRI-Method 40 (EPRI CS-3612. Project 1031-4. Final Report dated July, 1984).

**Soluble Salts.** Soluble salt impurities are one of the most important parameters affecting the physical properties of gypsum wallboard. Salts are a common impurity in natural and several different types of synthetic gypsums. It is common practice to mine around natural gypsum rock seams high in salt content. Chloride salts are common in natural and some synthetic gypsums. In addition, high amounts of magnesium salts can end up in some synthetic gypsums. Magnesium can originate from limestone sources used to neutralize waste acid and in desulfurization systems.

Salts readily go into solution when the calcined gypsum (stucco) is mixed with water and other additives in the board mixer. During the drying of the gypsum board in the kiln the salts migrate to the paper - core interface and interrupt the paper to core bond. Salts are very hygroscopic and cause moisture to deposit in the critical bond area of the board. On exposure to high moisture from joint finishing and wallpaper products the drywall paper can detach itself from the core.

The four soluble salt ions typically monitored are magnesium ( $Mg^{2+}$ ), potassium ( $K^+$ ), sodium ( $Na^+$ ), and chloride ( $Cl^-$ ). Soluble salts are analyzed by several different methods. Atomic absorption is used for the determination of magnesium. Atomic emission is used for the determination of potassium and sodium. Ion-selective electrode (ISE) is used for the determination of chloride. ISE can also be used for sodium and potassium determinations.

Table Two shows a typical soluble salt analysis for a synthetic gypsum sample. Total salts are based on a mathematical reconstruction. This mathematical reconstruction is based on the theoretical solubility of the ions.

**Trace Elements.** Trace elements and pH are evaluated on all natural and synthetic gypsum sources for industrial hygiene purposes. Trace elements normally evaluated are shown in Table Three. Trace elements are unwanted impurities. They arise from flyash contamination and increase process equipment wear. Also, trace elements are commonly found in most naturally occurring minerals including gypsum and limestone.

Trace elements can be determined through several methods including Atomic Absorption/Emission (AA) with a graphite furnace option, wet chemistry methods, Inductive Coupled Plasma (ICP) and XRF.

**Organic impurities.** Although not listed in the FGD guidelines, organic impurities even at trace (ppm) levels can have a dramatic effect on gypsum board operations. Organics are unwanted impurities in gypsum. The effects of organics found in natural and synthetic sources are observed during gypsum rehydration in the board conversion process. They can easily cause the rehydration time to dramatically lengthen and cause the board line to slow down and reduce production. Organics adversely affect crystal growth and reduce strength development of the gypsum core.

Residual organic impurities in synthetic gypsum from waste acid neutralization processes such as citric and lactic acid production can strongly retard the hydration of gypsum stucco.

Organic impurities can be identified through several methods including coulometric titrimetry, Infrared Spectroscopy (IR), Nuclear Magnetic Resonance (NMR) and High Performance Liquid Chromatography (HPLC).

**Physical Properties.** Although chemically the same, there can be significant physical property differences between natural and synthetic gypsums. It is well publicized that there are significant differences in particle size and shape between natural roller milled ground gypsum rock (land plaster) and most synthetic gypsums.

**Particle Size.** Most synthetic gypsums are formed in a solution environment supersaturated with respect to gypsum and accompanied with vigorous agitation. Under these conditions, the gypsum particles precipitate fairly uniformly in particle size and shape. The particular size and shape depends on the process conditions of the unit operations. USGC FGD guidelines list a 20 micron minimum median particle size. More commonly, synthetic gypsums have median particle size is in the 35 - 45 micron range.

Many synthetic gypsums have narrow or monolithic particle size distributions. Typical roller milled natural gypsum has a much broader particle size distribution. Figure Two shows SEM photomicrographs of natural and FGD gypsum. Figure Three shows a comparative particle size histogram between natural and a FGD gypsum.

A monolithic particle size distribution with a large mean particle size (40 - 60 microns median) for synthetic gypsum is preferred even though it creates processing challenges at the wallboard facility. Large particles (low surface area) will readily dewater. Low free moisture is a desired quality because of lower drying costs. Also, as free moisture is reduced through dewatering, the quantity of water soluble impurities will be reduced.

In general, synthetic gypsums that have poor dewatering characteristics also have high surface moisture and high surface area. In addition, the material has more challenging material handling properties and causes increased amounts of process water to be used during the continuous casting of gypsum board. The later point causes a higher thermal demand in drying the gypsum board.

Therefore, it is preferred that the gypsum supplier design the synthetic gypsum system to produce gypsum particles that will readily dewater. Despite engineering design challenges at the wallboard plant, synthetic gypsums with large particles are desired because they impart good dewatering properties.

Particle size is measured using laser scattering or sedimentation technique. The two methods do not always yield the same results. Figure Five shows particle size distribution for natural and synthetic gypsums using laser light scattering and sedimentation. Note that for both samples the laser technique yields a higher mean particle size than sedimentation.

Surface area is another method to measure particle fineness. The Blaine surface area technique is a common measuring method used for powders. The Fisher™ subsieve sizer is used as well. The surface area of natural roller milled gypsum is typically 2000 - 3000 cm<sup>2</sup>/gram. Wallboard grade FGD gypsum is commonly below 1000 cm<sup>2</sup>/gram.

**Aspect Ratio.** Some wallboard manufacturers will include an aspect ratio guideline (usually 10:1:1 - 20:1:1 maximum) on particle shape. The aspect ratio guideline is usually put into product specifications to insure against contending with problems associated with needle-like gypsum crystals in processing, calcining and wallboard manufacture. Since gypsum particles retain their shape after calcination, high aspect ratio particles can cause an increase in water demand during board conversion.

The synthetic gypsum producer needs to concern itself with aspect ratio because of its influence on internal processing issues. Needle shaped gypsum particles are more difficult to dewater than large blocky shaped crystals. Thus, under the same processing conditions, gypsum with a high aspect ratio will contain higher surface free moisture and water soluble impurities. It may also be more expensive to process in order to meet finished product guidelines. Hence, the material will have reduced value.

The aspect ratio of natural gypsum is generally 1: 1. The particle shape of gypsum can easily be determined using the SEM.

**Bulk Density.** Large monosized gypsum particles of many FGD gypsums tend to exhibit a high bulk density. Often, the synthetic gypsum is to be purchased sight unseen by the gypsum company. This can present engineering and process challenges to the wallboard manufacturer in designing suitable material handling systems due to the high bulk density. Loose bulk density of natural gypsum is about 50 pcf. The bulk density of synthetic gypsums can vary widely from less than 40 pcf to over 70 pcf. Table Four lists bulk densities of selected natural and synthetic gypsums used by USGC. Bulk density is easily measured through the weighing of a known volume of material.

## SUMMARY

Over the years of using natural and synthetic gypsums, USGC has developed and employed several methods of characterizing natural and synthetic gypsum. Synthetic and natural gypsum are chemically the same. The kind and amount of impurities will vary from source to source for both natural and synthetic gypsums. Chemical and physical property testing techniques are the same for natural and synthetic gypsum. It is the physical properties that commonly distinguish synthetic from natural gypsum.

In general, synthetic gypsum has a narrow particle size distribution. Natural gypsums are ground and have a much broader particle size distribution. Other physical properties differences such as surface area, bulk density and aspect ratio are related to the narrow particle size distribution of synthetic gypsum.

Synthetic gypsum is received at the wallboard plant in a wet cake form. It is important to the wallboard manufacturer that the gypsum be as low as possible in free moisture within the capability of the supplier. Lower free moisture reduces wallboard manufacturing costs.

## REFERENCES

1. P. J. Henkels and J.C. Gaynor, "Characterization of Synthetic Gypsum", The Fourth International Conference on FGD and Other Synthetic Gypsum, May 1995.
2. J. W. Barber, B. A. Hudgens, C. D. Byers and V. R. Nathan, "Characterization of Synthetic Gypsum", The Second International Conference of FGD and Chemical Gypsum, May 1991.

TABLE ONE

## FGD GYPSUM GUIDELINES

	USG	German Gypsum Association
Purity (CaSO <sub>4</sub> · 2H <sub>2</sub> O) (% min)	95	95
SO <sub>3</sub> (% min.)	44.2	—
Free Moisture (% max.)	10	10
Flyash (% max.)	1.0	---
SiO <sub>2</sub> (% max.)	1.0	---
Calcium Sulfite (% max.)	1.0	0.25
Chloride (max. ppm)	120	100
Total Water Soluble Salts (max. ppm)	600	---
Average Particle Size (min. microns)	20	---
Surface Area (cm <sup>2</sup> /gram)	3500 max.	---
pH	6 - 8	5 - 9

TABLE TWO

## SAMPLE SOLUBLE SALT ASSAY

Soluble Salts:	Synthetic (ppm)	Natural (ppm)
Potassium (K)	1	13
Sodium (Na)	7	15
Magnesium (Mg)	26	29
Chloride (Cl)	32	23
<b>Reconstruction</b>		
KCl	2	24
NaCl	17	19
Mg(Cl)2	27	0
Ca(Cl)2	0	0
K2SO4	0	0
Na2SO4	0	23
Mg2SO4	94	143
Total	141	209
Equivalent lbs/ton	0.28	0.42

TABLE THREE

## TRACE ELEMENTS

Zinc
Cadmium
Chromium
Nickel
Cobalt
Copper
Lead
Tin
Molybdenum
Fluorine
Arsenic
Antimony
Mercury
Selenium
Vanadium
pH

**TABLE FOUR**

**BULK DENSITY**

	Loose Bulk Density
Natural Gypsum	50 pcf
Synthetic Gypsum #1	75 pcf
Synthetic Gypsum #2	45 pcf
Synthetic Gypsum #3	53 pcf
Synthetic Gypsum #4	62 pcf

**FIGURE ONE SEM Photograph of Flyash Impurity in Synthetic Gypsum**

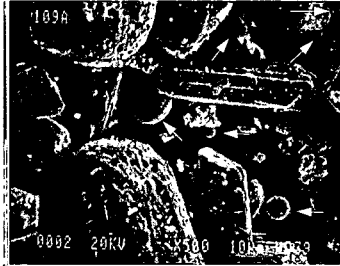


**FIGURE TWO SEM Photographs of FGD and Natural Gypsum**

**FGD GYPSUM**



**Natural Gypsum**

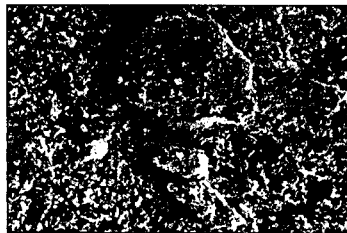


**FIGURE THREE**

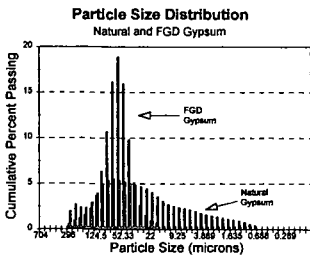
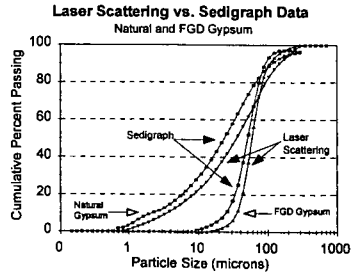


**FIGURE FOUR**



## BIOMASS PRODUCTION AND WATER QUALITY IN AN ACIDIC SPOIL AMENDED WITH Mg(OH)<sub>2</sub>-ENRICHED BY-PRODUCT GYPSUM

Humberto Yibirin, R.C. Stehouwer, J. Bigham, and P. Sutton.  
OARDC/School of Natural Resources, Williams Hall  
Wooster, OH 44691

Keywords: GYPSUM, MAGNESIUM, SPOIL, LAND RECLAMATION

Gypsum (G) and Mg(OH)<sub>2</sub> (FGD-Mg) are recovered from the thickener overflow of an experimental wet FGD scrubber in the Zimmer power plant of CInergy (Cincinnati Gas and Electric Company). The purity of recovered G ranges from almost 100 to 92%, with impurities occurring mainly as Mg(OH)<sub>2</sub>. Gypsum contaminated with Mg(OH)<sub>2</sub> is referred to as Mg(OH)<sub>2</sub>-enriched by-product gypsum (Mg-G).

Because of its Mg(OH)<sub>2</sub> content, Mg-G can potentially be used as a source of both Ca and Mg for green plants growing on soils and spoils with low levels of available Ca and Mg. In addition, the presence of Mg(OH)<sub>2</sub> should allow Mg-G to be used as an alkaline amendment for the reclamation of hyperacid spoils. The total abandoned surface coal mined land needing reclamation in eastern USA has been estimated to be more than 0.5 million ha (Sutton and Dick, 1987). Gypsum can reduce Al toxicity by: (1) increased ratio of Ca to Al in the soil solution (Kinraide et al., 1992), and (2) physical removal of Al from the soil profile through Ca exchange (Wendell and Ritchey, 1993). The Mg(OH)<sub>2</sub> in Mg-G may enhance the effectiveness of these mechanisms for amelioration of phytotoxic conditions below the zone of incorporation. The presence of Mg and sulfate increases the potential for salt loading (Stehouwer et al., 1995), which may enhance downward movement of Ca and Al.

The purpose of this greenhouse study was to investigate the effects of G and Mg-G, at three application rates, on spoil and leachate pH and electrical conductivity (EC), and movement of major and trace elements. Preliminary observations on plant growth are also reported.

### MATERIALS AND METHODS

Acidic minespoil was sampled from the upper 20 cm of an abandoned mineland (AML) site located at the Eastern Ohio Resource Development Center (EORDC). The samples were air-dried and passed through a 12.7-mm sieve. Initial Bray #1 P was 25 mg kg<sup>-1</sup>; NH<sub>4</sub>-acetate extractable Ca, K, Mg, and Al were 225, 54, 37, and 601 mg kg<sup>-1</sup> respectively; CEC was 30 cmol. kg<sup>-1</sup>, and pH was 2.9.

Three by-product materials were used: G (98% gypsum), and two Mg-G blends (4%Mg-G, and 8% Mg-G) which contained 4 and 8% (w/w) Mg(OH)<sub>2</sub> equivalent. Reagent grade Ca(OH)<sub>2</sub> was also mixed with G to produce two mixtures (4%Ca-G, and 8%Ca-G) with neutralizing potentials equal to 4%Mg-G and 8% Mg-G respectively.

Spoil material (8 kg) was poured into PVC columns (60 cm tall, 15 cm diam.) to a height of 36 cm forming an untreated sub-surface layer. A 15-cm surface layer of spoil (3.4 kg) was then thoroughly mixed with the various treatments and placed over the untreated spoil. The columns were mounted on flat PVC plates with a nipple in the center to allow for leachate collection.

Treatments consisted of G, 4%Mg-G, 8%Mg-G, 4%Ca-G, or 8%Ca-G applied at rates equivalent to 145, 290, and 580 Mg ha<sup>-1</sup>. These rates were calculated to supply Ca from G in amounts equal to 2.5, 5.0, and 10.0 times the spoil CEC in the treated layer. Control treatments included unamended spoil and spoil amended to pH 7.0 with limestone (112 Mg ha<sup>-1</sup>). Treatments were arranged in randomized complete blocks with three replications. Fertilizers were applied together with the treatments in amounts of 0.5 g NH<sub>4</sub>NO<sub>3</sub>, 0.4 g triple superphosphate, and 2 g KCl.

Columns were then leached with 2.5 L of deionized water and the first leachates (150-200 ml) were collected. Following this first leaching, 5 g of soil was collected from the surface 5-cm depth of each column for pH and EC measurements, and each column was planted with 30 seeds of Orchardgrass (*Dactylis glomerata* L.). After an initial 80-d growing period, orchardgrass was harvested monthly for a total of 4 harvests. Leachates were also collected at the end of the study. Columns were watered daily with deionized water such that the amount of water applied during the study was equivalent to the average annual rainfall for SE Ohio ( $\approx 1000$  mm).

Leachates were analyzed for pH, EC, and for As, B, Ba, Be, Ca, Cd, Co, Cr, Cu, Fe, K, Li, Mg, Mn, Mo, Na, Ni, P, Pb, S, Sb, Se, Si, and Zn by inductively coupled plasma emission spectrometry. Data analysis was conducted using analysis of variance procedures, and single degree of freedom orthogonal contrasts.

### RESULTS AND DISCUSSION

The Mg-G and Ca-G amendments were equally effective at increasing the pH of the acidic minespoil in the treated layer (Table 1). None of the amendments used, however, increased the pH of the first or final leachates compared to the untreated spoil. Increases in spoil pH led to increased growth of orchardgrass, however, the largest application rates of 4% and 8% Mg-G suppressed yield in the first two harvests. This initial yield suppression was associated with large increases in EC.

Mg-G increased spoil and leachate EC more than any other treatment (Table 1). The use of 4%Mg-G increased spoil EC 1.23 times compared to 4%Ca-G, 8%Ca-G, or gypsum, and 3.4 times compared to either the untreated or limed spoil. These differences were larger when the spoil was amended with 8%Mg-G. Leaching of salts out of the column during the course of the study reduced the EC in the final leachates, but Mg-G effects on EC were still present. Stehouwer et al. (1995) showed that the solubility of Mg in a spoil amended with materials containing  $\text{CaSO}_4$  and  $\text{Mg}(\text{OH})_2$  may be controlled by epsomite ( $\text{MgSO}_4 \cdot 6\text{H}_2\text{O}$ ) which is  $\approx 300$  times more soluble than gypsum. Enrichment of gypsum with Mg, therefore, increased the potential for salt loading. Gypsum-containing treatments increased the leachate concentrations of Ca, Mg, Al, Fe, Mn, and S (Table 2), and of Cd, Cr, Pb, Cu, and B (Table 3) relative to the control treatments. The largest increase occurred with Mg-G. Most cations were much less mobile with limestone and Ca-G treatments. The use of G alone increased the movement of Al, S, Fe, Mn, Cr, and B compared to Ca-G. The  $\text{Ca}(\text{OH})_2$  in Ca-G reduced the movement of metal cations in the spoil compared to G alone, thus making Ca-G behave more like limestone than G. By contrast, the  $\text{Mg}(\text{OH})_2$  in Mg-G increased the movement of metal cations in the spoil compared to G alone, limestone, or Ca-G. Effects of Mg-G on cation movement were most likely not due to pH differences since Mg-G and Ca-G had similar effects on pH. The increased transport of these metals with Mg-G appeared to be due to large concentrations of  $\text{Mg}^{2+}$  in solution. We believe the increases in metals in the leachates were due to mobilization of metals present in the spoil. These were brought into solution through exchange reactions with  $\text{Mg}^{2+}$  and then transported downward.

Amendment with Mg-G increased pH, thus allowing revegetation of otherwise phytotoxic spoils. In addition to being a source of Ca and Mg, Mg-G enhanced downward movement of Al, and Fe which may promote root penetration in untreated subsurface layers, and improve the chances of reclamation success. Amendment applications, however, should be limited to rates that will not cause phytotoxic salt concentrations, excessively high pH, or increase the concentrations of heavy metals in water to harmful levels.

Table 1. Initial and final electrical conductivity (EC) and pH in the spoil and leachate, averaged across rates, as affected by wet FGD Mg(OH)<sub>2</sub>-enriched gypsum, gypsum, Ca(OH)<sub>2</sub>-enriched gypsum, and calcitic limestone<sup>†</sup>.

	Spoil Init	Leach First	Leach Final	Spoil Init	Leach First	Leach Final
	pH			EC, S m <sup>-1</sup>		
4%Mg-G	5.60	2.27	2.58	0.27	0.64	0.32
8% Mg-G	7.31	2.26	2.67	0.32	0.64	0.29
4%Ca-G	5.82	2.27	2.55	0.23	0.44	0.24
8%Ca-G	7.23	2.26	2.55	0.21	0.47	0.21
Gypsum	3.09	2.26	2.60	0.22	0.53	0.28
Untreated	2.87	2.33	2.78	0.07	0.30	0.09
Limestone	7.09	2.33	2.71	0.09	0.30	0.10
avg.	5.71	2.27	2.61	0.23	0.52	0.25
lsd 0.05 <sup>†</sup>	0.31	NS	0.05	0.03	0.09	0.04

<sup>†</sup> lsd = least significant difference.

\* leachate and initial are abbreviated as leach and init.

Table 2. Major element composition of first leachate, averaged across rates, as affected by wet FGD Mg(OH)<sub>2</sub>-enriched gypsum, gypsum, Ca(OH)<sub>2</sub>-enriched gypsum, and calcitic limestone.

	Ca	Mg	Al	Fe	Mn	S
	mg L <sup>-1</sup>					
4%Mg-G	124	301	866	142	3	1821
8% Mg-G	105	249	950	150	3	1903
4%Ca-G	64	53	418	72	2	646
8%Ca-G	69	56	432	76	2	617
Gypsum	78	108	700	114	3	1201
Untreated	40	35	227	48	1	440
Limestone	36	37	246	53	1	479
avg.	82	139	622	104	2	1146
lsd <sup>†</sup> 0.05	22	57	170	22	1	258

<sup>†</sup> lsd = least significant difference.

Table 3. Trace element composition of first leachate, averaged across rates, as affected by wet FGD Mg(OH)<sub>2</sub>-enriched gypsum, gypsum, Ca(OH)<sub>2</sub>-enriched gypsum, and calcitic limestone.

	As	Cd	Cr	Pb	Cu	B
	mg L <sup>-1</sup>					
4%Mg-G	<0.04	0.05	0.28	0.22	0.64	4.41
8% Mg-G	<0.04	0.05	0.30	0.21	0.65	3.91
4%Ca-G	<0.04	0.04	0.14	0.11	0.50	0.40
8%Ca-G	<0.04	0.04	0.15	0.09	0.52	0.35
Gypsum	<0.04	0.05	0.24	0.18	0.63	1.30
Untreated	<0.04	0.03	0.09	0.08	0.35	0.27
Limestone	<0.04	0.03	0.08	0.19	0.32	0.23
avg.	<0.04	0.05	0.21	0.16	0.56	1.86
lsd <sup>†</sup> 0.05	NS	0.01	0.05	0.08	0.1	0.7

<sup>†</sup> lsd = least significant difference.

#### ACKNOWLEDGMENT

This study is part of an ongoing research program conducted at The Ohio State University. Support for this research was provided by The Ohio Coal Development Office, CInergy (Cincinnati Gas & Electric Co.), and Dravo Lime Company.

#### LITERATURE CITED

- Kinraide, T.B., P.R. Ryan, and L.V. Kochian. 1992. Interactive effects of  $Al^{+3}$ ,  $H^+$ , and other cations on root elongation considered in terms of cell-surface electrical potential. *Plant Physiol.* 99:1461-1468.
- Stehouwer, R.C, P. Sutton, R.K. Fowler, and W.A. Dick. 1995. Minespoil amendment with dry flue gas desulfurization by-products:Element solubility and mobility. *J. Environ. Qual.* 24:164-174.
- Sutton, P., and W.A. Dick. 1987. Reclamation of acidic mined lands in humid areas. *Adv. Agron.* 41:377-405.
- Wendell, R.R., and K.D. Ritchey. 1993. Use of high-gypsum flue gas desulfurization by-products in agriculture, p. 40-45. In Shiao-Hung (ed.), *Proceedings of the Tenth Annual International Pittsburgh Coal Conference*. September 20-24, 1993. Pittsburgh, PA.

**This page left intentionally blank.**

# MANUFACTURE OF AMMONIUM SULFATE FERTILIZER FROM GYPSUM-RICH BYPRODUCT OF FLUE GAS DESULFURIZATION - A Prefeasibility Cost Estimate

M.-I. M. Chou, M. Rostam-Abadi, and J.M. Lytle  
Illinois State Geological Survey  
615 E. Peabody Dr.  
Champaign, IL 61820

F.P. Achorn,  
Southeast Marketing Chem. Process Inc.  
Suite 404, Florence, AL 35631

**KEYWORDS:** ammonium sulfate, gypsum, desulfurization

## ABSTRACT

Costs for constructing and operating a conceptual plant based on a proposed process that converts flue gas desulfurization (FGD)-gypsum to ammonium sulfate fertilizer has been calculated and used to estimate a market price for the product. The average market price of granular ammonium sulfate (\$138/ton) exceeds the rough estimated cost of ammonium sulfate from the proposed process (\$111/ton), by 25 percent, if granular size ammonium sulfate crystals of 1.2 to 3.3 millimeters in diameters can be produced by the proposed process. However, there was at least  $\pm 30\%$  margin in the cost estimate calculations. The additional costs for compaction, if needed to create granules of the required size, would make the process uneconomical unless considerable efficiency gains are achieved to balance the additional costs. This study suggests the need both to refine the crystallization process and to find potential markets for the calcium carbonate produced by the process.

## INTRODUCTION AND BACKGROUND

The 1990 amendments to the Clean Air Act mandate a 2-stage 10-million ton reduction in sulfur dioxide emissions in the United States. Emission controls using flue gas desulfurization (FGD) technologies have been commercially demonstrated. However, in addition to capital costs for equipment and operating expenses, plants burning high sulfur coal and using FGD technologies must also bear increasingly expensive landfill disposal costs for the solid waste produced. FGD technologies would be much less of a financial burden if successful commercial uses were developed for the gypsum-rich byproducts of wet limestone scrubbing.

A process for converting FGD-gypsum to calcium carbonate and ammonium sulfate by allowing it to react with  $\text{CO}_2$  and ammonia or by allowing it to react with ammonium carbonate was studied at the ISGS. A variation of this process could provide electric utilities a means converting the  $\text{CO}_2$  and  $\text{SO}_2$  in their flue gas to useful commercial products. The fertilizer industry would also be provided with an abundant source of ammonium sulfate to supply sulfur nutrient in NPK fertilizer blends. If successful, the results of this project could provide a solution, from both the environmental and economic standpoints, to the problem of disposing of large quantities of by-products from FGD processes. The technical feasibility of producing fertilizer-grade ammonium sulfate from FGD-gypsum has been assessed (Chou et al., 1995). It is important, therefore, to assess the economic feasibility of producing commercial-grade ammonium sulfate fertilizer from FGD-gypsum. The preliminary process flow diagram and the rough cost estimates of the process are presented in this paper.

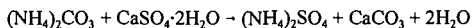
## PROCESS FLOW DIAGRAM

The proposed process is similar to the one used in Europe and India in the 1960s to produce large quantities of ammonium sulfate from natural gypsum (Sauchelli, 1964). Some modifications were made on the gypsum conversion reactor based on pilot plant tests by the TVA (Meline et al., 1971).

Figure 1 shows the proposed flow diagram for the conversion of gypsum to ammonium sulfate fertilizer and calcium carbonate. The flow diagram contains four major units: 1) absorption tower, 2) gypsum converter, 3) concentrator-crystallizer, and 4) solid handling system.

In an absorption tower, ammonium carbonate, a major reactant, is formed by reacting carbon dioxide and ammonia in aqueous solution. The ammonium carbonate solution is then mixed with gypsum ( $\text{CaSO}_4 \cdot 2\text{H}_2\text{O}$ ) and delivered to a gypsum conversion unit.

In the gypsum converter, the mixture is converted to ammonium sulfate solution and calcium carbonate by the following reaction:



The overflow from the gypsum converter, containing all of the  $(\text{NH}_4)_2\text{SO}_4$  produced, will give a solution of 35% ammonium sulfate. The solution will be concentrated from 35 to about 42 to 45% in a standard Swenson vacuum-type concentrator with forced circulation. A vacuum crystallizer equipped with a heat exchanger (evaporator-crystallizer) designed to control the conditions for crystal formation is used. The ammonium sulfate solution should be supersaturated within a metastable field during the process of crystallization, in order to produce the larger crystals (particle size 1.2 to 3.3 millimeters with average 2.4 millimeters) required for fertilizer application. Two medium-sized crystallizers are used to provide a shorter retention time during crystallization.

The slurry with crystals from the crystallizer is centrifuged and the crystals are washed with dilute aqueous ammonia. The solution from the centrifuge is used to dissolve fines from screening the product. The  $(\text{NH}_4)_2\text{SO}_4$  crystals are first dried then cooled in rotary type equipment. Material from the cooler is screened on double deck vibrating screens. Oversized and undersized crystals from the screens are directed to the dissolution tank. Suitable size crystals (1.2 to 3.3mm) are delivered to bulk storage.

#### ASSUMPTIONS FOR RAW MATERIALS ESTIMATION

**Gypsum** - The yearly production of FGD-gypsum from a 550 Mw electrical generating plant was calculated based on data (Hillenbrenner, 1995) from the City Water Light and Power Utility of Springfield, IL. This company uses a limestone scrubbing process to remove sulfur dioxide from the exhaust gases by converting it to gypsum ( $\text{CaSO}_4 \cdot 2\text{H}_2\text{O}$ ). The plant consumes coal at a rate of 0.96 pounds per kwh and the sulfur content of the coal is about 3%. Based on a load factor of 65% for 300 days per year of operation, the plant produces 200,000 tons gypsum per year.

**Ammonia gas** - Assuming 98% recovery, one ton of gypsum could produce 0.752 tons of ammonium sulfate. This requires 0.22 tons of ammonia gas (10% excess) consumption per ton of gypsum (Bennett, 1962; Hillenbrenner, 1995) or 0.292 tons of ammonium gas consumption per ton of ammonium sulfate. The proposed plant will require about 123.4 tons of ammonia gas per day (or 43,800 tons per year to produce 150,000 tons of ammonium sulfate per year.

**Carbon dioxide** - The proposed plant would be built near a utility or a lime producing plant that could supply the carbon dioxide. It was assumed, for this estimate, that the  $\text{CO}_2$  would be obtained from the utility or a lime producing plant at no cost.

It is assumed that the 0.581 tons of  $\text{CaCO}_3$  produced per ton of gypsum processed (or 0.773 tons of  $\text{CaCO}_3$  per ton of ammonium sulfate) will be recycled to the scrubber. This will result in recycling 325.9 tons of  $\text{CaCO}_3$  per day.

#### EQUIPMENT AND COST ESTIMATIONS

The cost estimates are based on the assumption that a linear projection of the TVA pilot plant equipment (Meline et al, 1971) to a commercial scale plant will result in at least a 30 percent increase in production capacity and allow for usual plant down-time while producing 150,000 tons of ammonium sulfate per year. All cost estimates are for a conceptual plant design. Additional references used in the calculation include the sixth edition of the Chemical Engineer's Handbook by Perry & Green and economics factors for 1993 and 1994 found in the chemical engineering journals. See Tables 1 to 3 for the cost summary.

#### COMPACTION ALTERNATIVE

A specific size of ammonium sulfate is demanded by the fertilizer and chemical industries. If sufficiently large crystals of ammonium sulfate can not be produced, an alternative is to compact the smaller crystals. Based on available literature information (Compaction, 1983), a process for compacting the smaller size product was developed and used to estimate the additional costs.

For the compaction process, the smaller size ammonium sulfate is delivered to a fresh feed hopper. The crystals are weighed and then delivered to the compactors, which are two rolls that are

hydraulically operated so that the materials passing between the rolls are compressed into flakes. The flakes are broken to desired sizes by a specially designed coarse crusher. Materials from the crusher are screened to extract the desired particle size. Oversize materials from the screens are returned to the crusher, fines from the screens are recirculated to the compactor. The sized product is usually passed through a rotary drum to remove the rough edges from the product.

## RESULTS AND DISCUSSION

The total cost and individual unit costs for the installed equipment for the basic process are shown in Table 1. The fixed capital and working capital investments are shown in Table 2. Table 3 lists the costs for raw material, operating cost, other cost, in-plant (transfer) cost and the ex-gate cost. These estimates assume the cost of ammonia in Illinois is \$200 per ton (Green Markets, March '95) and the total material cost is to be \$58.40 per ton of product. The operating cost was calculated to be \$26.14 per ton (Table 3). Since the calcium carbonate will be recycled, the process receives a credit for the cost of the limestone that is replaced (based on \$15 per ton for limestone). The calculations show this credit should be \$11.60 per ton of ammonium sulfate. The net production cost of the ammonium sulfate without considering capital cost is \$72.94 per ton. The capital costs shown in Table 2, were used to determine the cost of depreciation, taxes, and insurance. With these costs the subtotal cost was estimated to be \$86.58. In addition, the cost of interest, the minimum equity return, and pre-tax incentive return need to be added. These costs are calculated using the capital cost in Table 2. These data show the total in-plant cost to be \$106.78 per ton of ammonium sulfate. This in-plant cost of ammonium sulfate is used in the next section to calculate the plant sale price for compacted material. A general sales and administrative cost (\$4.00 per ton of ammonium sulfate) added to the in-plant cost, yields an estimated sale price of \$110.78 of no compaction is needed to produce crystals of the required size.

**Price Comparison with Commercial Products-** As recorded in "Green Markets," a respected publication of the fertilizer industry, the March price for granular ammonium sulfate in Illinois for the past 3 years were \$137 to \$154/ton, \$134 to \$141\$/ton, and \$123 to \$135 \$/ton for 1995, 1994, and 1993 respectively. These data give an average market price of granular ammonium sulfate of \$138/ton.

The average market price of granular ammonium sulfate (\$138/ton) exceeds the estimated cost of ammonium sulfate from the proposed process (\$110.78/ ton), by a margin of 25 percent. However, there is a margin of error of  $\pm 30$  percent in the cost estimates. The product could have a very competitive price if the crystals produced fall in the required size range (1.2 to 3.3 millimeters) for granular products.

**Costs Including Compaction-** If desired size crystals can not be produced, compaction of the smaller crystals will be necessary. A cost estimate (Tables 4 to 6) was made including the additional cost of compaction. In this estimate, the raw material costs include ammonium sulfate at the in-plant transfer price (\$106.78/ton) and a binder cost at \$0.6/ton. The total raw material cost, therefore, is \$107.38 per ton. The additional operating cost for compaction was estimated to be \$8.40 per ton. After capital costs, taxes and insurance were added, the total estimated production cost was \$126.49/ ton. This results in an estimated in-plant price of \$143.09 per ton. When general sales and administrative cost are added, the sale price would be \$147.09 per ton. This is about \$10 per ton higher than the average March commercial price for the last 3 years, but, close to the average March price for this year (\$146).

## CONCLUSIONS AND RECOMMENDATIONS

Considering that the costs are for a conceptual plant design and as such subject to the usual margin of error, the results of this study indicate that the proposed process could be economically feasible if crystals of 1.2 to 3.3 millimeters can be produced without compaction. Because the average market price of granular ammonium sulfate (\$138/ton) exceeds with the estimated cost of ammonium sulfate without compaction from the proposed process (\$110.78/ ton), a profit margin of 25 percent could be possible. If smaller crystals are produced and compaction is necessary, cost estimates show a negative margin between the market price and the sale price. This study indicates the need both to refine the crystallization process and, perhaps, to find other potential markets for

the by-product calcium carbonate.

#### ACKNOWLEDGMENT & DISCLAIMER

This report was prepared by the authors through a research project supported, in part, by grants made possible by the U.S. Department of Energy (DOE) cooperative Agreement Number DE-FC22-PC92521 and the Illinois Coal Development Board (ICDB) and the Illinois Clean Coal Institute (ICCI). Neither the authors nor any of the subcontractors nor the U.S. DOE, ISGS, ICDB, ICCI nor any person acting on behalf of any of them assumes any liability with respect to the use of, or for damages resulting from the use of, any information disclosed in this report. The authors are grateful to Drs. J. H. Goodwin and S.B. Bhagwat, staff members of the ISGS, for their reviewing of this manuscript.

#### REFERENCES

- Bennett, R.C., Product Size Distribution in Commercial Crystallizer, *Chemical Eng. Prog.* Vol. 58, No. 9, 1962.
- Chou, M.I. M., J.A. Briunius, Y.C. Li, J.M. Lytle, and M. Rostam-Abadi, Manufacture of ammonium sulfate fertilizer from FGD-gypsum, preprint of the American Chemical Society Fuel Chem. Div., Chicago, August 20-24, 1995.
- Compaction, IFDC Technical Bulletin EFD6-T-25, June, 1983.
- Green Markets, March 1993, March 1994, and March 1995.
- Hillenbrenner, J., City Water Light and Power, Springfield, IL via telephone during March 1995.
- Higson, G.I., The Manufacture of Ammonium Sulphate from Anhydrite, *Chemistry and Industry*, 750-754, September 8, 1951.
- Journal of Chemical Engineering* 1993 and 1994. Economic Factors Relating to Cost of Plant Facilities.
- Kachelman, D.L., Fluid Fertilizer Reference Manual, TVA Report Y 210 November, 1989.
- Kenton, J.R., Fertilizer Components: Ammonium Sulfate, *Encyclopedia of Chemical Processing and Design*, vol 21, 274-283, Marcel Dekker, Inc., New York, 1985.
- Kirk-Othmer, *Encyclopedia of Chemical Technology*, fourth edition, vol. 2, 706, John Wiley & Sons, New York, 1992.
- Meline, R.S., H.L. Faucett, C.H. Davis, and A.R. Shirley Jr., Pilot-Plant Development of the Sulfate Recycle Nitric Phosphate Process, *Ind. Eng. Process Des. Develop.*, vol. 10, 257-264, 1971.
- Perry, R.H., and D.W. Green editors, *Perry's Chemical Engineers Handbook*, 6th Edition, McGraw Hill, 1984.
- Sauchelli, V., Fertilizer Nitrogen, American Chemical Society's Series of Chemical Monographs, Reinhold Publishing Co, 1964.

Table 1. Plant Equipment and Costs

Unit	Dollars
Absorption Tower	\$ 625,000
Tower, Air filter, Pumps, and handling equipment and Installation	\$1,500,000
Gypsum Converter	\$ 330,000
Equipment, Foundations, auxiliary equipment, and Installation	\$ 330,000
Concentrator	
Auxiliaries and Incidentals Equipment and Installation	\$2,330,000
Crystallizer	
crystallizer, centrifuge, and Installation	\$2,100,000
Solids Handling	
Dryer, Cooler, Screens Elevator, Conveyors, Dust controlling system, and Installation	
<b>Total</b>	<b>\$6,885,000</b>



Table 2. Plant Capital Investment for Ammonium Sulfate (non-granular) Production at a capacity of 422 tons per day or 150,000 tons per year.

ITEM_NO.	COST (x 10 <sup>6</sup> \$)
A. Fixed Capital - Depreciable	21.985
■ Installed Equipment	6.885
■ Design Engineering, etc.	3.400
■ Site Preparation	1.000
■ Auxiliary Facilities	3.525
■ Dry Storage	2.000
■ Incidental and Overheads	5.175
B. Fixed Capital - Nondepreciable	0.94
■ Spare Parts, 2% A	0.44
■ Land	0.50
C. Working Capital - Nondepreciable	1.293
■ 30 - day raw materials cost	0.739
■ 15 - day Inventory Value	0.554
D. Total Fixed Capital (A+B)	22.923
E. Total Capital (A+B+C)	24.218
F. Average Capital (0.53 A+B+C)	13.885

Table 3. Cost estimate - Production of ammonium sulfate crystalline fertilizer from FGD-gypsum at a capacity of 422 tons per day or 150,000 tons per year (355 days)

Raw Materials	Units	Units/ton	\$/Unit	Cost, \$/ton
Ammonia	TON	0.292	200	58.40
Gypsum	TON	1.328	0	0
Carbon Dioxide	TON	0.374	0	0
<b>Total raw material cost</b>			<b>A</b>	<b>58.40</b>
<b>Operating</b>				
Direct labor (calculated 0.408 man-hrs/ton X \$17.00/hr)				6.94
Maintenance (calculated 0.15mh/ton x \$20/hr)				3.00
Utilities (estimated)				12.61
Supplies (20% maintenance)				0.60
Plant overhead (\$/ton) calculated				2.99
Operating costs,			<b>B</b>	<b>26.14</b>
Cr. for rec. limestone (0.773 tons/ton (NH <sub>4</sub> ) <sub>2</sub> SO <sub>4</sub> X \$15/ton)			<b>C</b>	<b>11.60</b>
<b>Net operating cost</b>			<b>B - C</b>	<b>14.54</b>
<b>Capital</b>				
Depreciation 6.7% A (from Table 2)/TY*				9.82
Ins. & taxes 2.5% (A+B, from Table 2)/TY				3.82
<b>Total capital cost</b>			<b>D</b>	<b>13.64</b>
<b>Others</b>				
Interest 10% F (from Table 2) X 0.5/TY				4.62
Minimum equity return 0.075x F(from Table 2) X 0.5/TY				3.47
Pre-tax incentive return 0.075x E(from Table 2)/TY				12.11
<b>Total other costs</b>			<b>E</b>	<b>20.20</b>
In-Plant Transfer				
<b>General Sales &amp; administrative cost</b>			<b>F</b>	<b>4.00</b>
<b>Ex-gate price, \$/ton</b>		<b>A + (B - C) + D + E + F</b>		<b>\$110.78</b>

\*TY is tons of ammonium sulfate produced in one year.

Table 4. Compaction Plant Equipment and Costs

Unit	Dollars
Compaction Plant Equipment, Installation, Additional building, offsites	\$ 16,000
<b>Total</b>	<b>\$ 16,000</b>

Table 5. Additional Capital investment for Compaction of Ammonium Sulfate

ITEM	COST (x 10 <sup>6</sup> \$)
A. Fix Capital - Depreciable	17.47
■ Installed Equipment	16.00
■ Start-up Allowance	0.48
■ Construction Capital	0.99
B. Fixed Capital-Nondepreciable	0.00
C. Working Capital-Nondepreciable	2.11
30 - day raw materials cost	1.37
15 - day Inventory Value	0.74
D. Total Fixed Capital (A+B)	17.47
E. Total Capital (A+B+C)	19.58
F. Average Capital (0.53A+B+C)	11.36

Table 6. Cost estimate - Production of ammonium sulfate crystalline fertilizer from FGD-gypsum at a capacity of 422 tons per day or 150,000 tons per year (355 days), with compaction.

Raw Materials	Units	Units/ton	\$/Unit	Cost, \$/ton
Ammonium Sulfate	TON	1	106.78	106.78
Binder	TON	0.01	0.60	0.60
<b>Total raw material cost</b>			A	107.38
<b>Operating</b>				
Direct labor (calculated 0.408 man-hrs/ton X \$17.00/hr)				2.70
Maintenance (calculated 0.15mh/ton x \$20/hr)				1.00
Electricity (45kwh/ton X \$ 0.10 /kwh) (estimated)				3.00
Supplies (20% maintenance)				0.20
Plant overhead (\$/ton) calculated				1.50
<b>Total operating costs,</b>			B	8.40
<b>Capital</b>				
Depreciation 6.7% A (from Table 2)/TY*				7.80
Ins. & taxes 2.5% (A+B, from Table 2)/TY				2.91
<b>Total capital cost</b>			C	10.71
<b>Others</b>				
Interest 10% F (from Table 2) X 0.5/TY				3.97
Minimum equity return 0.075x F(from Table 5) X 0.5/TY				2.84
Pre-tax incentive return 0.075x E(from Table 5)/TY				9.79
<b>Total other costs</b>			D	16.60
<b>In-Plant Transfer</b>				
<b>General Sales &amp; administrative cost</b>			E	4.00
<b>Ex-gate price, \$/ton</b>			<b>A + B + C + D + E</b>	<b>\$147.09</b>

\*TY is tons of ammonium sulfate produced in one year.

**COAL COMBUSTION FLY ASH--  
OVERVIEW OF APPLICATIONS AND OPPORTUNITIES IN THE USA**

Sam Tyson, P.E. and Tom Blackstock, P.E.  
Executive Director and Director of Technical Services  
American Coal Ash Association, 2760 Eisenhower Ave, Suite 304,  
Alexandria, VA 22314

Keywords: fly ash, CCBs, ash utilization

**ABSTRACT**

The American Coal Ash Association, Inc. (ACAA) is an organization representing the coal combustion byproducts industry. Since 1968, the goal of ACAA has been to gain recognition and acceptance of coal fly ash as an engineering material on par with competing virgin, processed and manufactured materials by advancing uses that are technically sound, commercially competitive and environmentally safe.

An annual survey of coal-burning electric utilities is conducted by ACAA to determine the quantities of coal fly ash produced and used in the USA. In 1993 approximately 43.4 million metric tonnes (47.8 million short tons) of coal fly ash were produced. Approximately twenty-two percent or 9.5 million metric tonnes (10.5 million short tons) was used while the remaining portion was deposited in disposal areas. The major markets for coal fly ash include cement and concrete products, structural fills, road base stabilization, flowable fills, mineral filler in asphalt, grit for snow and ice control, grouting, coal mining applications, and waste solidification and stabilization.

**INTRODUCTION**

An annual survey of electric utilities is conducted by ACAA to determine the quantities of CCBs produced and used in the United States (Ref. 1; ACAA 1994). In 1993 approximately 80.3 million metric tons (88.5 million short tons) of CCBs were produced in the U.S. in the form of fly ash, bottom ash, boiler slag and flue gas desulfurization (FGD) material. Approximately twenty-two percent of the combined production of these byproducts was used, while the remaining portion was deposited in disposal areas. Production and use quantities for these byproducts are summarized in Table 1.

**Table 1. Production and Use of Coal Ash.**  
[1993 Data; Million metric tons (million short tons)]

	Fly Ash	Bottom Ash	Boiler Slag	FGD Mat'l
Production	43.4 (47.8)	12.8 (14.2)	5.6 (6.2)	18.4 (20.3)
Use	9.5 (10.5)	3.8 (4.2)	3.1 (3.4)	1.0 (1.1)
% Use	22%	30%	55%	6%

It is clear from survey data gathered by ACAA over the years that the annual use of 18.2 million metric tons (20.3 million short tons) of CCBs represents a major continuing effort by a number of parties, including the electric utility producers of CCBs and their marketers. It is equally clear, however, that

significant quantities of CCBS are not used each year. Therefore it is essential for ACAA to promote the use of coal combustion byproducts in numerous applications that are technically sound, commercially effective and environmentally safe.

CCBs are engineering materials and are similar in use to competing virgin, processed and manufactured materials. CCBS are affected by local and regional factors, which include production rates, processing and handling costs, transportation costs, availability of competing materials, seasonal adjustments, and the experience of materials specifiers, design engineers, purchasing agents, contractors, and other construction professionals.

#### COAL FLY ASH APPLICATIONS

It is instructive to consider the total amounts of coal fly ash that are used in the leading markets based on ACAA's 1993 survey results, presented in Table 2.

**Table 2. Summary of Fly Ash Uses.**  
[1993 Data; Million metric tons (million short tons)]

Fly Ash Uses	Million Tons	
	Used	Percent
Cement and concrete products	6.17(6.8)	65.0
Road base/subbase	0.91(1.0)	9.5
Structural fills, embankments	0.83(.91)	8.7
Flowable fill	0.34(.38)	3.6
Filler in asphalt mixes	0.10(.11)	1.0
Grouting	0.02(.02)	0.2
Waste stabilization	0.40(.44)	4.2
Other	0.76(.84)	17.8
Total Used	9.53(10.5)	100.0

#### CEMENT AND CONCRETE PRODUCTS

In 1993 approximately 6.17 million metric tons (6.8 million short tons) of coal fly ash was used in the U.S. in cement and concrete products (Ref. 1; ACAA 1994). The amount of coal fly ash in typical structural concrete applications ranges from 15 to 35 percent by weight, with amounts up to 70 percent for massive walls and girders, concrete road bases, and dams.

Various concrete mixtures are produced with coal fly ash including 2500 to 6000 psi normal weight and lightweight concretes, high strength (>6000 psi) concrete, early strength concrete for form removal requirements, low-slump paving concrete, controlled low strength material (CLSM), and architectural concrete.

With the principal exception of high strength concrete, all of these coal fly ash concrete mixtures are routinely air-entrained for added workability and for resistance to freezing and thawing. A state-of-the-art report on the use of coal fly ash in concrete has been prepared by the American Concrete Institute (ACI) (Ref. 2; ACI, 1987). Fly ash for use in concrete is covered in an ASTM specification (Ref. 3; ASTM, 1994).

#### Flowable Mixtures (CLSM)

ACI Committee 229 deals with certain flowable grout-like materials under a general designation, "Controlled Low Strength Materials" (CLSM). Such materials have compressive strengths of 1200 psi or less, as currently defined by ACI, and may also represent a wide range of fly ash contents. Applications of CLSM currently being reviewed by ACI 229 include but are not limited to: backfills, structural fills, insulating fills, road and slab base, trench bedding and so on.

While flowable mixtures can be produced without fly ash, it is very easy demonstrate that economical mixtures with the most desirable characteristics, including flowability, cohesiveness, minimal bleeding, and controlled density, can be produced only with fly ash in combination with relatively small amounts of portland cement. The percentage of fly ash used in grout mixtures may be in a wide range from 20 to 95 percent by weight.

CLSM mixtures can be proportioned to provide a desired flowability and unit weight, and to have a compressive strength which is equal to or greater than that of well-compacted soil. CLSM can also be designed for a maximum strength where future excavation may be necessary.

The use of CLSM flowable mixtures is open to numerous innovative engineering solutions for everyday problems that would otherwise be viewed as traditional soils backfilling and foundations problems.

#### **ROAD BASE AND SUBBASE**

The ACAA pavement manual (Ref. 4; ACAA, 1991) offers pavement design engineers, materials engineers, and construction managers guidance in the design and construction of low- to high-strength "pozzolanic stabilized mixture" ("PSM") base and subbase layers having coal fly ash in combination with activators, aggregates and water.

To capture the long-term service and cost-saving features of PSM design, the document details a mixture proportioning system, a thickness design procedure, and established mixing and construction techniques. The user can apply the contents of this manual with professional advice to produce satisfactory pavement structures of acceptable uniformity in accordance with current specifications and QC/QA requirements of individual state departments of transportation.

The ACAA pavement manual is supported by guidelines and guide specifications in four chapters that comprise a publication (Ref. 5; AASHTO, 1990) developed by a Joint Committee of the American Association of State Highway and Transportation Officials (AASHTO), the Associated General Contractors (AGC) and the American Road and Transportation Builders Association (ARTBA).

## STRUCTURAL FILLS

Fly ash may be used as a borrow material in the construction of fills. When the fly ash is compacted in lifts, a structural fill is constructed which is capable of supporting buildings or other structures. An embankment is constructed when the fly ash is placed to support roads or to impound water. The size of structural fills/embankments that have previously been constructed with fly ash ranges from small fills, consisting of a few thousand cubic yards of material covering less than one acre, to fills covering several acres.

When used in structural fills and embankments, fly ash offers several advantages over soil and rock. These advantages include low unit weight and high shear strength. The compacted maximum dry density of fly ash is typically within the range of 70 to 105 pcf. Compared to fills of silty sand that have a compacted maximum dry density of about 115 pcf, placing fly ash over weak, compressible foundation soils results in lower total settlement. Hauling costs will also be reduced because there is less tonnage for a given volume of fill. Another significant characteristic of fly ash used as a fill material is its strength. Compacted fly ash is as strong or stronger than many compacted soils. Class C ash will self-harden, resulting in a fill that is stronger than most compacted soil.

## REGULATORY AND LEGISLATIVE ISSUES

The U.S. Environmental Protection Agency (EPA) issued a final regulatory determination on the four large volume CCB streams from coal-burning electric utilities in August 1993 (Ref. 6; EPA, 1993). The EPA determined that "large volume wastes from coal-fired electric utilities pose minimal risks to human health and the environment. Therefore, it is unnecessary to manage these wastes as hazardous." This determination continues to provide for the management of CCBs under Subtitle D of the Resource Conservation and Recovery Act (RCRA).

The U.S. Department of Energy (DOE) issued a report on the barriers to the increased use of CCBs in July 1994 (Ref. 7; DOE, 1994). The report is expected to have a significant effect on the use and management of CCBs. This report was developed as the result of the Energy Policy Act of 1992 [Public Law No. 102-486, October 24, 1992] in which DOE was charged with the task of conducting a detailed and comprehensive study on the "institutional, legal and regulatory barriers to increased utilization of CCBs by potential governmental and commercial users".

The recommendations in the DOE report address a network of related barriers which can be overcome only through cooperative efforts among federal and state government and industry. ACAA has addressed many of these issues in its business plan and will expand these activities in the future.

## SUMMARY

Throughout ACAA's history, its goal has been to gain recognition and acceptance of CCBs as engineering materials on par with competing virgin, processed and manufactured materials by advancing CCB uses that are technically sound, commercially competitive and environmentally safe. It is clear from survey data gathered by ACAA over the years that the annual use of some 18.2 million metric tons (20 million tons) of CCBs represents a

major continuing effort by a number of parties, including CCB producers, marketers and other organizations. It is equally clear, however, that significant quantities of CCBs are not used each year. Therefore it is essential for ACAA to promote the use of coal combustion byproducts in numerous applications.

#### REFERENCES

1. 1993 Coal Combustion Byproduct Production and Consumption, American Coal Ash Association, Inc., Washington, D.C., 1994, 1 page.
2. Use of Fly Ash in Concrete, American Concrete Institute, Committee 226 Report, ACI Materials Journal, Detroit, September-October 1987, pages 381-409.
3. Standard Specification for Fly Ash and Raw or Calcined Natural Pozzolan for Use As a Mineral Admixture in Portland Cement Concrete, ASTM C 618, American Society for Testing and Materials, Philadelphia, PA, 1994, 3 pages.
4. Flexible Pavement Manual, American Coal Ash Association, Inc., Washington, D.C., 1991, 64 pages plus Appendices.
5. Guidelines and Guide Specifications for Using Pozzolanic Stabilized Mixture (Base Course or Subbase) and Fly Ash for In-Place Subgrade Soil Modification, AASHTO/AGC/ARTBA Joint Committee, Task Force 28 Report, 1990, 40 pages plus Appendices.
6. Environmental Fact Sheet, Large-volume Wastes from Coal-fired Electric Utilities Exempt as Hazardous Waste, EPA530-F-93-014, United States Environmental Protection Agency, Washington, D.C., August 1993, 2 pages.
7. Barriers to the Increased Utilization of Coal Combustion/Desulfurization Byproducts by Governmental and Commercial Sectors, DOE Office of Fossil Energy, Morgantown Energy Technology Center, July 1994, 36 pages.

## HIGH STRENGTH LIGHT WEIGHT FLY ASH COMPOSITES

Gerald P. Wirtz, John M. Bukowski, H. Dale DeFord and Asif Ahmed  
Department of Materials Science and Engineering  
University of Illinois at Urbana-Champaign  
Urbana, IL 61801

Keywords: Fly Ash, Extrusion, Monolithic Honeycombs

### ABSTRACT

Fly ash is a valuable by-product of coal-fired power generation. After beneficiation to recover valuable minor constituents, a fine powder of spherically shaped, largely amorphous, calcium aluminosilicate particles is left, which is well suited for processing into useful shapes without further milling. With the addition of Portland cement or lime, the formed body may be autoclaved at near 200°C to form a pozzolanic bond between fly ash particles. Light weight is achieved by extruding honeycomb structures with parallel open channels. Maximum strength to weight ratio would be achieved for pore-free honeycomb walls. The strength to density ratio of the honeycomb structures is independent of weight, since both weight and strength decrease linearly with fractional channel volume.

### INTRODUCTION

The long range objective of this effort is to utilize fly ash from coal burning power plants to manufacture lightweight construction materials. To this end, selected processing methods from advanced ceramics and advanced cement based materials were adapted, chief among them the extrusion of fine monolithic honeycomb structures. This technology was developed by the automotive industry for the manufacture of cordierite catalyst carriers. While high surface area and high thermal shock resistance are the principal attributes of interest in automotive exhaust catalyst carriers, high strength, low weight, thermal insulation and acoustic isolation are of primary interest in construction materials. Building components envisioned range from brick size blocks to 4x8 foot panels, as well as a variety of posts, beams and other configurations. The size of components which could be produced in this study was severely limited by the extrusion equipment.

Since the density of silicates is largely dominated by the silica network, which is the lightest component, achieving densities less than about 2.3 gm/cc in a silica rich composition such as fly ash or Portland cement can only be achieved by incorporating open space in the structure. The most obvious way of accomplishing this is to increase the porosity of the final body. The difficulty is that the strength of a ceramic body decreases exponentially with porosity according to the Ryshkewitch equation<sup>1,2</sup>:

$$\sigma = \sigma_0 e^{-\beta P} \quad (1)$$

where  $\sigma_0$  is the theoretical, pore-free strength of the material,  $P$  is the fractional porosity and  $\beta$  is an empirical constant for the material. Rewriting equation (1) for a honeycomb structure, the theoretical strength will be multiplied by the area fraction of the solid walls in cross section and the porosity in the equation will be replaced by the porosity within the solid walls:

$$\sigma = A_w \sigma_0 e^{-\beta P_w} \quad (2)$$

Defining the macroscopic bulk density of the honeycomb structure,  $\rho_b$ , as the weight of the honeycomb divided by its total volume, the area fraction of the walls perpendicular to the extrusion direction can be expressed as the ratio of this bulk density to the density of the walls,  $\rho_w$ . The pore fraction in the walls will be one minus the solid fraction in the walls. The solid fraction in the walls will be equal to the ratio of the wall density to the theoretical density of the fly ash. The Ryshkewitch equation may thus be expressed for a honeycomb structure as:

$$\sigma = \frac{\rho_b}{\rho_w} \sigma_0 e^{-\beta \left(1 - \frac{\rho_w}{\rho_0}\right)} \quad (3)$$

Rewriting equation (3) slightly, the macroscopic strength to density ratio may be related to the maximum, pore free, strength to density ratio and the fractional porosity of the honeycomb walls.

$$\frac{\sigma}{\rho_b} = \frac{\sigma_0}{\rho_0} \frac{e^{-\beta P_w}}{(1 - P_w)} \quad (4)$$

Equation (4) says that for zero porosity in the honeycomb wall, the strength to density ratio of the honeycomb will correspond to the pore free strength to density ratio. For a given wall porosity, the density of the honeycomb will be determined by the relative dimensions of the channels and walls in the honeycomb, which are fixed by die design. The strength will scale in exactly the same fashion.

Achieving any given macroscopic density requires fabricating honeycombs with specific numbers of channels and wall thicknesses. Assuming square channels of side  $d$  with wall thickness  $t$ , the

relationship between honeycomb dimensional parameters and macroscopic bulk density may be written:

$$\frac{t}{d} \left( 1 + \frac{1}{n} \right) = \sqrt{\frac{1}{1 - \frac{\rho_b}{\rho_w}}} - 1 \quad (5)$$

where  $n$  is the total number of channels in the sample being tested. In the limit of large  $n$ , the bulk density may be expressed as a function of the wall density and the ratio of the wall thickness to the channel width.

$$\rho_b = \rho_w \left[ 1 - \frac{1}{\left( 1 + \frac{t}{d} \right)^2} \right] \quad (6)$$

The fundamental approach to achieving high strength lightweight honeycomb structures is to develop the extrusion process to produce honeycombs with dense, thin walls, and to develop the curing process to further enhance the wall density in the final structure. Extrusion parameters, such as pressure and extrusion rate, affect the green density of the extruded body, which will be reflected in the final solidified product. Similarly, plasticizers, water and lubricants may be transient components of the green body. In leaving the body during firing or drying they leave behind void spaces in the structure which can affect the ultimate density. The relative fractions of these components added to promote extrudibility affects the ultimate wall density of the honeycomb structure, and thus the ultimate strength. Porosity in the green extruded body may be reduced during autoclaving by filling the pores with reaction products. In fired bodies, the porosity is reduced by normal vitreous sintering, with concomitant changes in sample dimensions. In autoclaved bodies, residual plasticizer and binder will affect both density and the hydration reaction.

#### SAMPLE PREPARATION

The minimum achievable wall thickness in the extruded honeycomb will be limited by the maximum particle size of the fly ash in the mix. The raw fly ash was therefore separated by sieving into fractions of particle size greater than 90  $\mu\text{m}$  and less than 90  $\mu\text{m}$ . The latter comprised greater than 98 weight % of the ash and was used exclusively in the extrusion of honeycombs.

Extrusion batches need to have sufficient plasticity to allow flawless knitting of the honeycomb walls during extrusion, with sufficient stiffness to support thin walls (0.05-0.13 cm). This required optimization of the water and binder additions, adequate shredding of the batch before extrusion to enable thorough de-airing, and optimization of the speed of extrusion. Methyl cellulose (MC), with additions of polyethylene oxide (PEO) to improve water retention during extrusion, was the initial binder studied, in the range of 0.5-5 weight % of solids<sup>3</sup>. Binders and plasticizers used in hydrothermally processed honeycombs had to be chosen to avoid adversely affecting the hydration reactions which are responsible for strength development. Methyl cellulose exhibits limited solubility in hot water, and appeared to impede the development of strength during autoclaving. In subsequent batches, the methyl cellulose was replaced by a mixture of hydroxyethyl cellulose (HEC) and polyethylene glycol (PEG), with small amounts of PEO again added. These exhibit higher solubility in hot water, and higher strengths were attained on autoclaving.

All specimens were extruded on a 40 ton, vacuum de-airing, piston extruder (Loomis Products Co.), with dies fabricated in house. A 2.54 cm square honeycomb with rounded corners and a nominal wall thickness of 0.16 cm, has evolved as the standard test piece, but different configurations have been fabricated. Fly ash samples containing 10-100 weight % Type I Portland cement (OPC, ordinary Portland cement) were hydrated at 60°C for 1-7 days after extruding, then autoclaved at temperatures from 150-210°C for 1-24 hours.

#### RESULTS AND DISCUSSION

Variables whose effects on strength were systematically measured included composition, reaction temperature and reaction time. Within very broad limits, the effects of each of these variables on strength mirrored their effects on sample porosity. Figure 1 shows the measured crushing strength as a function of fractional porosity of sintered samples, determined from density measurements on the samples. The data are plotted on a semilogarithmic plot in accordance with equation (1). Samples in Figure 1 were prepared by a variety of methods, and with a variety of compositions. Samples sintered at moderate temperatures (800-1000°C) contained up to 5% borax or boric acid as a sintering aid. Pure fly ash samples were sintered at temperatures above 1100°C. High porosity cast samples were foamed and contained 5-10% calcium lignosulfonate as a foam stabilizer<sup>4</sup>. Extruded cylinders contained from 1-5% methyl cellulose. The autoclaved honeycombs shown in the figure for comparison contained 40% OPC. The solid line in Figure 1 represents the linear regression fit of the data to equation (1). The empirical constants in equation (1) corresponding to this fit are:  $\sigma_0 = 615 \text{ MPa}$ , and  $\beta = 6.6$ .

The data on extruded honeycombs in Figure 1 are plotted as if the open channels in the honeycomb were ordinary porosity, and can be seen to exhibit as much as an order of magnitude greater strength for a given weight than the cast cylinders. This serves to illustrate the advantage of the honeycomb configuration for achieving high strength, light weight materials, but the

appropriate equation to compare these data qualitatively would be equation (4). Alternatively, the crushing force can be divided by the cross-sectional area of the wall to give the wall strength, which can be plotted against the wall porosity to compare directly with Figure 1. Figure 2 shows such a plot of wall strength vs. wall porosity, where the wall porosity was determined by mercury intrusion porosimetry. Included in the plot is the solid line representing equation (1) with the values of the empirical constants determined from Figure 1. Two different compositions are represented in Figure 2, 30% and 40% OPC, both autoclaved at 180°C, the former for 12 hours, the latter for 13 hours. The average strength of the latter is higher, as might be anticipated in light of the higher OPC content and longer curing time. The difference, however, can be attributed entirely to the difference in porosity of the two compositions. They both fall within the anticipated range for agreement with equation (1), with empirical constants determined from fly ash samples fired at high temperatures and containing no Portland cement. Mechanistically, this indicates that the strength of samples in both figures was determined by the strength of the fly ash framework. The mechanism of bonding between fly ash particles did not affect the strength achieved. The fact that in all autoclaved samples tested thus far the wall porosity has exceeded 20% is of major relevance to the direction of future work.

Figure 3 shows electron micrographs of fractured surfaces of autoclaved honeycomb samples containing 40 and 10 weight % Portland cement. In the former, the fracture is transgranular, passing through the fly ash grains. The transgranular nature of the fracture in Figure 3A is particularly notable when the fracture passes through hollow fly ash particles (cenospheres), as illustrated by the arrow (a) on the micrograph, but is also evident by the general planar character of the fracture surface, with little evidence that the body is made up of spherical fly ash particles. The fracture has the appearance of a typical ceramic fracture surface. In Figure 3B, by comparison, the fracture is clearly intergranular. The spherical fly ash particles are evident as the fracture proceeded between the particles, leaving many of the spherical surfaces unmarred. The 40 % OPC composition of Figure 3A exhibited about 8 times the crushing strength of the 10 % OPC sample of Figure 3B. In samples where the weakness of the bonding between particles permitted intergranular fracture, the strength was no longer represented by equation (1), at least not with the empirical constants determined from Figure 1.

Figure 4 shows an electron micrograph of the fracture surface of a sintered fly ash honeycomb, such as used to determine the empirical constants in equation (1) from Figure 1. Fracture is again clearly transgranular, and the only evidence of the spherical nature of the initial particles is the spherical pores observed where the fracture passed through the hollow cenospheres. The bonding mechanism in this case can be seen to be vitreous sintering, whereas the bonding in the samples of Figure 3 was the pozzolanic reaction of the lime in the Portland cement with the free silica at the surface of the fly ash particles to form tobermorite and other calcium silicate hydrates.

## CONCLUSIONS

High strength light weight honeycomb composites can be formed by autoclaving a mixture of fly ash and Portland cement, as well as by typical ceramic firing of fly ash honeycomb structures at high temperatures. A comparison of strength and density of fly ash honeycomb samples with typical construction materials is presented in Table 1. Materials are listed in order of increasing strength to density ratio, which has been normalized to 1.0 for construction grade pine. Typical values for both autoclaved and sintered honeycombs from the present study are shown. Differences in the strength to density ratio of honeycomb samples is determined primarily by differences in the fractional porosity of the walls for honeycombs with very different compositional modifications, as well as processing variations. This is attributed to the fact that the fracture mechanism is the same and occurs through the fly ash grains. This indicates that the solid grains form the weak link in the system and that the strength is proportional to the cross sectional area fraction of the solid, which may be converted directly to density of the wall. When intergranular fracture was observed, as seen in Figure 3(B), the same strength-porosity relationship no longer held.

In no case was the wall density greater than 80% of theoretical for autoclaved honeycombs. With the experimentally determined value of  $\beta = 6.6$ , a wall porosity of 20% yields a strength to density ratio of only 33% of theoretical from equation (4). For the honeycomb samples in Table 1, the total porosity, as determined by mercury intrusion porosimetry, was about 25 and 18% respectively. These values would predict a maximum normalized strength to density ratio of about 5. There is clearly still much room for improvement. Future efforts will be concentrated on the attainment of greater wall densities, i.e., eliminating the porosity in the walls.

## REFERENCES

1. E. Ryshkewitch, "Compression Strength of Porous Sintered Alumina and Zirconia- 9th Communication to Ceramography," *J. Amer. Cer. Soc.*, **36**, [2] 65-68 (1953)
2. W. Duckworth, "Discussion of Ryshkewitch Paper", *J. Amer. Cer. Soc.*, **42**, [8] 68 (1953)
3. H. D. DeFord and G. P. Wirtz, "Extrusion of Lightweight Construction Materials from Fly Ash", *Ceram. Eng. Sci. Proc.* **14**[1-2] pp. 298-308 (1993)
4. J. R. Wylder, Processing and Characterization of a Foamed Fly Ash Construction Material, M.S. Thesis, University of Illinois at Urbana-Champaign (1989)

**Table 1. Strength/density comparison with typical construction materials**

Material	Bulk Density (gm/cc)	Compressive Strength		Normalized Strength/Density Ratio
		(MPa)	(psi)	
Aerated Concrete	0.69	4.4	640	0.10
Concrete	2.2	35	5100	0.25
Clay Brick	2.3	45	6500	0.31
Steel	7.8	455	66000	0.91
Pine	0.48	30	4350	1.00
Autoclaved Honeycomb	1.13	95	14000	1.36
Fired Honeycomb	1.32	155	22500	1.89

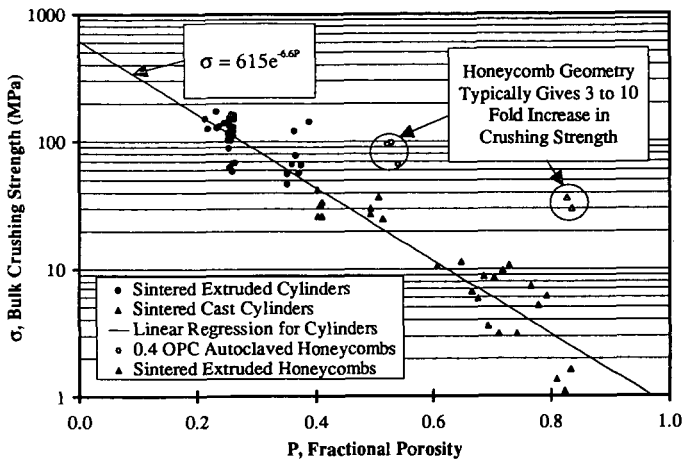


Figure 1. Crushing strength vs. fractional porosity for fired fly ash bodies.

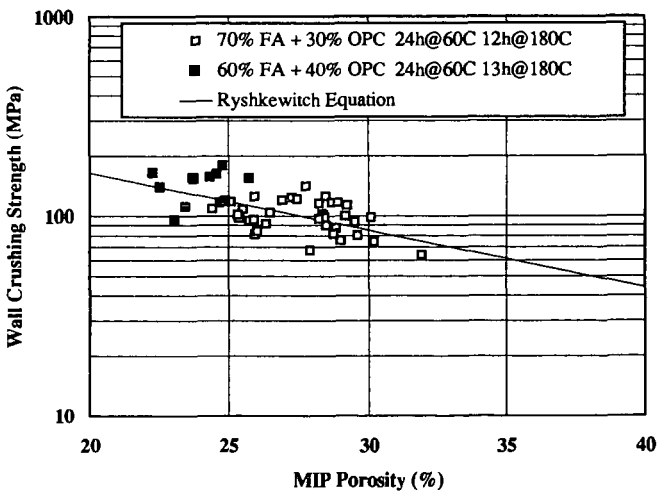
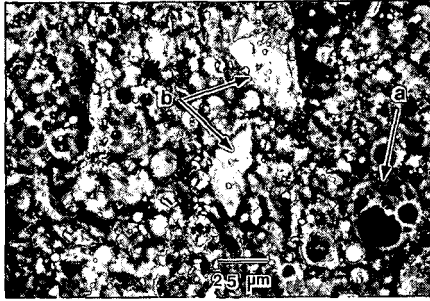
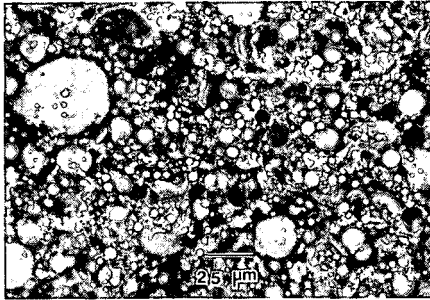


Figure 2. Crushing strength of the honeycomb wall vs. fractional porosity of the wall.



(A) SEM of 40 % OPC fly ash honeycomb illustrating transgranular fracture surface.  
 (a) Cross section of hollow fly ash particle (cenosphere)  
 (b) Unhydrated cement paste grains



(B) SEM of 10 % OPC fly ash honeycomb illustrating intergranular fracture surface. Note spherical morphology retained by fly ash particles in fracture surface.

Figure 3. Scanning electron micrographs of fracture surfaces of fly ash honeycombs illustrating (A) transgranular fracture in 40% OPC composition, and (B) intergranular fracture and pullout in 10% OPC composition.

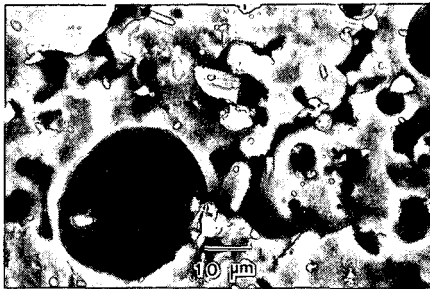


Figure 4. Scanning electron micrograph of fracture surface of pure fly ash honeycomb densified by firing at 1075 °C for 24 ho

## UTILIZATION OF FLY ASH IN STRUCTURAL AND DECORATIVE CERAMIC PRODUCTS

R. E. Hughes, G. B. Dreher, M. R. Rostam-Abadi, D. M. Moore, and P. J. DeMaris  
Illinois State Geological Survey  
Champaign, IL 61820

Keywords: Utilization of fly ash, manufacture of bricks, decorative and structural ceramics

### INTRODUCTION AND BACKGROUND

The main objective of this study is to promote the use of fly ash from electric power plants in Illinois in the manufacture of bricks. Fly ash that is produced during the burning of coal represents a continuing disposal problem and thus a disincentive to coal's use. Each year, approximately  $5 \times 10^6$  metric tons of fly ash are produced from burning Illinois coals. Use of brick clays for ceramic products in the Illinois area amounted to about  $0.5 \times 10^6$  metric tons in 1994. If significant amounts of fly ash were used in the manufacture of fired-clay products such as brick, the fly ash disposal problem would be reduced, a valuable construction product would be created, and mining of brick clays would be slowed. Furthermore, the clay minerals in the green bricks are dehydroxylated during the firing process. Fly ash already has been through dehydroxylation, therefore this energy for dehydroxylation is "saved" during brick manufacture. Six tasks were defined to meet our objectives: 1) manufacture bricks that contain 20 wt% or more of fly ash under normal plant-scale conditions; 2) measure the firing characteristics of mixtures created by using extremes in chemical composition of Illinois fly ashes and brick clays and shales; 3) from those measurements, derive equations that predict the firing characteristics of any mixture of clay and fly ash; 4) optimize mixtures of brick clays with sources of fly ash near existing ceramic plants; 5) perform tests to determine the leachability of toxic constituents, if any, from the bricks; and 6) integrate the results of tasks 1 and 2 with preliminary engineering and market assessments to evaluate the feasibility of large-scale use of fly ash in fired-clay products.

Although general principles guiding the selection of raw materials for fired-clay products have been known for many years (Grim, 1962; Burst and Hughes, 1994), the complexity of the firing reactions suggested the need for improved methods (Hughes, 1993) of predicting the firing behavior of bricks and related products. This need is emphasized by our plant-scale experiments with Colonial Brick Company in Cayuga, Indiana. Because we lack adequate methods for prediction, we were obliged to resort to trial-and-error methods for our first plant-scale test. The improvement of methods for predicting the properties of fired fly ash, shale, and underclay mixtures is now possible, and an approach based on mineral content is expected to provide significant improvements in accuracy of prediction.

An improved method for the prediction of coal ash fusion temperature is an important outcome expected from this study. Laboratory methods for the estimation of coal ash fusion temperature are the same as those for testing ceramics. As for ceramic products, the methods used to predict coal ash fusion temperatures are notoriously inaccurate because they are based on chemical analyses. For the ceramic and the coal ash fusion tests, we suggest that equations based on mineralogical composition will yield improved accuracy and precision. A mineralogical basis for prediction also should elucidate the underlying mechanisms that cause problems and suggest solutions to those problems.

The manufacturing process at most brick plants is similar. Clays are blended in a crusher, pulverized, and water and dispersant are added in a pugmill to produce a plastic clay that can be extruded. The preferred raw materials for these fired-clay products occur as underclays and roof shales associated with coals. They contain variable amounts of three basic groups of minerals: 1) relatively low-melting-point illite, mixed-layered illite/smectite (I/S), and chlorite; 2) refractory kaolinite and mixed-layered kaolinite/expandables (K/E); and 3) somewhat refractory quartz. Common red-firing roof shales generally contain nearly ideal amounts of group 1 and 2, and adequate firing characteristics are obtained by blending clay-rich shale zones with sandier, quartz-rich zones. The mixture must contain enough clay minerals for adequate plasticity, and enough coarse grains to insure access of air so that the core of the brick is completely oxidized in the shortest possible time during firing.

Many of the shales immediately above coals (roof shales) in the Illinois Basin are nearly ideal raw materials. Their progressive change in grain size from smaller at the base to larger at the top, makes blending for plasticity and firing rate possible. Many underclays below Illinois coals are fireclays, which, unlike shales, contain more kaolinite and significant amounts of K/E. This K/E gives special properties to fired-clay products because it is composed at the atomic scale of a 2:1 clay mineral layer that melts at relatively low temperatures and a 1:1 layer that is refractory. Quartz also can have special properties during firing. Quartz acts as a framework grain in normal shale and fireclay bricks, but at high enough temperature, it can melt and act as a bonding agent. For these reasons, predictive equations must be made with different groupings of mineralogical factors.

Background information on clays for bricks and similar ceramic products is summarized in Hughes (1993). Slonaker (1977) showed that acceptable bricks were produced from feeds of 72% fly ash, 25% bottom ash, and 3% sodium silicate. A general discussion of the properties of fly ash that are important to its use in fired-clay products can be found in Kurgan, Balestrino, and Daley (1984). They reported that the high alkalinity of fly ash from Illinois could improve dispersion of the clay body during mixing and extrusion of bricks. Talmy *et al.* (1995) described two approaches for using 100% fly ash plus additives to make bricks.

The development and use of leaching tests for the measurement of environmental impacts of coal combustion residues was reviewed in Dreher, Roy, and Steele (1993). Improved methods for the mineralogical characterization of coal samples and coal combustion wastes have been described recently by Kruse *et al.* (1994) and Moore, Dreher, and Hughes (1995). Characterization methods for clay minerals are described in Hughes and Warren (1989) and Moore and Reynolds (1989).

If successful, the results obtained from this project should lead to an attractive solution, from an environmental and economic standpoint, for the recycling of fly ash to high-value marketable products. Success also could revitalize the ceramics industry in Illinois, an industry that has been in decline for several years. Finally, high-calcium fly ashes may be useful for capture of sulfur that volatilizes from brick clays during firing.

## EXPERIMENTAL PROCEDURES

Brick manufacturing tests were made using fly ash from Illinois Power Company's Wood River Power Plant. Colonial Brick Company conducted a manufacturing run of about 5,000 bricks without fly ash and a similar number with about 20% fly ash added to the normal clay. A batch of bricks of each of the two compositions was fired side-by-side in the kiln and tested for standard market specifications, *i.e.*, samples of the bricks with and without fly ash were taken during firing to provide a measure of "clearing" or time required to completely oxidize the core of the bricks. Water absorption tests and of color determinations also were made by Colonial Brick on the fired products. These proved acceptable to them.

Mineralogical characterization was made by X-ray diffraction (XRD), X-ray fluorescence, instrumental neutron activation analysis, and a step-wise dissolution in 2N HCl with inductively coupled plasma (ICP) analysis of the supernates and XRD of the solids. The X-ray diffractometer was a Scintag® unit that used a Cu tube, a  $\theta/\theta$  goniometer, a 12-position sample changer, a liquid N<sub>2</sub>-cooled germanium detector, and computer controls and peak deconvolution programs. The XRF spectrometer was a Rigaku® wavelength-dispersive model that has a chromium radiation source and a 6-position sample changer. The ICP spectrometer was a Jarrell-Ash Model 1155V vacuum spectrometer equipped with 35 element channels. Instrumental neutron activation analysis was accomplished by irradiating solid samples in a neutron flux at the University of Illinois Advanced TRIGA MARK II reactor. After suitable decay times, gamma-ray spectra for various elements in the irradiated sample were recorded by a multi-channel analyzer. For step-dissolution experiments, about 1 gm samples were ground in a McCrone micronizer®, ultrasonically dispersed in 50 mL of H<sub>2</sub>O, and added to 550 mL of 2N HCl. Stirred, 40 mL aliquots were extracted from the suspension at selected intervals for up to a month, *e.g.*, 2 hr, 4 hr, 8 hr, etc. To increase solubility, one fireclay sample was heated to 500°C to dehydroxylate most of its kaolinite and K/E.

Leaching procedures developed by Dreher *et al.* (1988, 1989) are being used to determine the extent to which constituents of environmental concern might leach from bricks exposed to weathering. Batch extraction and wet-dry leaching experiments, in which the substrate is exposed to deionized water for a given time period, are being conducted on crushed and whole bricks. To simulate exposure in a building, five faces of the bricks are protected from leaching by application of an epoxy coating. Batch extraction experiments are being conducted at a solution-to-solid ratio of 4:1 for periods of 3, 10, 30, 90, and 180 days. Each solid was analyzed chemically and mineralogically prior to extraction and leaching experiments, and the solids from the 180-day extraction will be analyzed mineralogically.

Estimates of the composition of Illinois fly ashes were obtained from Moore, Dreher, and Hughes (1995) and by calculation from the composition of coals reported by Demir *et al.* (1994). These two sources of fly ash chemical composition were plotted in various ways to find the range of composition available as a replacement for clays in bricks (Figs. 1 and 2). Results from laboratory and plant tests will be analyzed by factorial analysis and regression analysis to obtain equations that measure the effect on fired properties of additions of each of the basic components from the raw materials.

## RESULTS AND DISCUSSION

**Plant-scale tests.** The results of the production run were somewhat unexpected. During firing, we expected the fly ash to increase gas movement into and out of the bricks, but the reverse occurred. Essentially, the fly ash decreased the rate of oxidation. The bricks with fly ash also had noticeably more "scumming," which also was unexpected. This scumming causes a white to cream-colored dusting on the outside of the bricks and is mostly due to the migration of calcium sulfates to the surface during drying, firing, or both. We will attempt to confirm this assumption with chemical analyses. The problem can be corrected by adding barium carbonate, or possibly by moistening the fly ash and precipitating the salts, or it may be possible to simply select a fly ash with a smaller calcium sulfate content. A benefit resulting from the effect of fly ash on gas permeability was the lack of an expected increase in water absorption by the products. In general, the bricks from the manufacturing run were within local and regional market specifications. However, the scumming reduces their marketability.

On a matter of importance to the plant operator, the amount of dust associated with unloading fly ash at Colonial Brick was an unexpected problem that must be solved because of environmental regulations. It may be possible to wet the ash at the power plant or use pneumatic facilities at the brick plant.

**Characterization of materials.** The mineralogical and chemical analyses of clay and fly ash samples are given in Tables 1 and 2. The shales used are typical red-firing Pennsylvanian shales, which are common as the roof shale of most coals. At Colonial Brick Company's pit, about 30 ft of roof shale overlies a 6-12 in carbonaceous or coaly zone, which overlies about 6 ft of fireclay. The coaly zone may be equivalent to the Colchester (No. 2) Coal. Our second-year collaborator, Marseilles Brick Company, mines shale and fireclay from different pits. The shale is middle or upper Pennsylvanian and the fireclay occurs in the Cheltenham Formation, immediately below the underclay of the Colchester Coal.

For the approximately 25,000 samples of ceramic clays that have been collected since 1930 at the Illinois State Geological Survey, a database was constructed for this study. This database lists locations and material types. The location and selection of fly ash standards proved more difficult than the selection of clays. Data for each of the coals in Demir *et al.* (1994) were modified in an Excel® spreadsheet to estimate the chemical composition of fly ash from each of these coals (Figs. 1 and 2). The chemical composition of 8 fly ash samples that were part of the characterization study by Moore, Dreher, and Hughes (1995), and the chemical analyses of the fly ash and brick clays used in this investigation, were added to the spreadsheet and plotted (Figs. 1 and 2).

Most fly ashes contain more iron and calcium than brick clays (Figures 1 and 2). Because they were fused, the fly ashes may differ in the degree to which chemical constituents are segregated between phases and glass. However, to represent the range of available materials, we selected fly ash compositions that were relatively rich in: 1)  $\text{SiO}_2 + \text{Al}_2\text{O}_3$ , 2)  $\text{Fe}_2\text{O}_3$ , and 3) CaO. Differences in the contents of these constituents represent the important compositional variation for most Illinois fly ashes. In order to better understand the relationship between the chemical and mineralogical contents of coals, we plan to calculate regression equations of the chemical and mineralogical contents of the Illinois Basin Coal Sample Program (IBCSP) coals (Kruse *et al.*, 1994) and use those equations to estimate the mineralogical content of the 34 commercial coals of Demir *et al.* (1994).

Figure 2 shows that  $\text{SiO}_2:\text{Al}_2\text{O}_3$  is nearly constant. This ratio ranges from 1.9 to 3.6 with a mean of about 2.5 in the data set of Demir *et al.* (1994), and a range of 2.3 to 3.9 with a mean of about 2.5 in the data of Moore, Dreher, and Hughes (1995). The differences in the contents of CaO,  $\text{Fe}_2\text{O}_3$ ,  $\text{K}_2\text{O}$ , and  $\text{Na}_2\text{O}$  in fly ashes and brick clays account for most of the significant variation in these materials. For purposes of selecting standards for optimization studies, the fly ash used in production runs this year (Table 2) can be used to represent fly ashes that are rich in  $\text{SiO}_2$  and  $\text{Al}_2\text{O}_3$ . Samples 2 and 8 from the set of fly ashes analyzed by Moore, Dreher, and Hughes (1995) can be used to represent CaO-rich and  $\text{Fe}_2\text{O}_3$ -rich types, respectively. We selected and analyzed two standard optimization clays from Marseilles Brick Company.

**Step-dissolution analysis and optimization.** We believe that the solution to the problem of predicting the firing behavior of mixtures of materials depends on the accurate measurement of the major and minor mineral phases that make up a material. For unfired materials, XRD analysis of the mineral content is the technique of choice. However, some of the clay minerals are difficult to determine accurately, and we have chosen step-dissolution methods with ICP and XRD analyses to improve the determinations (Cicel and Komadel, 1994; Moore, Dreher, and Hughes, 1995). Figures 3 and 4 show the results of step-dissolution analyses of shale samples used at Colonial Brick Company. Because chlorite has two octahedral sites that can be occupied by Al, Fe, or Mg, it is the most difficult non-mixed-layered clay mineral to determine by XRD. In addition, of the minerals of concern in the shale, it is the most soluble in HCl. Therefore, XRD analyses of the solid fraction of the samples showed a decrease in chlorite content as time of reaction in 2N HCl increased (Fig. 3). Similarly, results of elemental analyses of the supernates recorded the increase in chlorite-forming elements with increased reaction time (Fig. 4). These plots of elemental concentration versus time can be used to calculate a structural formula of the chlorite in the sample and will make the optimization equations more accurate. The formula for chlorite derived from Fig. 4 is  $\text{Al}_{1.6}\text{Fe}_{2.9}\text{Mg}_{1.4}\text{Mn}_{0.1}\text{Si}_{3.0}\text{Al}_{1.0}\text{O}_{10}(\text{OH})_8$ .

After chlorite has been dissolved, step dissolution analysis of fireclays and shales becomes difficult because of the low solubility of the minerals remaining in the system. There are no easily dissolved minerals in fireclay and fly ash samples, therefore this becomes a major analytical problem. For fireclays, only 3 to 5% of the untreated sample was dissolved. A pre-treatment at 500°C increased the solubility of kaolinite and K/E, and gave meaningful estimates of the composition of those phases. To improve the method, it appears that we will have to grind the samples longer, leave them in acid longer, increase the strength of the acid, increase the temperature, or use some combination of these methods to dissolve all the amorphous material from fly ash samples.

**Future studies.** Recent studies of the firing behavior of bricks and related materials suggested that we may need to expand the number of tests used to measure fired-clay properties. This expansion will add tests for shrinkage, rate of burnout, hardness, strength, pyrometric cone equivalent (PCE), color, and water adsorption. Many of these determinations can be done on the samples used for PCE analysis and most of the tests would increase the analytical costs only moderately. The amounts of CaO,  $\text{CaSO}_4$ , and  $\text{Fe}_2\text{O}_3$  (from pyrite and marcasite) in some fly ashes are too large to be used for manufacture many ceramic products. The excess calcium from these sources can be corrected for by adding water in the cooling part of the firing cycle. This method was used in the manufacture of bricks known as "Chicago Commons." The scumming problem from calcium sulfates in fly ash may be solved by adding 5-15% water to the fly ash and eliminating it by processing fly ashes into various fractions. Both the color and lower melting

point caused by high levels of  $\text{Fe}_2\text{O}_3$  are best adjusted for by increasing the quartz and/or kaolinite content of the clay-shale. Problems with  $\text{SO}_2$  emissions are common in brick production, and we plan to test high-Ca fly ash for its ability to capture sulfur from the clays during firing.

## SUMMARY AND RECOMMENDATIONS

Additions of fly ash to bricks at the 20% level in plant-scale tests increased scumming and "burn-out" problems, but, contrary to our expectations, failed to increase water absorption. Although these problems are not expected to cause insurmountable difficulties, better characterization of the mineralogical composition of fly ashes is needed to find solutions to such problems.

Characterization of the clays used at Colonial and Marseilles Brick Companies showed that they are typical of the Pennsylvanian-age clays associated with coals of the Illinois Basin. A computer database of approximately 25,000 ceramic clays of Illinois was constructed, and the database of chemical composition of marketed Illinois coals reported in Demir *et al.* (1994) was processed to estimate the composition of fly ash that would be produced from burning each of those coals. The chemical composition of the eight fly ash samples from the study of Moore, Dreher, and Hughes (1995) also were added to a composite database. Characterization by XRD, XRF, INAA, and step-dissolution/ICP analyses of the fly ashes, shales, fireclays, green bricks, and fired bricks showed that the fly ashes contained more CaO and  $\text{Fe}_2\text{O}_3$  than the brick clays. However, there is a wide range of chemical composition and an unknown variation in the mineralogical content of fly ashes. Low solubilities of minerals in fly ashes and fireclays made it difficult to use the step-dissolution method for the mineralogical characterization of those materials. Preheating fireclays to dehydroxylate kaolinite and mixed-layered kaolinite/expandables (K/E) in fireclays and more intense grinding of fly ashes seemed to give adequate step-dissolution results. Environmental leaching studies are being conducted to evaluate the leaching of potential pollutants.

To broaden the comprehensiveness of the fundamental studies, future studies will include determinations of water absorption, shrinkage, rate of burnout, hardness, color, and pyrometric cone equivalent (PCE) on mixtures of fireclay, fly ash, and shale. To reduce  $\text{SO}_2$  emissions from brick clays, fly ashes rich in Ca will be tested to determine the amount of sulfur that can be captured during firing. Comparisons between the composition of fly ash calculated from the elemental compositions of coals and the actual fly ash samples and between predicted and actual coal ash fusion temperatures will be made to assess the accuracy of predictive methods from this study.

## ACKNOWLEDGMENTS

The authors gratefully acknowledge the Illinois Department of Commerce and Community Affairs, Illinois Coal Development Board, Illinois Clean Coal Institute, and the U.S. Department of Energy. We also thank our project officer Dr. Daniel D. Banerjee, and Robert R. Frost and John D. Steele for chemical analyses.

## REFERENCES

- Burst, J.F. and R.E. Hughes. 1994. Clay-Based Ceramic Raw Materials; In D.D. Carr, (ed.), 6<sup>th</sup> Edition, Industrial Minerals and Rocks, Soc. Mining Eng., Denver, CO, 317-324.
- Cícel, B., and P. Komadel. 1994. Structural Formulae of Layer Silicates: Quantitative Methods in Soil Mineralogy, Soil Science Society of America Miscellaneous Publication, p. 114-136.
- Demir, I., R.D. Harvey, R.R. Ruch, H.H. Damberger, C. Chaven, J.D. Steele, and W.T. Frankie. 1994. Characterization of Available (Marketed) Coals from Illinois Mines: III State Geological Survey Open File Series No. 1994-2, 16 p.
- Dreher, G. B., M. Rostam-Abadi, W. R. Roy, D. M. Rapp, S. C. Mravik, I. Demir, J. D. Steele, R. R. Ruch, and R. L. Berger. 1988. Factors Affecting Management of ISGS Aggregate Flotation Waste Solids. Final Technical Report to the Illinois Coal Development Board, Center for Research on Sulfur in Coal, Champaign, IL, 29 p.
- Dreher, G. B., M. Rostam-Abadi, W. R. Roy, J. D. Steele, D. M. Rapp, W.-T. Chen, and R. L. Berger. 1989. Factors Affecting Management of Fine-Coal Cleaning Waste Solids. Final Technical Report to the Illinois Coal Development Board, Center for Research on Sulfur in Coal, Carterville, IL, 50 p.
- Dreher, G. B., W. R. Roy, and J. D. Steele. 1993. Geochemistry of FBC Waste-Coal Slurry Solid Mixtures, Final Technical Report to the Illinois Coal Development Board, Center for Research on Sulfur in Coal, Carterville, IL, 26 p. and Appendix, 10 p.
- Grim, R.E. 1962. Applied Clay Mineralogy. McGraw-Hill Book Company, Inc., New York, 422p.
- Hughes, R. E., B. L. Bargh, and W. A. White. 1983. The Expansion and Weathering of Brick. Proceedings of the 18<sup>th</sup> Forum on the Geology of Industrial Minerals, Bloomington, Indiana. 183-197.
- Hughes, R. E. and R. L. Warren. 1989. Evaluation of the Economic Usefulness of Earth Materials by X-Ray Diffraction. Proceedings of the 23<sup>rd</sup> Forum on the Geology of Industrial Minerals, R. E. Hughes and J. C. Bradbury, eds., North Aurora, Illinois, May 11-15, 1987,

- Hughes, R.E., and P.J. DeMaris. 1992. DUCCR Program Final Report: Utilization of Coal Conversion Residues; Coal Combustion Residues Management Program, Southern Illinois University, Carbondale, IL, 49p.
- Hughes, R.E. 1993. Clay Resources Associated with Lower Pennsylvanian Coals. In Preprints Symposium on Economic Resources of the Lower Pennsylvanian of the Illinois Basin, Indiana Geological Survey, Bloomington, IN, November 10-11, 1993, 29-37.
- Kruse, C.W., R.E. Hughes, D.M. Moore, R.D. Harvey, and J. Xu, 1994, Illinois Basin Coal Sample Program, Final Technical Report to the Illinois Coal Development Board, Center for Research on Sulfur in Coal, Cartersville, IL.
- Kurgan, G.J., J.M. Balestrino, and J.R. Daley. 1984. Coal Combustion By-Products Utilization Manual, Volume 1: Evaluating the utilization option. Electric Power Research Institute, CS-3122, Volume I, Research Project 1850-1, Palo Alto, CA, 3-1 to 3-34.
- Moore, D. M., G. B. Dreher, and R. E. Hughes. 1995. New Procedure for X-Ray Diffraction Characterization of Flue Gas Desulfurization (FGD) and Fluidized Bed Combustion (FBC) By-Products. Final Technical Report to the Coal Combustion Residues Management Program, Carbondale, IL.
- Moore, D. M. and R. C. Reynolds Jr. 1989. X-Ray Diffraction and the Identification and Analysis of Clay Minerals, Oxford University Press, New York, 337 p.
- Slonaker, J. F. 1977. The Role of Fly Ash Brick Manufacturing in Energy Conservation; Coal Research Bureau, College of Mineral and Energy Resources, W. Virginia University, Report No. 149, Morgantown, WV, 6p.
- Talmy, I. G., C. A. Martin, A. G. Cade, and W. D. Sudduth. 1995. Utilization of Fly Ash in Building Materials; *In Abstracts for the International Ash Utilization Symposium*, Lexington, KY, October 23-25.

Table 1. Mineralogical composition (%) of Colonial Brick and Marseilles Brick clays

Sample	I/S	I	K/E	K	C	Q	Kf	Pf	Cc	Py	Other
sh3521A	10	25	0	8.9	11	39	0.1	5.9	0.0	0.0	
sh3521C	15	19	0	5.7	6.5	47	0.2	6.0	0.0	1.5	
fc3521B	45	10	0	7.8	0.0	34	0.0	1.3	0.0	2.1	
fc3521BR	45	10	0	7.8	0.0	33	0.0	1.3	0.0	3.1	
fc3538A	19	3.4	22	7.6	0.0	44	0.4	0.0	0.0	2.9	
sh3538B	17	18	0	3.1	7.4	48	0.4	5.8	0.0	0.0	
sh3528A	17	16	0	5.3	5.1	47	1.3	8.2	0.0	0.0	
sh3528AR	15	19	0	6.1	7.6	46	0.0	6.8	0.0	0.0	
fc3528B	27	6.9	14	7.6	2.1	37	0.0	1.7	0.8	2.1	
fc3528BR	33	6.4	13	7.0	1.6	34	0.4	1.4	0.8	2.0	
sh3548A	19	21	0.0	4.0	7.7	42	0.8	5.4	0.0	0.0	apatite?
sh3548AR	19	20	0.0	3.9	7.5	44	0.6	5.8	0.0	0.0	apatite?
fc3548B	18	2.5	32	9.0	0.0	33	0.0	0.0	0.4	4.5	
flsh3538E						11					glass, M, H
flsh3538F						12					glass, M, H
shbr3521F	16	19	0.0	5.7	5.8	48	0.2	5.6	0.0	0.0	apatite?
shbr3521G	17	27	0.0	6.5	8.3	36	0.0	4.9	0.0	0.0	apatite?
shbr3521J	15	20	0.0	4.9	7.7	46	0.4	5.3	0.0	0.0	apatite?
shbr3521K	15	19	0.0	4.0	6.4	50	0.7	5.6	0.0	0.0	apatite?
br3521D						25					glass, M, H
br3521E						21					glass, M, H
br3521H						27					glass, M, H
br3521I						28					glass, M, H

Key: Samples 3521, 3538 = Colonial Brick 3/94 and 4/95; samples 3528, 3548 = Marseilles Brick 10/94 and 6/95; I/S = mixed-layered illite/smectite; I = illite; K/E = mixed-layered kaolinite/expandables; K = kaolinite; C = chlorite; Q = quartz; Kf = K-feldspar; Pf = plagioclase feldspar; Cc = calcite; Py-Ma = pyrite-marcasite; M = mullite; H = hematite; R = repeat; sh = shale; fc = fireclay; flsh = fly ash; shbr = unfired brick; br = fired brick; (3521D, E, F, G = bricks with 20% fly ash; 3521H, I, J, K = bricks without fly ash).

Table 2. Chemical composition (%) of Colonial Brick Co. clays, Marseilles Brick Co. clays, and bricks from the manufacturing run at Colonial

Sample	SiO <sub>2</sub>	Al <sub>2</sub> O <sub>3</sub>	Fe <sub>2</sub> O <sub>3</sub>	CaO	MgO	K <sub>2</sub> O	Na <sub>2</sub> O	TiO <sub>2</sub>	LOI	P <sub>2</sub> O <sub>5</sub>	Sr	Ba	Zr
sh-3521A	61.33	17.7	6.52	0.57	1.9	3.09	1.08	0.98	6.44	0.16	0.14	0.53	0.23
shbr-3521C	60.81	17.66	6.47	0.6	1.91	3.07	1.07	0.97	6.82	0.16	0.15	0.54	0.23
sh-3538A	59.96	18.86	6.5	0.39	2.07	3.36	1.04	0.98	6.34	0.17	0.14	0.65	0.13
fc-3521B	57.47	21.37	4.71	1.67	1.47	2.68	0.35	1.1	7.98	0.16	0.25	0.44	0.25
fc-3538C	58.27	21.49	5.06	0.78	1.38	2.35	0.47	1.11	8.15	0.1	0.18	0.41	0.19
fc-3528A	59.22	26.18	1.99	0.31	0.5	0.96	0.04	1.27	8.93	0.06	0.16	0.09	0.29
sh-3528B	66.38	16.81	4.96	0.32	1.95	3.22	1.3	1.03	3.52	0.14	0.10	0.43	0.27
grbr1-3521F	61.09	18.18	6.12	0.88	1.78	2.83	1.04	1.01	6.27	0.17	0.20	0.62	0.17
grbr2-3521J	62.81	17.02	5.89	0.56	1.75	2.74	1.02	0.98	6.52	0.17	0.19	0.46	0.18
br1-3521D	64.71	19.71	6.68	0.86	1.95	3.08	1.08	1.07	0.13	0.18	0.21	0.69	0.18
br2-3521H	66.44	18.61	6.39	0.65	1.96	3.05	1.07	1.04	0.19	0.17	0.16	0.62	0.19
br2R-3521H	66.37	18.51	6.42	0.64	1.94	3.04	1.09	1.04	0.21	0.18	0.18	0.56	0.20
flsh1-3538E	54.5	25.5	6.39	2.55	1.29	2.22	1.13	1.34	3.42	0.19	0.75	1.27	0.24
flsh2-3538F	54.73	25.42	6.38	2.54	1.3	2.22	1.11	1.35	3.18	0.19	0.75	1.25	0.20

Key: Samples with clay numbers 3521 and 3538 are from Colonial Brick Co.; 3528 are from Marseilles Brick Co.; grbr1 = unfired brick with 20% fly ash; grbr2 = unfired brick without fly ash; br1 = fired brick with 20% fly ash; br2 and br2R = fired brick samples without fly ash; flsh1 and flsh2 are duplicate fly ash samples.

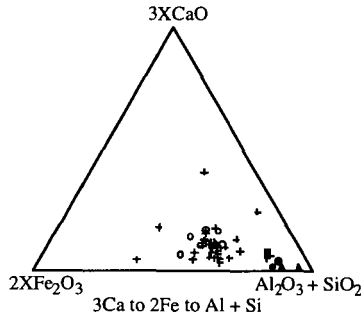


Figure 1. Triangular plot of CaO:SiO<sub>2</sub>+Al<sub>2</sub>O<sub>3</sub>:Fe<sub>2</sub>O<sub>3</sub>. Symbols: + = data set of Demir et al. (1994); o = data set of Moore, Dreher, and Hughes (1995); ● = Colonial Brick Company's shale and fireclay; ▲ = Marseilles Brick Company's shale and fireclay; ■ = fly ash used for tests at Colonial Brick.

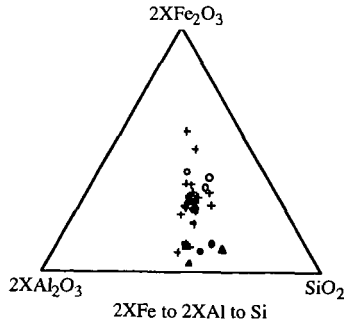


Figure 2. Triangular plot of Fe<sub>2</sub>O<sub>3</sub>:Al<sub>2</sub>O<sub>3</sub>:SiO<sub>2</sub>. Symbols: + = data set of Demir et al. (1994); o = data set of Moore, Dreher, and Hughes (1995); ● = Colonial Brick Company's shale and fireclay; ▲ = Marseilles Brick Company's shale and fireclay; ■ = fly ash used for tests at Colonial Brick.

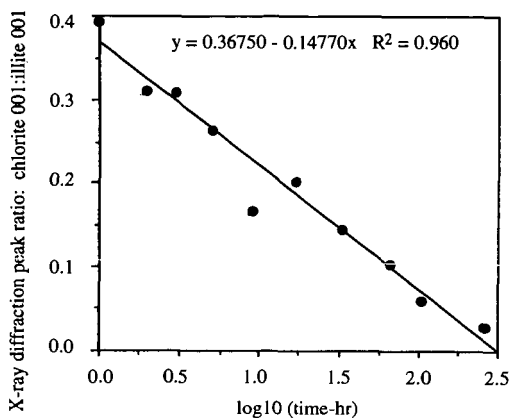


Figure 3. Plot of the XRD peak intensity ratio of the chlorite 001 to the illite 001 peaks from solid samples. This plot shows the dissolution of chlorite in 2N HCl with time. (See figure 4 for a plot of the dissolved species from chlorite.)

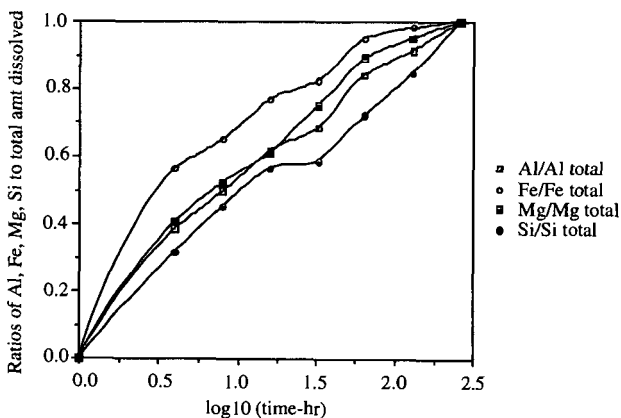


Figure 4. Plot of the ratio of Al, Fe, Mg, and Si ions in solution to the total amount of that constituent in solution at the end of the experiment. This plot shows variation in Al and Si versus Fe and Mg solution rate, which reflects the lower solubility of the tetrahedral sheet of the chlorite structure. The concentration when all chlorite has been dissolved gives a structural formula for the chlorite, *i.e.*,  $\text{Al}_{1.6}\text{Fe}_{2.9}\text{Mg}_{1.4}\text{Mn}_{0.1}\text{Si}_{3.0}\text{Al}_{1.0}\text{O}_{10}(\text{OH})_8$ .

## VALUABLE PRODUCTS FROM UTILITY FLY ASH

Joseph A. DeBarr<sup>1</sup>, David M. Rapp<sup>1</sup>, Massoud Rostam-Abadi<sup>1</sup> and Mark J. Rood<sup>2</sup>

<sup>1</sup>Illinois State Geological Survey, 615 E. Peabody Dr., Champaign, IL 61820

<sup>2</sup>University of Illinois, 3213 Newmark, 205 N. Mathews, Urbana, IL 61801

**Key Words:** fly ash utilization, activated carbon, magnetite

### INTRODUCTION

Fly ash is a potentially important engineering raw material that has yet to be extensively utilized. Of the 48 million short tons of fly ash produced in 1993 from burning coal in power stations in the U.S., only 22% was utilized, with the major use occurring in cement and concrete products [1]. Utilization of fly ash represents a potential for utilities to both reduce costs and increase revenues. A major barrier to fly ash use is its variable nature, both chemical and physical, due to differences in source coals, boiler design and stack removal processes.

Because the variability of fly ash is manifested in the diversity of its chemical and mineral components, a novel way of exploiting the variability would be to physically separate these components and use them as raw materials for the manufacture of various value-added materials. Figure 1 shows components that may be separated from fly ash, and some of their potential uses. For example, the reactive aluminosilicate glass could be reacted to microengineer zeolites or other high surface area phases, or to prepare structural and insulation components. Unburned carbon can be converted to activated carbons or carbon black, or used as a supplementary fuel. Iron oxides (magnetite) can be used as a raw material for making ferrites (magnetic ceramics), in heavy media coal cleaning equipment to provide a high specific gravity suspension, and as cement additives. Cenospheres, hollow spheres composed mostly of silica, alumina and iron oxides, can be used as polymer fillers, in light-weight ceramics and as low dielectric constant substrates.

Recovery of useful components from fly ash can improve the economics of fly ash utilization and can offset costs associated with disposal. The Illinois State Geological Survey (ISGS) has a program to find new uses for fly ash. One objective of this work is to investigate the potential of recovering adsorbent carbon, magnetite and cenospheres from fly ash. Removing these components may improve the quality of the remaining fly ash so that it can be used in cement and concrete products. In this paper, results of preliminary efforts to recover adsorbent carbons and magnetite from fly ash are described.

### EXPERIMENTAL

Fly ash was obtained from an Illinois utility burning high sulfur Illinois coal. The fly ash was sieved into plus 90- $\mu\text{m}$  and minus 90- $\mu\text{m}$  fractions. Only the plus 90- $\mu\text{m}$  fraction was used in this work. Ash composition (major and minor oxides) was determined by X-ray fluorescence (XRF) spectrometry. Samples were dried overnight at 110°C, then ignited at 1000°C for one hour to determine loss-on-ignition (LOI). The ignited sample was fused at 1000°C for 15 minutes with 50% lithium tetraborate/50% lithium metaborate flux and formed into a 30-mm diameter disk. The specimen was analyzed with a Rigaku model 3371 wavelength dispersive X-ray fluorescence spectrometer with an end-window rhodium X-ray tube.

Magnetic components were recovered by dispersing 500 grams of fly ash in one liter of water and stirring by hand to wet the sample fully. A plunger type hand magnet was used to recover magnetic components that were transferred to another vessel. The procedure was repeated until very little magnetic component was collected by the magnet. The concentrate was dried and weighed to determine the amount of sample obtained.

The unburned carbon in fly ash was concentrated in a two-step process involving sieving through a 170-mesh screen and cleaning the -170 mesh particles by oil agglomeration/froth flotation. Activation of the carbon concentrate was done to develop further the surface area and porosity of the sample. About 10 g of carbon concentrate was placed in a ceramic boat (1.9 cm x 1.2 cm x 7.5 cm) and centered in a 5 cm ID x 90 cm mullite tube in a Lindberg split-tube furnace. The sample was heated at 20°C/min to 950°C in flowing N<sub>2</sub>. The N<sub>2</sub> was replaced by 50% H<sub>2</sub>O/50% N<sub>2</sub> for 1 h. The sample was then cooled under N<sub>2</sub> to room temperature.

The SO<sub>2</sub> adsorption capacities of samples were determined by thermogravimetric analysis (Cahn TG-131). In a typical run, a 30-50 mg sample was placed in a platinum pan and heated at 20°C/min in

flowing  $N_2$  to 360°C to remove moisture and impurities. The sample was cooled to 120°C. Once the temperature stabilized, a mixture of gases containing 5%  $O_2$ , 7%  $H_2O$  and the balance  $N_2$  was substituted for the  $N_2$ . Once there was no further weight gain due to adsorption of  $O_2$  and  $H_2O$ ,  $SO_2$  was added in concentrations representative of a flue gas from combustion of high sulfur coal (2500 ppmv  $SO_2$ ). The weight gain was recorded versus time by a computerized data acquisition system.

Surface areas were determined from the amount of  $N_2$  adsorbed at 77 K using a dynamic sorption method in conjunction with a single point BET adsorption equation. Single point  $N_2$  BET surface areas were determined from  $N_2$  (77 K) adsorption data obtained at a relative pressure ( $P/P_0$ ) of 0.30 with a Monosorb flow apparatus (Quantachrome Corporation).

## RESULTS AND DISCUSSION

The results of analyses of the +90  $\mu m$  and -90  $\mu m$  fractions are shown in Table 1. The two major components of the fly ash, silica and alumina, were equally distributed between the two size fractions. Most other elements, except carbon (as evidenced by the LOI), are concentrated in the size fraction with smaller particle diameters. The majority of the carbon in this fly ash had particle diameters larger than 90  $\mu m$ .

### Magnetite

The magnetic concentrate represented about 1% of the feed fly ash. Microscopic evaluation of the concentrate revealed the material was black spherulites (about 90% of the sample) and that no magnetite crystals (octahedrons) were observable, suggesting the particles probably were composed of microcrystalline magnetite. X-ray diffraction spectrometry confirmed that the magnetic concentrate was predominantly magnetite. The spherulites were less magnetic than regular magnetite suggesting they also contained some nonmagnetic material. Semiquantitative analysis of the sample indicated that the concentrate was approximately 90% magnetite and most of the remainder was hematite. The spherulites were somewhat fragile, and could probably be easily ground. This could be a useful property if a simple grinding step could be done to liberate nonmagnetic material and provide a relatively pure microcrystalline magnetite product. Fly ash-derived magnetite has potential for application as a heavy medium in coal cleaning [2, 3]. It has been reported that the most effective magnetite for heavy medium cyclones is magnetite having a mean particle size of 12  $\mu m$  [4]. A process called the Micromag process was recently patented and specifies that a majority of the magnetite particles be less than 5  $\mu m$  in size.

### Carbon

The unburned carbon in fly ash was concentrated from about 3 wt% to about 70 wt% in this study. Screening at 170 mesh resulted in a 11.6% carbon concentrate (assuming all the LOI is attributed to carbon, Table 1), and flotation increased the carbon content to 70 wt%. Screening has been reported effective for concentrating carbon in fly ash [2] as has air classification [2] and electrostatic separation [5, 6]. Others have used froth flotation to prepare a concentrate of up to 56 wt% carbon [7].

The surface area of the carbon concentrate was about 11  $m^2/g$ . During activation, weight loss was 18%, and surface area of the carbon increased from 11  $m^2/g$  to more than 160  $m^2/g$ . It is known that surface area, corrected for ash content, increases monotonically during activation up to about 80% weight loss [8], suggesting that optimization of separation and activation steps may result in the production of even higher surface area carbons from fly ash.

A low-surface-area carbon has many potential applications. One such application would be in processes for removing air toxics from waste incinerator and utility flue gas [9, 10]. STEAG, a German-based multinational corporation, has licensed technology for carbon-based systems installed on commercial medical, hazardous and municipal waste incinerators in the European Community [9]. The carbon used in the STEAG process, Herdofenkoks, is an activated char produced from lignite, with pore surface area of 300  $m^2/g$  [11]. The  $SO_2$  adsorption capacity of a carbon is reported to be a reliable guide to acceptability in the STEAG process [12]. The kinetics of  $SO_2$  adsorption for a carbon prepared by the ISGS from Illinois coal [13] are compared in Figure 2 with that for Herdofenkoks. The ISGS activated carbon had a  $N_2$  BET surface area of only 110  $m^2/g$ , but had an  $SO_2$  adsorption capacity of 7% by weight after 4 h, almost twice that of the Herdofenkoks. Early pilot scale test results showed that the ISGS activated carbon was effective in the STEAG process. The activated carbon prepared in this study from fly ash adsorbs much more  $SO_2$  than either the ISGS or Herdofenkoks carbons (Figure 2), suggesting that it has potential for application in the STEAG process.

## CONCLUSIONS

A quality adsorbent carbon and a quality magnetite concentrate were recovered from an Illinois utility fly ash. There remains significant room for improvement in the quantity and quality of both these products recovered from fly ash. The quantity of recoverable cenospheres has not yet been evaluated. Co-recovery of cenospheres, currently a commercial product, could make the economics of processing fly ash even more attractive. Adsorbent carbons sell for up to \$2,500 per ton, magnetite for approximately \$60-\$70 per ton and cenospheres for as much as several hundred dollars per ton. Removing these valuable products from fly ash may improve the characteristics of the remaining ash for application in cement and concrete products. Future efforts will focus on recovery of products from fly ashes with a wide range of characteristics.

## ACKNOWLEDGMENTS

This work is to continue with support, in part, by grants made possible by the Illinois Department of Commerce and Community Affairs through the Illinois Coal Development Board and the Illinois Clean Coal Institute.

## REFERENCES

1. American Coal Ash Association, 1993, "Coal Combustion Byproduct (CCB) - Production and Use," pamphlet, American Coal Ash Association, Alexandria, VA.
2. Boux, J. F., 1969, "Canadians Pioneer New Fly Ash Processing System," *Minerals Processing*, 10:3.
3. Roy, N. K., Murtha, M. J. and Burnet, G., 1979, "Use of Magnetic Fraction of Fly Ash as a Heavy Medium Material in Coal Washing," Proceedings of the 5th International Ash Utilization Symposium.
4. Stoessner, R.D., Chedgy, D.G., and Zawadzki, E.A., 1988, "Heavy Medium Cyclone Cleaning 28x100 Mesh Raw Coal," from *Industrial Practice of Fine Coal Processing*, 1988 SME, Edited by R.R. Klimpel and P.T. Luckie, 57-64.
5. Makansi, J., 1994, *Power*, Aug, 37-41.
6. Inculet, I.I., Bergougnou, M. A. and Brown, J.D., 1977, "Electrostatic Separation of Particles Below 40 Micron in a Dilute Phase Continuous Loop," *Institute of Electrical and Electronic Engineers Transactions*, 1A-13:4.
7. Groppo, J.G., Robl, T.L. and McCormick, C.J., 1995, "A Selective Beneficiation Process for High LOI Fly Ash," Proceedings of the 1995 International Ash Utilization Symposium, Lexington, KY, October 23-25.
8. Lizzio, A.A and Radovic, L.R., "On the Usefulness of Total Surface Area for Predicting Carbon Gasification Reactivity Profiles", 19th Biennial Conference on Carbon, University Park, PA, 1989.
9. Brueggendick, H. and Pohl, F.G., 1993, "Operating Experience with STEAG's Activated Carbon Process-a/c/t<sup>TM</sup> in European Waste Incineration Plants," brochure from STEAG AG.
10. Tsuji, K. and Shiraishi, I., 1991, "Mitsui-BF Dry Desulfurization and Denitrification Process Using Activated Coke," in Proceedings of the EPRI SO<sub>2</sub> Control Symposium, Washington, D.C., p. 307.
11. Thielen, W. and Seipenbusch, J., 1992, "Flue Gas Cleaning with Activated Coke in Waste Incineration," *La Rivista dei Combustibili*, 46 (4), p. 129.
12. Rummenhol, V., 1994, Presentation to Illinois Coal Development Board, Illinois Clean Coal Institute and Illinois State Geological Survey, Champaign, IL, March 2.
13. Lizzio, A.A., DeBarr, J.A. and Kruse, C.W., 1995, "Development of Low Surface Area Char for Cleanup of Incinerator Flue Gas," Proceedings of the 22nd Biennial Conference on Carbon, San Diego, CA, p. 74.

Table 1. Composition of +90- $\mu\text{m}$  and -90- $\mu\text{m}$  fly ash (wt%).

Oxide	+90 $\mu\text{m}$	-90 $\mu\text{m}$
SiO <sub>2</sub>	45.91	44.86
Al <sub>2</sub> O <sub>3</sub>	25.15	26.91
Fe <sub>2</sub> O <sub>3</sub>	4.38	7.10
CaO	6.31	9.46
MgO	1.61	2.26
K <sub>2</sub> O	0.67	0.76
Na <sub>2</sub> O	0.91	1.37
TiO <sub>2</sub>	1.07	1.53
P <sub>2</sub> O <sub>5</sub>	1.12	2.12
MnO	0.01	0.01
SO <sub>3</sub>	0.43	0.71
SrO	0.17	0.32
BaO	0.24	0.47
Loss on Ignition (carbon)	11.62	1.75

# FLY ASH: AN INDUSTRIAL CHEMICAL RESOURCE

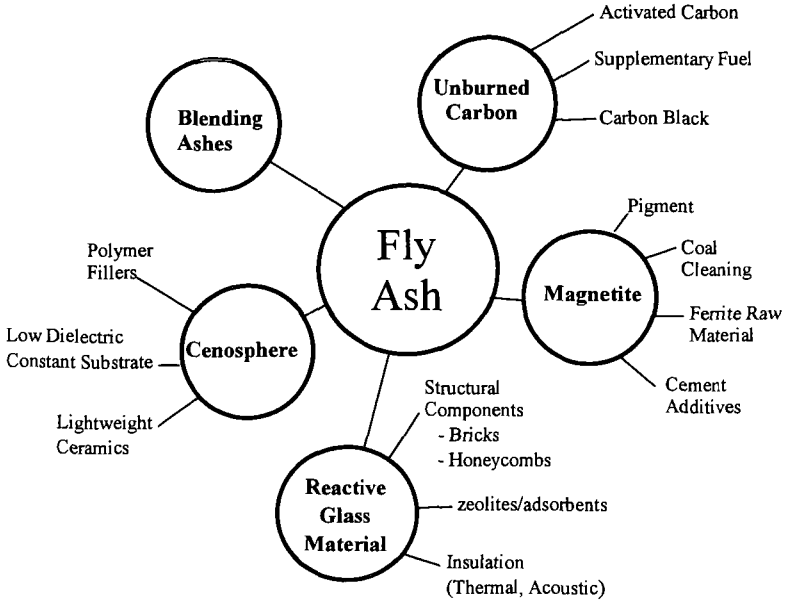


Figure 1. Components of fly ash.

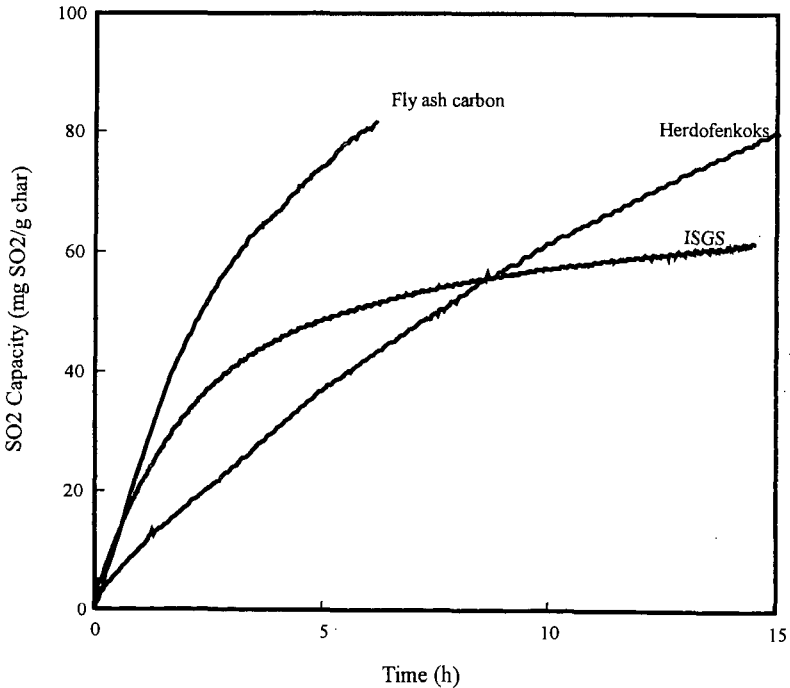


Figure 2. SO<sub>2</sub> adsorption for activated carbons.

# TRIBOELECTROSTATIC SEPARATION OF UNBURNED CARBON FROM FLY ASH

Heng Ban, Tian X. Li, John L. Schaefer and John M. Stencil  
Center for Applied Energy Research, University of Kentucky  
3572 Iron Works Pike, Lexington, KY 40511-8433, U.S.A.

Keywords: Fly ash; Triboelectrostatic; Beneficiation

## ABSTRACT

Due to differences in the surface physical and chemical properties of the carbon and ash, particles of unburned carbon and fly ash can be electrically charged to opposite polarity, and can be separated by passing them through an external electric field. A laboratory scale triboelectrostatic separation system was used to study fly ash beneficiation. Fly ash samples, characterized by size analysis and carbon content, were subjected to triboelectrostatic separation. The separated fractions were collected and evaluated for carbon content, and subjected to SEM. The results indicate the potential for applying dry separation technology for removing unburned carbon from coal ash.

## INTRODUCTION

Fly ash from pulverized coal power plants is a marketable commodity, provided acceptable levels of carbon are maintained.<sup>1</sup> With the advent of low NO<sub>x</sub> burners, the carbon content in fly ash in many cases has increased to the point where it is no longer marketable and becomes a disposal liability. Dry triboelectrostatic separation technology is just beginning to be applied to recover purified ash from fly ash streams which contain high concentrations of carbon.<sup>2</sup> Due to differences in the surface physical and chemical properties of the carbon and ash, they can be electrically charged to opposite polarity by particle-to-particle or by particle-to-surface contact. By manipulating the polarity and magnitude of this charge, the carbon and ash can be separated by passing them through an external electric field, see Figure 1. The successful application of dry separation technology to ash purification would be significant because it would eliminate water handling and treatment problems associated with wet beneficiation methods.

Dry electrostatic separation technology has been utilized in the mineral processing industry and most recently has been considered for coal beneficiation.<sup>3-7</sup> The US DOE has funded several projects focusing on both the fundamentals and development of dry coal beneficiation technologies based on electrostatics.<sup>8</sup> As a consequence of these efforts, a greater understanding of factors relating to the particle charging and electrostatic separation has been achieved. While the cost of processing is a major factor in the economic feasibility of coal beneficiation, it is not as important in the case of fly ash beneficiation. Economic factors of equal or higher importance include the avoided cost of ash disposal and the market value of the processed ash. Depending on geographic location, it is possible that the application of efficient dry ash separation technologies could be very beneficial to coal utilization systems.

Very little has been published on the application of dry triboelectrostatic separation to fly ash beneficiation. There is a need for optimizing dry fly ash separation technologies because of the vast amount of coal ash produced in the US and the growing interest in applying superior technologies with respect to their economical and environmental performance. In this paper, results from the triboelectrostatic separation of two coal fly ashes are presented. These experiments were conducted at a laboratory scale. The design of the triboelectrostatic separation system and the data obtained on the ashes in this study will be used in future work to optimize ash separation using feed rates typical to industrial and utility systems.

## EXPERIMENTAL

A laboratory scale triboelectrostatic separation system, shown in Figure 2, was used in the fly ash beneficiation study. The fly ash was metered by using a vibratory feeder, contained in a sealed environment tank, into a pneumatic transport tube where it was entrained in a N<sub>2</sub> carrier gas. The gas-particle mixture was then passed through a tribocharging unit where the fly ash was charged by particle-particle or particle-wall frictional contact. The exit of the charger was connected to a separation chamber which contained parallel copper plates across which was established a high intensity electric field. A filter was placed at the bottom of the separation chamber to catch any entrained fly ash particles. The exit of the separation chamber was connected to an induced draft fan.

About 10 grams of ash sample were weighed and used for each separation test. The average carrier gas flow velocity was about 15 m/s. The electric field strength was maintained at 200 kV/m.

The fly ash samples were acquired from either ESP hoppers or storage silos at two pulverized coal boilers. Prior to separation tests, the samples were evaluated for particle size and carbon content.

After the triboelectrostatic separation, samples were collected from predetermined locations throughout the separation chamber, and their weight and carbon content determined. Representative sample fractions were also prepared and examined using scanning electron microscopy (SEM) and energy dispersive spectrometry (EDS).

## RESULTS AND DISCUSSIONS

During separator operation, fractions of carbon and ash were deposited on the electrodes. For both electrodes, the depositions appeared to be long narrow ribbons of material, starting from near the exit of the transporting tube and extending to the end of the copper plates. Analysis of sequential axial sections of the depositions showed the carbon content to be highest at the top of the negative electrode and lowest at the top of the positive electrode. The carbon content on the positive electrode increased with distance while that on the negative electrode decreased with distance. In other words, the ash was the purest at the top of the positive plate and the carbon the purest at the top of the negative plate. Since the carbon and ash content on the electrodes could be represented by a continuous distribution, it was possible to make an arbitrary split of the separated products that satisfied desired purity requirements. However, as in any physical separation processes, higher purity products are achieved at the expense of lower yield.

A procedure was established for separated sample collection and analysis. For each test, there were a total of ten sample fractions collected; eight from four axial regions of the two electrodes, one from the center filter, and one removed from the vertical plexiglass windows. These fractions along with the feed were weighed and analyzed for their carbon content. An eleventh data point, which represents the material which was not captured anywhere in the separator, was determined by performing a mass and carbon balance. The separation results were plotted in a manner similar to a washability or release analysis curve, using the analogy of each fraction being either a float or sink product. These data include an assessment of mass balances. A second stage separation could be performed by putting the fraction collected on the center filter back to the feeder, and process the data with those from the first stage separation.

Carbon and ash recovery, and particle size and carbon distributions, for the fly ash sample A are shown in Figure 3-5. This sample was obtained from a utility boiler burning bituminous coal having an intermediate sulfur content. Over 65% of the ash was recovered with a carbon content of less than 3%, while about 50% of the carbon in the ash was recovered with a carbon content greater than 35%. The particle size distribution data show that there is a significant amount of the ash with sizes greater than 150  $\mu\text{m}$  and with sizes below 25  $\mu\text{m}$ . This wide distribution of particle size presents a significant challenge to dry separation systems due to an order of magnitude range in aerodynamic drag and gravitational forces. For this particular ash, the carbon concentrations for each size fraction are in a descending order, as shown in Figure 3, from the highest in the largest size fraction to the lowest in the smallest size fraction.

Separation results for fly ash sample B are presented in Figure 6-7. This sample was obtained from a utility burning intermediate-to-high sulfur coal. The ash recovery data is plotted for a one stage and a two stage processing scheme. The application of the second stage increased the ash recovery by about 15% and, hence, may be important to the overall processing scheme. These data show that nearly 55% of the ash was recovered with a carbon content of less than 3% while over 60% of the carbon could be recovered with a carbon purity greater than 40%. These results suggest the utility of dry ash separation. Important chemical and physical properties of the fly ashes which affect or control efficient dry ash separation are currently under investigation.

## CONCLUSIONS

This study has shown that dry triboelectrostatic separation of fly ash has the potential to be an effective method of separating unburned carbon from fly ash. Laboratory tests on a simple parallel flow separator showed that 60-80% of ash could be recovered at carbon contents below 5%, and 50% of carbon could be recovered at carbon concentrations over 50%. Additional studies should be initiated to evaluate the effects of ash properties on separation with the goal of optimizing the beneficiation process.

## REFERENCES

1. Manz, O.E., 1993, Worldwide Production of Coal Ash and Utilization in Concrete and Other Products: *Proceedings, 10th International Ash Use Symposium, Volume 2: Ash Use R&D and Clean Coal By-Products*, EPRI, Orlando, FL, p. 64/1-64/12.
2. Whitlock, D.R., 1993, Electrostatic Separation of Unburned Carbon from Fly Ash: *Proceedings, 10th International Ash Use Symposium, Volume 2: Ash Use R&D and Clean Coal By-Products*, EPRI, Orlando, FL, p.70/1-70/12.
3. Schaefer, J.L., J.M. Stencel and H. Ban, 1992, Non-Intrusive Measurement of Particle Charge

Relating to Electrostatic Dry Coal Cleaning: *Proceedings, 9th Annual International Pittsburgh Coal Conference*, University of Pittsburgh, Pittsburgh, PA, p. 259-264.

4. Ban, H., J. Yang, J.L. Schaefer, K. Saito and J.M. Stencel, 1993, Measurement of Charge and Charge Distribution on Coal and Mineral Mater During Electrostatic Dry Coal Cleaning: *Proceedings, 7th International Conference on Coal Science*, Banff, Alberta, Canada, Vol. 1, p. 615-618.

5. Ban, H., J.L. Schaefer and J.M. Stencel, 1993, Velocity and Size Effect on Particle Triboelectrification: *Proceedings, 10th Annual International Pittsburgh Coal Conference*, University of Pittsburgh, Pittsburgh, PA, p. 138-143.

6. Schaefer, J.L., H. Ban and J.M. Stencel, 1994, Triboelectrostatic Dry Coal Cleaning: *Proceedings, 11th Annual International Pittsburgh Coal Conference*, University of Pittsburgh, Pittsburgh, PA, Vol. 1, p. 624-629.

7. Ban, H., J.L. Schaefer, K. Saito and J.M. Stencel, 1994, Particle Tribocharging Characteristics Relating to Electrostatic Dry Coal Cleaning, *Fuel*, Vol. 73, p. 1108-1115.

8. Finseth, D., T. Newby and R. Elstrodt, 1993, Dry Electrostatic Separation of Fine Coal: *Proceedings, 5th International Conference on Processing and Utilization of High-Sulfur Coals*, University of Kentucky, Lexington, KY, p. 91-98.

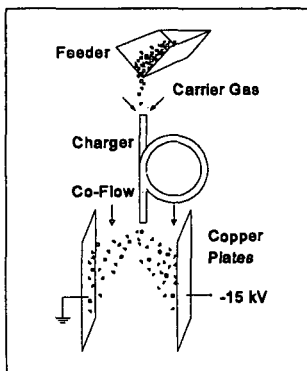


Figure 1: Electrostatic separation principle

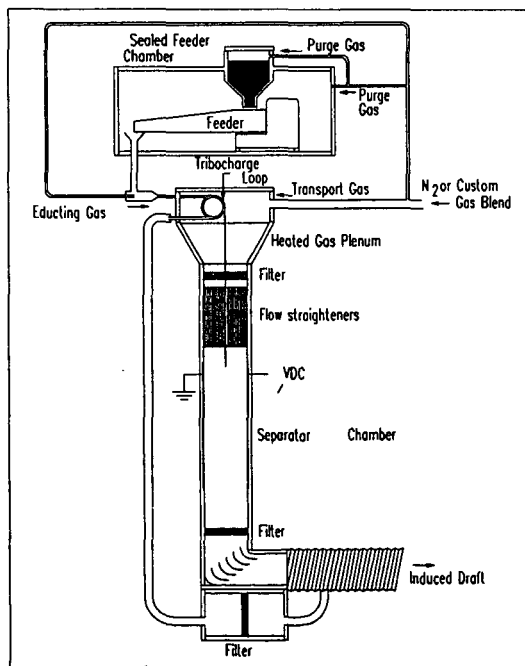


Figure 2: The schematic of the test system.

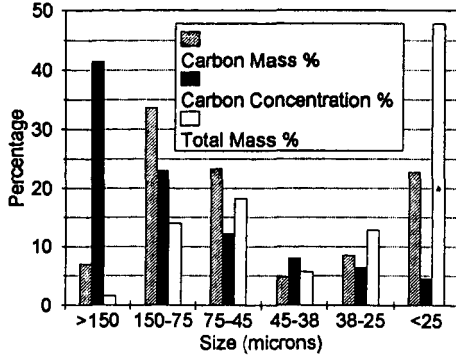


Figure 3: Percentage fly ash weight, carbon concentration, and carbon mass distributions in each size fractions for fly ash sample A.

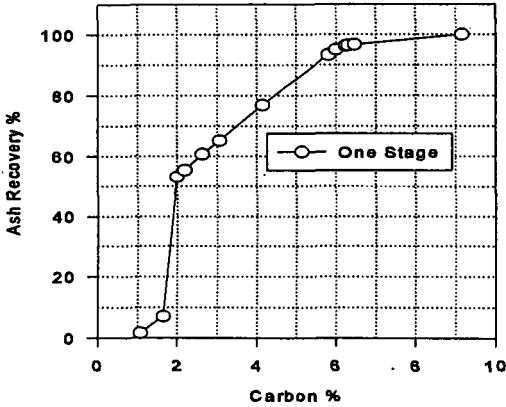


Figure 4: Ash recovery curve for sample A.

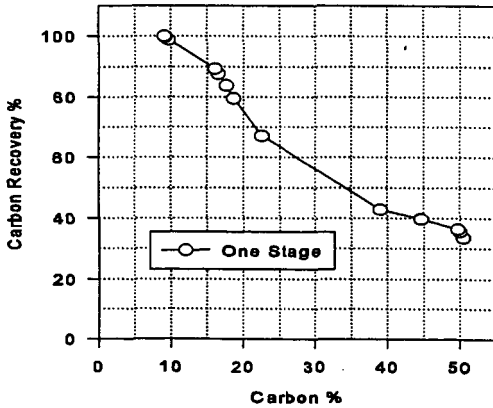


Figure 5: Carbon recovery curve for sample A.

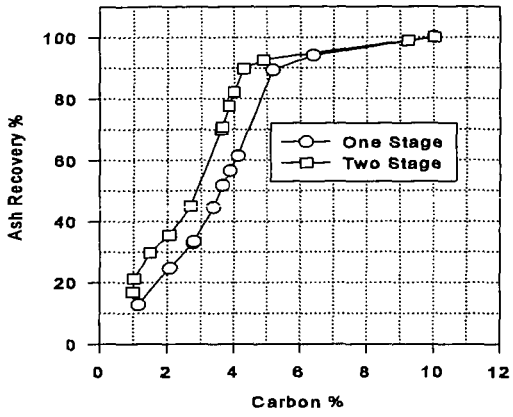


Figure 6: Ash recovery curve for sample B.

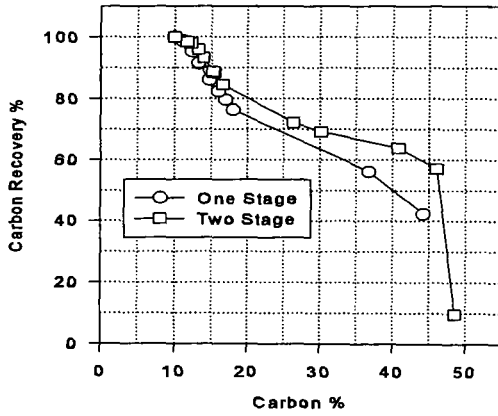


Figure 7: Carbon recovery curve for sample B.

## REGENERATION AND REUSE OF A LIME-BASED SORBENT FOR SULFUR OXIDES

S. B. Jagtap and T. D. Wheelock  
Chemical Engineering Department  
and Engineering Research Institute  
Iowa State University  
Ames, Iowa 50011

Keywords: Lime-based sorbent, sulfur oxides, regeneration

### INTRODUCTION

The purpose of this work was to study the feasibility of regenerating and reusing lime employed as a sorbent for sulfur oxides in an industrial, circulating fluidized bed boiler that is fired with petroleum coke. At present ground limestone is supplied continuously to the boiler, and the resulting sulfated bed ash and fly ash are discarded. By regenerating the sorbent, much less limestone would be required and waste disposal would be minimized.

Since the sorbent is converted to calcium sulfate in the boiler, regeneration requires converting calcium sulfate back to calcium oxide. Previous studies showed that such conversion can be achieved by employing reductive decomposition with carbon monoxide as indicated below (1,2):



By such means it is also possible to produce by-product sulfur dioxide in sufficient concentration for conversion into sulfuric acid or possibly elemental sulfur.

To study the feasibility of regenerating and reusing the lime sorbent, samples of sulfated bed ash and fly ash from an industrial boiler were subjected to a number of regeneration and sulfation cycles, and changes in the apparent reactivity and sorptive capacity of the materials were observed. The experiments were conducted by employing thermogravimetric analysis (TGA) which made it possible to monitor sulfation and regeneration by observing the change in sorbent weight.

### EXPERIMENTAL METHODS AND MATERIALS

The limestone supplied to the boiler is largely calcium carbonate with the principal impurity being silica. Chemical analysis of samples of fluidized bed ash and fly ash from the boiler showed the principal components of the ash to be  $\text{CaSO}_4$  (58.2%, 33.6%),  $\text{CaO}$  (30.4%, 29.3%),  $\text{CaCO}_3$  (1.8%, 21.5%), and  $\text{SiO}_2$  (2.1%, 7.2%). For each component, the first number is for bed ash and the second number is for fly ash. Both materials were also found to contain small amounts of iron, vanadium, and nickel oxides arising from the combustion of petroleum coke. Approximately 98% of the bed ash particles were larger than 230 mesh size, whereas 82% of the fly ash particles were smaller than this size. The composition of the bed ash indicates that 37% of the  $\text{CaO}$  was converted to  $\text{CaSO}_4$  in the boiler, while the composition of the fly ash suggests a lower level of conversion.

For some regeneration and sulfation experiments larger particles of fluidized bed ash or limestone were used as received, whereas for other experiments the materials were pelletized first, and fly ash was always pelletized first. The pellets were formed in a double-acting stainless steel die by application of high pressure with a hand-operated hydraulic press. The pellets were 6.35 mm in diameter and 1-2 mm thick. For some experiments the pellets were used directly, whereas for others the pellets were crushed, and the material screened.

The experiments were conducted with conventional TGA apparatus consisting of a vertical tubular reactor in which a balance pan for holding the reacting solids was suspended from a Cahn model 2000 electrobalance. Both the 10 mm diameter pan and 25 mm diameter reactor were made of quartz. The reactor was surrounded by a temperature-controlled electric furnace. During operation the reactor was supplied with a mixture of gases produced by combining various pure component gases which were metered separately by calibrated rotameters.

When starting with sulfated particles of fluidized bed ash or fly ash, the particles were first heated in a stream of nitrogen to 1100°C. The particles were then regenerated by treatment with a reducing gas mixture consisting of 2% CO, 5% SO<sub>2</sub>, 20% CO<sub>2</sub>, and 73% N<sub>2</sub>. When the reaction appeared complete, the gas mixture was replaced by nitrogen and the temperature was lowered to 900°C. At this point the particles were sulfated by treatment with a gas mixture consisting of either 1% or 3% SO<sub>2</sub>, 5% O<sub>2</sub>, and sufficient N<sub>2</sub> to make up the balance. When the reaction appeared complete, the cycle was repeated.

The conversion during each sulfation step was based on the following relation:

$$\text{Sulfation (\%)} = \frac{\text{moles SO}_2 \text{ adsorbed}}{\text{moles Ca present}} \times 100 \quad (2)$$

For each regeneration step the conversion was estimated by employing the relation shown below.

$$\text{Conversion (\%)} = \frac{\text{Wt. loss during regeneration}}{\text{Wt. gain during sulfation}} \times 100 \quad (3)$$

## RESULTS AND DISCUSSION

A number of runs were made with the TGA apparatus to determine the regeneration and sulfation characteristics of the parent limestone, fluidized bed ash, and fly ash. Typical results obtained with bed ash are shown in Table 1. For this experiment the bed ash was pelletized, crushed, and screened to provide -25/+40 mesh particles. The particles were first regenerated and then subjected to the seven cycles of sulfation and regeneration listed. The first sulfation step required 98 min. and resulted in the conversion of 44.6% of the CaO to CaSO<sub>4</sub>. The subsequent regeneration step only took 25 min. and appeared to result in the complete conversion of CaSO<sub>4</sub> to CaO. As the cycles were repeated, both the cycle time and the extent of sulfation decreased gradually from cycle to cycle. The decrease in sulfation indicated that an increasing portion of each particle became inaccessible or unreactive. This result could have been caused by sintering and closure of some of the particle micropores. Nevertheless, even during the eighth cycle of sulfation (recalling that the first cycle took place in the boiler), the capacity of the sorbent was still 26% of the maximum theoretically possible if all of the calcium were converted to CaSO<sub>4</sub>. Even more encouraging were the results of the regeneration step which always seemed to achieve, nearly complete conversion of CaSO<sub>4</sub> to CaO.

Similar results were obtained with -25/+40 mesh unreacted limestone particles which were prepared in the same manner as the bed ash particles by pelletizing, crushing, and screening. Upon heating the limestone particles to 900°C in a stream of nitrogen, the CaCO<sub>3</sub> was converted to CaO. The particles were then subjected to a series of sulfation and regeneration cycles using the same conditions employed with bed ash. For the early cycles the level of sulfation was nearly the same as that observed with bed ash while for the later cycles it was slightly greater. The similarity in results achieved with the two materials suggests that the small amount of petroleum coke ash present in the bed ash had little effect on the sulfation and regeneration characteristics of the bed ash.

The results observed with -25/+40 mesh fly ash particles differed in several respects from those described above when the particles were prepared and treated like the bed ash particles. For the fly ash particles the time required for the sulfation step was about half that required for the other materials. The level of sulfation achieved in the first TGA cycle was 37.7% compared to 44.6% for bed ash, and in the fifth TGA cycle it was 19.7% compared to 31.4% for bed ash. Therefore, it is apparent that the sorptive capacity of the fly ash decreased more rapidly than that of the other materials. This result was probably due to the difference in grain size of the various materials. The initial particle size of the fly ash was considerably smaller than that of the bed ash. Consequently, when the two materials were heated to reaction temperature, there would have been a greater tendency for the fly ash particles to sinter causing a greater decrease in microporosity.

## CONCLUSIONS

The results of this work indicate that it would be feasible to regenerate and recycle the sulfated bed ash produced by burning petroleum coke in a fluidized bed of limestone particles. Although the experimental results showed a decline in the sulfation capacity of bed ash particles as the number of sulfation and regeneration cycles increased, it was still possible to convert 30% or more of the CaO to CaSO<sub>4</sub> after five cycles. Regeneration was more rapid than sulfation, and it was nearly always complete. The results also indicate that it would be feasible to regenerate and recycle pelletized fly ash. However, the sulfation capacity of this material declined more with each cycle than the sulfation capacity of bed ash declined.

## ACKNOWLEDGMENT

This work was supported by the Engineering Research Institute of Iowa State University.

## REFERENCES

1. T. D. Wheelock and D. R. Boylan, Reductive Decomposition of Gypsum by Carbon Monoxide, *Ind. Eng. Chem.*, **52**, 215-218 (1960).
2. J. S. Oh and T. D. Wheelock, Reductive Decomposition of Calcium Sulfate with Carbon Monoxide: Reaction Mechanism, *Ind. Eng. Chem. Res.*, **29**, 544-550 (1990).

Table 1. Results of run made with granulated bed ash\*

Cycle	Time, min.	Initial wt., mg	Final wt., mg	Δ wt., mg	Sulf., %	Regen Sulf., %
1-S	98	39.2	58.5	19.3	44.6	
1-R	25	58.5	39.2	19.3		100
2-S	90	39.2	56.1	16.1	39.1	
2-R	24	56.1	39.3	16.8		104
3-S	89	39.3	54.2	14.9	34.5	
3-R	20	54.2	39.4	14.8		99
4-S	86	39.3	53.6	14.3	33.1	
4-R	22	53.6	39.4	14.2		99
5-S	86	39.4	53.0	13.6	31.4	
5-R	22	53.0	39.6	13.4		99
6-S	88	39.3	51.7	12.4	28.7	
6-R	20	51.7	39.4	12.3		99
7-S	80	39.3	50.7	11.4	26.4	
7-R	20	50.7	39.4	11.3		99

\*Particle size: -25/+40 mesh

Weight before calcination: 54.6 mg

Sulfation conditions: 905-910°C, 1% SO<sub>2</sub>, 5% O<sub>2</sub>, 94% N<sub>2</sub>

Regeneration conditions: 1105-1110°C, 2% CO, 5% SO<sub>2</sub>, 20% CO<sub>2</sub>, 73% N<sub>2</sub>.

## ABSORPTION STUDIES OF ACIDIC GASES USING DRY FGD WASTES.

Darrell N. Taulbee and Thomas L. Robl  
University of Kentucky-Center for Applied Energy Research  
3572 Iron Works Pike, Lexington, KY 40511

**Keywords:** Acid gases, absorption, CO<sub>2</sub>, NO<sub>2</sub>, H<sub>2</sub>S, SO<sub>2</sub>, Flue-gas desulfurization or FGD,

### ABSTRACT

Utility boilers and tail-gas desulfurization units that utilize limestone-based sorbents to remove sulfur oxides generate ~20 million tons of flue-gas desulfurization (FGD) wastes each year in the U.S.<sup>1</sup> A substantial portion of the Ca in these wastes remains unsulfated (as CaO or Ca(OH)<sub>2</sub>), particularly in units that produce *dry* wastes. When hydrated, these materials exhibit a strong affinity to absorb acid gases at ambient temperature in proportion to their available-calcium content and particle size. The work reported here is a continuation of previous investigations of CO<sub>2</sub> and H<sub>2</sub>S absorption that includes more recent studies with NO, NO<sub>2</sub>, and SO<sub>2</sub>. The relative affinity for the gases examined thus far is SO<sub>2</sub> > CO<sub>2</sub> > H<sub>2</sub>S. CH<sub>4</sub> and NO are not absorbed and NO<sub>2</sub> apparently decomposes at first to NO and HNO<sub>3</sub> before eventually being absorbed as calcium nitrate following depletion of hydration water. The role of available calcium and particle size on absorption capacity and mineralogic changes in the wastes during exposure are discussed.

### INTRODUCTION.

In recent years, numerous flue-gas desulfurization (FGD) technologies that utilize limestone-based sorbents, such as fluidized-bed combustors (FBC), spray dryers, and wet scrubbers, have been or will be added to existing utility boilers in an effort to satisfy federally-mandated limits on SO<sub>2</sub> emissions. Such units are normally classified as either *wet* or *dry* depending on whether the absorbent is used in an aqueous slurry (*wet*) or as a dry or hydrated solid. In addition to differences in the proportions of sulfites and sulfates formed during sulfur capture, dry FGD by-products differ from their wet-scrubber counterparts in that a significant portion of the calcium in the dry waste remains unsulfated. The fraction of unreacted Ca, available as lime (CaO) or slaked lime (Ca(OH)<sub>2</sub>) can be quite high (> 1/2) depending on scrubber design and operation.

When hydrated, dry FGD wastes strongly absorb acid gases at ambient temperature, e.g. CO<sub>2</sub>. Further, absorption can be both rapid and near complete. Such a sorbent may have numerous commercial uses such as the removal of CO<sub>2</sub> from natural gas (the focus of a prior study<sup>2</sup>). Further, considering that about 95% of the ~20 million tons of flue-gas desulfurization (FGD) wastes generated annually in the US is discarded in landfills or holding ponds, commercial utilization of FGD wastes could stand to benefit from both a plentiful low-cost raw material as well as a significant savings in disposal.

In our ongoing study, gas absorption has been examined using waste samples generated in four commercial boilers, a Coolside demonstration-plant run<sup>3</sup>, and four tests conducted in the Coolside pilot plant.<sup>4</sup> With the exception of a utility-derived fly ash that served as a control, all study samples are dry-FGD materials. In addition to the absorption studies with CO<sub>2</sub>, CH<sub>4</sub> and H<sub>2</sub>S previously reported, results from tests with NO, NO<sub>2</sub>, and SO<sub>2</sub> are reported here.

### EXPERIMENTAL.

Details for the most recent round of testing with NO, NO<sub>2</sub>, and SO<sub>2</sub> plus a brief description of the reactor system, study samples, and run procedures are presented in the section to follow. The reader is referred to previous manuscripts for additional information on the latter.<sup>2,5,6</sup>

**Absorption Reactors.** A schematic of the reactor system shown with a pair of 4" x 3/8"-i.d. ss tube reactors as configured for hydrated solids is shown on the left of Figure 1. Essentially the same system was used to measure absorption by aqueous waste slurries except that a pair of 250 mL-capacity gas scrubbers were substituted for the tube reactors (Figure 1-right). It should be noted that due to the high solubility of SO<sub>2</sub> in and the tendency for NO<sub>2</sub> to decompose on contact with water, only tests with hydrated solids were conducted for these two gases.

**Samples.** A total of 11 waste samples have been used throughout this investigation.<sup>2,5</sup> Nine of the samples are fly ashes, designated with a -FA suffix. The remaining two, designated with a -BA suffix, are bed ashes. A Class F fly ash (L-FA) from a pulverized-coal-combustion (PCC) utility boiler served as a control and was the only non-FGD sample examined. The four fluidized-bed combustion wastes (FU-FA/BA and CC-FA/BA) were derived from circulating or entrained flow units operating on high-sulfur bituminous coal. Two types of dry, post-combustion flue-gas scrubber material were also examined, a spray-dryer ash from an industrial

boiler in the Midwest, and materials from the Coolside duct-injection technology. The Coolside materials include one sample generated in Ohio Edison's 1990 demonstration of the technology at its Edgewater power plant<sup>3</sup> (CS) as well as materials from the CONSOL's Coolside pilot plant in Library, PA (PP1-PP4).<sup>4</sup> The major differences in the waste samples with respect to absorption appears to be in the particle size (BA > FA) and the proportions of free lime which ranged from <3% in the L-FA control to ~20% or greater in the FU-FA, FU-BA, CC-BA, and PP4 samples. Because absorption of CO<sub>2</sub> has been reported for all 11 samples in a previous report, tests conducted in this round were limited for the most part to the FU-FA and PP4 which represent the two samples of fly ash with the highest free-lime content.

**Run Procedures.** All absorption tests were conducted at ambient temperatures. Hydrated samples were obtained by blending distilled water with dry waste under N<sub>2</sub>. 0.5-2 g of the hydrated sample and 6 g of Ottawa sand were packed to the absorbent and bypass reactors, respectively. For the slurry tests, ~5 g of dry sample were added to 200 mL of distilled water in a 250-mL gas scrubber. The bypass scrubber contained distilled water only (200 ml).

Gas flow through the reactors was comprised solely of N<sub>2</sub> in the bypass line. Standard-gas blends containing various combinations of CO<sub>2</sub>, H<sub>2</sub>S, CH<sub>4</sub>, and Ar were metered through the absorbent line.<sup>2,5</sup> Standard-gas blends containing 0.509 vol% NO, 3.82 vol% NO<sub>2</sub>, or 3.81 vol% SO<sub>2</sub> were used in this round of testing. These blends were either quantitatively combined with high-purity Ar or with a blend of Ar/CO<sub>2</sub>/CH<sub>4</sub> (30.3/49.6/20.1 vol%) prior to entering the reactor system. Argon was generally included in all blends as a tracer gas.

The exit streams from both the bypass and sample reactors were combined and continuously sampled with a capillary tube connected to the inlet of a VG-quadrupole mass spectrometer (QMS). The QMS was operated in a selected-ion-monitoring mode in which ion intensities for m/e 15-CH<sub>3</sub><sup>+</sup> (for methane), 18-H<sub>2</sub>O<sup>+</sup>, 20-Ar<sup>2+</sup>, 28-N<sub>2</sub><sup>+</sup>, 30-NO<sup>+</sup>, 34-H<sub>2</sub>S<sup>+</sup>, 40-Ar<sup>+</sup>, 44-CO<sub>2</sub><sup>+</sup>, 46-NO<sub>2</sub><sup>+</sup>, and/or 64-SO<sub>2</sub><sup>+</sup> were recorded at approximately 1-second intervals.

For both reactor configurations, data collection was initiated with the switching valve in the bypass position, i.e., the test-gas stream passing through the sand-packed bypass reactor. After a timed interval, the valve was rotated so that the test-gas stream was switched to the absorbent reactor as the N<sub>2</sub> stream was simultaneously switched to the bypass reactor. Following exposure, the valve was returned to the initial position to reestablish the QMS baseline. At the conclusion of a run, the QMS molecular-ion signal for each gas of interest was ratioed to the Ar-ion signal. The curves described by these ratios were then numerically integrated over the interval of exposure. By comparing these integrals to the test gas/Ar ratios obtained during passage through the bypass bed (before and after valve switch), the fraction of the test gas absorbed was determined. Since gas flows and sample weights are known, absorption could be converted to an absolute basis (standard cubic feet (SCF)/ton of waste). The same procedure was used for those runs in which more than one test gas was passed through the reactor in the same run.

## RESULTS

It was shown in prior studies that the absorption of CO<sub>2</sub> required wetting of the dry FGD waste (hydration or slurry formation). For non-wetted samples, absorption proceeded at a prohibitively slow rate.<sup>2,5</sup> This is illustrated in Figure 2 where absorption of CO<sub>2</sub> is observed to increase in a linear manner up to about 25 wt% added water. Further water addition created a mud-like consistency accompanied by a dramatic decline in the apparent absorption capacity. This decline is presumably due to decreased permeability of the hydrated sample preventing gaseous CO<sub>2</sub> from freely entering the sample bed.

Absorption curves are shown in Figure 3 for a hydrated sample (top) and an aqueous slurry (bottom) prepared from PP4. This figure shows CH<sub>4</sub>, CO<sub>2</sub>, and H<sub>2</sub>S response curves as these gases were concurrently passed through the reactor. These plots indicate that CH<sub>4</sub> was not absorbed, H<sub>2</sub>S was moderately absorbed, and CO<sub>2</sub> was extensively absorbed. Closer inspection of the absorption curves reveals that the H<sub>2</sub>S response rose to greater than baseline levels in both runs as H<sub>2</sub>S was passed through the sorbent bed. This implies that some of the H<sub>2</sub>S absorbed early in the exposure was displaced by CO<sub>2</sub> as the capacity of the PP4 sample was depleted. The absorption kinetics were more rapid for the hydrated sample than for the aqueous slurry though on an absolute basis, absorption was about twice as great for the latter (~3,800 SCF/t vs ~1,800 SCF/t). It was previously concluded that CO<sub>2</sub> incorporated into the hydrated sample to form calcite whereas absorption by the waste slurry resulted in capture as HCO<sub>3</sub><sup>-</sup> ions which remain in solution. Thus, each CaO unit in the hydrated solids could capture one CO<sub>2</sub> molecule to form CaCO<sub>3</sub> or lead to the capture of two CO<sub>2</sub> molecules to form aqueous-phase HCO<sub>3</sub><sup>-</sup> ions.

CO<sub>2</sub> absorption by waste slurries is plotted as a function of available-calcium content for the 11

study samples in Figure 4. The majority of the samples plot along a straight line with the exception of the two points on the lower right. These two outliers represent the two samples of bed ash (FU and CC) whereas the other points in Figure 4 represent samples of fly ash. This plot emphasizes the dependency of CO<sub>2</sub> absorption on both available calcium and particle size. That is, the significantly larger particle size of the bed-ash samples as well as potential blockage of particle pores by chemisorbed SO<sub>2</sub> likely limits diffusion of CO<sub>2</sub> to the particle interior.

**Tests with NO, NO<sub>2</sub>, and SO<sub>2</sub>.** Absorption curves for NO, NO<sub>2</sub>, and SO<sub>2</sub> are shown in Figure 5 as these gases were passed through either an aqueous slurry (NO) or a hydrated sample of PP4 (NO<sub>2</sub>/SO<sub>2</sub>). CO<sub>2</sub> was blended to the test-gas stream prior to routing to the absorption reactor for all three runs shown in Figure 5. The top plot shows essentially no absorption of NO. Likewise, no significant absorption of NO was measured when this gas was passed through the slurry without CO<sub>2</sub> (not shown) or when passed through a sample of hydrated PP4 (not shown).

The middle plot in Figure 5 shows simultaneous removal of NO<sub>2</sub> and CO<sub>2</sub>. Both gases were extensively absorbed immediately after the valve switch to expose mode. However, ~5 min into the exposure, the response curve for CO<sub>2</sub> exceeded its baseline established during bypass mode (before and after exposure). This suggests that CO<sub>2</sub> initially absorbed was displaced as the run proceeded (absorption capacity of the slurry was depleted). Unlike CO<sub>2</sub> which is chemisorbed by portlandite (Ca(OH)<sub>2</sub>) to form CaCO<sub>3</sub>, it is not believed that NO<sub>2</sub> is absorbed as such. Rather, it appears to decompose on contact with hydration water to form HNO<sub>3</sub> and NO. This is supported by the NO and H<sub>2</sub>O curves shown in the same plot. Immediately after switching to expose mode, the NO<sub>2</sub> signal is lower than that of NO. However, about 40-45 min into the run, the NO<sub>2</sub> response increases above that of NO concurrent with the depletion of H<sub>2</sub>O. This is congruent with a decrease in NO<sub>2</sub> decomposition as the hydration water is consumed. HNO<sub>3</sub> ultimately reacts with portlandite to produce H<sub>2</sub>O and calcium nitrate hydrate but not until much of the hydration water is depleted. Finally, integration of the CO<sub>2</sub>-response curve revealed a net release of CO<sub>2</sub> of ~150 SCF/t. This production of CO<sub>2</sub> likely derives from calcite (CaCO<sub>3</sub>) inherent to the FGD waste which is attacked by the newly-formed nitric acid (later discussion).

The bottom plot in Figure 5 shows SO<sub>2</sub>/CO<sub>2</sub> absorption. Again, CO<sub>2</sub> was initially absorbed but later displaced by SO<sub>2</sub> as the run proceeded. Integration of the absorption curves (60 min interval) indicated an average absorption of ~3,800 SCF/t SO<sub>2</sub> and a net release of ~550 SCF/t CO<sub>2</sub>. Again, the released CO<sub>2</sub> is believed to originate from pre-existing calcite in the PP4 sample as indicated by XRD. The calcite peaks were totally absent in the XRD spectra of wastes following exposure to SO<sub>2</sub>. At the end of the 60' exposure, absorption of SO<sub>2</sub> and release of CO<sub>2</sub> is essentially complete. In contrast, during exposure to a blend of NO<sub>2</sub>/CO<sub>2</sub> (Figure 5b), NO<sub>2</sub> decomposition and CO<sub>2</sub> displacement is not complete despite the fact that essentially the same volumes of NO<sub>2</sub> and SO<sub>2</sub> were flowed through the reactors during these runs. In a single run with SO<sub>2</sub> and NO<sub>2</sub> (w/o CO<sub>2</sub>), SO<sub>2</sub> response began to return to baseline well before NO<sub>2</sub> which again exhibited an inverse relation to water availability. Thus, it would appear that SO<sub>2</sub> removal is controlled by the chemistry of the waste sample whereas NO<sub>2</sub> removal seems more dependent on water content.

**Changes in mineralogy.** X-ray diffraction (XRD) spectra of hydrated-PP4 waste samples are shown in Figure 6. The top plot (Figure 6a) is for a hydrated sample simultaneously exposed to CO<sub>2</sub> and H<sub>2</sub>S, the middle spectrum (Figure 6b) is following exposure to NO<sub>2</sub>/CO<sub>2</sub>, and the bottom (Figure 6c) is following exposure to SO<sub>2</sub>/CO<sub>2</sub>. A spectrum of a hydrated sample of PP4 that had not been exposed to the test gases is shown in all three plots for comparison (darker lines). In the top plot, the major mineralogic change was depletion of portlandite (Ca(OH)<sub>2</sub>) and formation of calcite (CaCO<sub>3</sub>). There is no indication of CaS formation. When H<sub>2</sub>S was passed through the sample without CO<sub>2</sub> (not shown), portlandite was again depleted only this time accompanied by the formation of an unidentified mineral with peaks near 9 and 20 (2-theta). The suspected stoichiometry of the unknown is Ca(OH)<sub>2-x</sub>(HS)<sub>x</sub> though this structure is yet to be confirmed.

Again, depletion of portlandite from the parent to the exposed sample can be seen in Figure 6b in which NO<sub>2</sub> and CO<sub>2</sub> were passed through the hydrated sample. Several new peaks appear which are identified as a hydrated form of calcium nitrate. However, in runs aborted prior to water depletion, these peaks were not observed in the exposed sample. This is consistent with the decomposition of NO<sub>2</sub> to NO and HNO<sub>3</sub> since NO would be released and surface adsorbed HNO<sub>3</sub> would not exhibit an XRD pattern. Thus, the absorbed NO<sub>x</sub> species must exist as either HNO<sub>3</sub> or in an amorphous structure. It is speculated that at some point during the exposure as water is depleted, the HNO<sub>3</sub> reacts with portlandite to form H<sub>2</sub>O and Ca(NO<sub>3</sub>)<sub>2</sub>·2H<sub>2</sub>O.

Depletion of portlandite from the parent to the exposed sample is again evident in Figure 6c in

which a mixture of  $\text{CO}_2/\text{SO}_2$  was used. The minor calcite peaks present in the parent are absent in the exposed sample. Several new peaks appear in the exposed sample which, for the most part, can be attributed to hannebachite ( $\text{CaSO}_3 \cdot 0.5\text{H}_2\text{O}$ ). Thus, it appears that  $\text{SO}_2$  is mostly incorporated by substitution for the hydroxyl ions in portlandite with some substitution for  $\text{CO}_2$  in the inherent carbonates.

#### SUMMARY

Hydrated FGD wastes exhibit a strong affinity for  $\text{CO}_2$ ,  $\text{H}_2\text{S}$ , and  $\text{SO}_2$  ranging upwards of 4,000 SCF/t for  $\text{SO}_2$  in tests with the PP4 and FU-fly ash. The relative order of affinity appears to be  $\text{SO}_2 > \text{CO}_2 > \text{H}_2\text{S}$ .  $\text{NO}_2$  was found to decompose on contact with the hydrated samples to form  $\text{NO}$  and  $\text{HNO}_3$  with eventual incorporation as hydrated calcium nitrate. Little or no absorption of  $\text{CH}_4$  or  $\text{NO}$  was observed. In tests of  $\text{CO}_2$  absorption, absorption capacity was found to be directly related to the available-calcium content and inversely to the particle size of the waste. Further, absorption did not proceed at a significant rate without the addition of water to the dry wastes. XRD analyses showed that exposure of hydrated FGD wastes to  $\text{CO}_2$ ,  $\text{H}_2\text{S}$ ,  $\text{SO}_2$ , and  $\text{NO}_2$  resulted in the depletion of portlandite ( $\text{Ca}(\text{OH})_2$ ) and subsequent formation of calcite ( $\text{CaCO}_3$ ), an unknown mineral, hannebachite ( $\text{CaSO}_3 \cdot \text{H}_2\text{O}$ ), and initially either an amorphous nitrate/nitrite mineral or absorbed  $\text{HNO}_3$  followed by formation of  $\text{Ca}(\text{NO}_3)_2 \cdot 2\text{H}_2\text{O}$ , respectively.

#### ACKNOWLEDGEMENT

The authors wish to thank Dr. U. Graham, Dr. R. Rathbone, and M. Gust for assistance with the XRD analyses; G. Thomas, B. Schram, and M. Grider for sample analyses; and K. Baker of Jefferson Gas Transmission for useful discussions. This work was supported in part by the Morgantown Energy Techn. Ctr., USDOE, under Coop. Agreement DE-AC21-91MC28162 (such support does not constitute an endorsement by the USDOE of the views expressed in this manuscript).

#### REFERENCES.

1. *Coal Combustion Byproduct (CCB); Production & use: 1966-1993. Report for Coal Burning Utilities in the United States.* American Coal Ash Association, 1995, Alexandria, VA, 68p.
2. Taulbee, D.N., Graham, U., Rathbone, R.F., and Robl, T.L.; *Prepr., ACS Div. of Fuel Chem.*, 1995, 40, #4, American Chemistry Society, Washington, DC, 858-862.
3. Kanary, D.A., R.M. Stanick, H.Yoon, et al., 1990, Coolside Process Demonstration at the Ohio Edison Company Edgewater Plant Unit 4-Boiler 13. *Proceedings, 1990 SO<sub>2</sub> Control Symposium 3*, EPRI/U.S. EPA, Session 7A., New Orleans, LA, 19p.
4. Withum, J.A., W.A. Rosenhoover and H. Yoon, 1988 *Proceedings, 5th Pittsburgh Coal Conf.* University of Pittsburgh, 84-96.
5. Taulbee, D.N.; Graham, U.; Rathbone, R.F.; Robl, T.L.; submitted for publication in *Fuel*, anticipated publication, late 1996.
6. Taulbee, D. N., *Prepr., ACS Div. of Fuel Chem.*, 1993, 38, #1, American Chemistry Society, Washington, DC, 324-329.

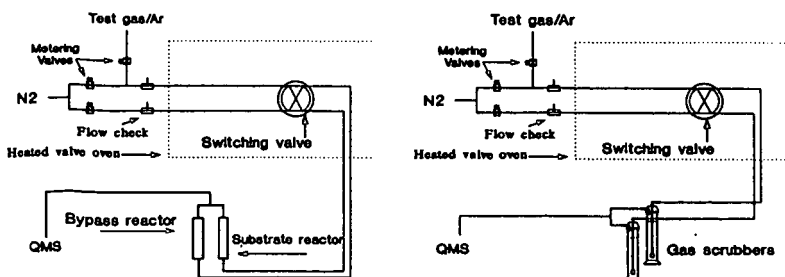


Figure 1. Schematic of the absorption reactors used to measure gas absorption by hydrated-FGD wastes (left) and waste slurries (right).

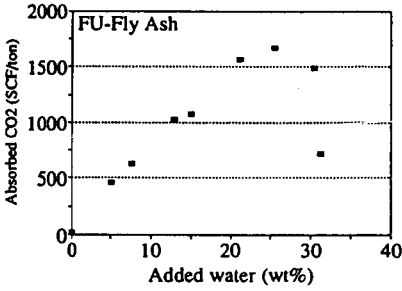


Figure 2. Absorption of CO<sub>2</sub> as a function of prehydration for samples of FU-FA.

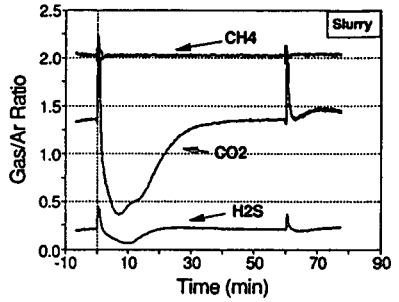
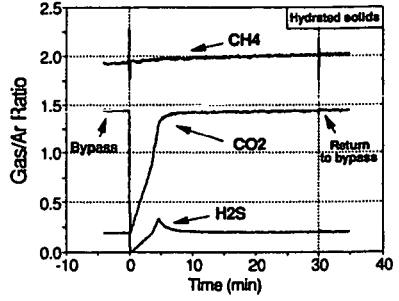


Figure 3. Absorption curves for CH<sub>4</sub>, CO<sub>2</sub>, and H<sub>2</sub>S simultaneously passed through a hydrated sample (top) and aqueous slurry (bottom) of PP4.

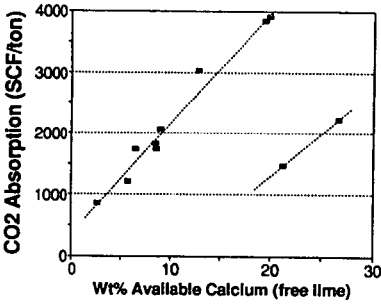


Figure 4. CO<sub>2</sub> absorption as a function of the available calcium. The two points on the bottom right represent samples of bed ash; all others are fly ash samples.

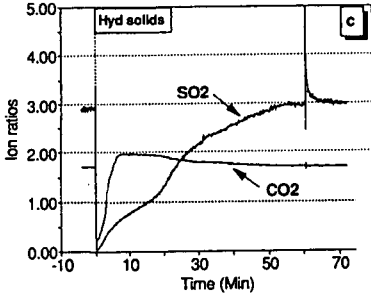
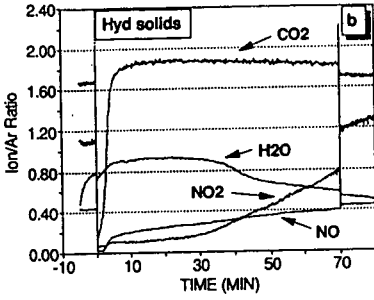
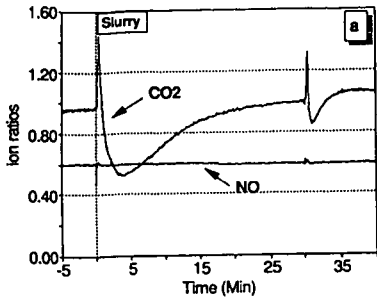


Figure 5. Test gas/Ar ion ratios for NO (a), NO<sub>2</sub> (b), and SO<sub>2</sub> (c) during exposure hydrated PP4 (a) and PP4 slurry (b/c). C absorption shown in all three plots.

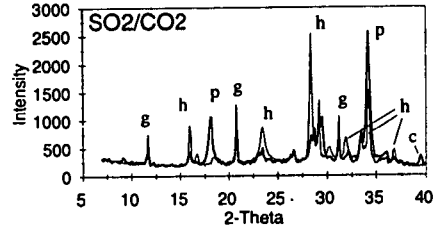
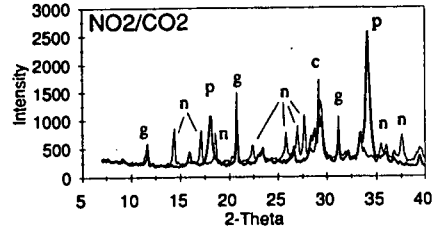
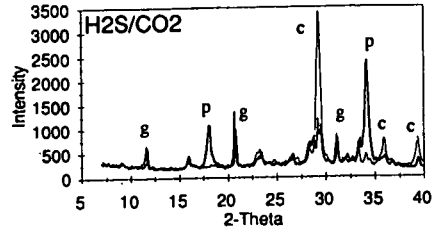


Figure 6. XRD spectra of PP4; hydrated only-darker lines; exposed sample-lighter shading. c-calcite (CaCO<sub>3</sub>); n-calcium nitrate hydrate; g-gypsum (CaSO<sub>4</sub>·H<sub>2</sub>O); h-hannebachite (CaSO<sub>3</sub>·5H<sub>2</sub>O); p-portlandite-(Ca(OH)<sub>2</sub>).